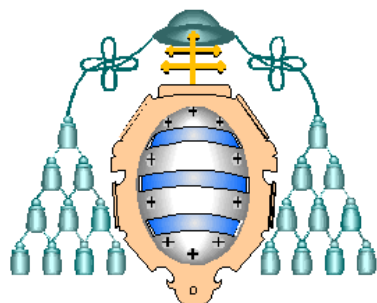


**DEPARTMENT OF CHEMICAL AND ENVIRONMENTAL  
ENGINEERING**

**UNIVERSITY OF OVIEDO**



***PRODUCTION OF EMULSIONS WITH  
CONTROLLED DROPLET SIZE  
CONTAINING BIOACTIVE COMPOUNDS  
USING MEMBRANES***

**DOCTORAL THESIS**

**BY**

***MARÍA MATOS GONZÁLEZ***

**NOVEMBER, 2013**

## **AGRADECIMIENTOS**

Al Prof. José Coca por haberme dado la oportunidad de llevar a cabo este trabajo, de participar en varios proyectos, cursos y congresos, por las enseñanzas recibidas y por el apoyo mostrado durante todo este tiempo.

A la Prof. Carmen Pazos, por permitirme formar parte del Grupo de Investigación de Emulsiones y Fenómenos Interfaciales, por sus consejos a la hora de ayudarme a estructurar y desarrollar este trabajo, por toda su paciencia y comprensión, y por sus extraordinarias correcciones.

A la Dra. Gemma Gutiérrez, no sólo por supervisar este trabajo, sino por su amistad incondicional y grata compañía a lo largo de todos estos años.

Al Dr. José Manuel Benito, por siempre estar ahí cuando se le necesita, a pesar de encontrarse a muchos kilómetros de distancia, y responder desinteresadamente con esa rapidez tan sorprendente a todas las dudas que se me han planteado.

A la Dra. Marilyn Rayner y al Prof. Petr Dejmek, por permitirme llevar a cabo una breve pero fructífera estancia en el Departamento de Tecnología de Alimentos, Ingeniería y Nutrición de la Universidad de Lund (Suecia). Agradezco también a la Dra. Malin Sjöö por haberme dejado participar en el proyecto Speximo y a la Dra. Anna Timgren, que desgraciadamente ya no está entre nosotros, por su apoyo constante en el laboratorio durante mi estancia.

Al programa de Formación de Personal Investigador (FPI) del Ministerio de Economía y Competitividad, cofinanciado por el fondo social europeo (FEDER), por el apoyo económico para la realización de la presente Tesis Doctoral, así como a los proyectos CTQ2007-65348 y CTQ2010-20009-C02-01.

A los becarios que durante estos dos últimos años han pertenecido al Grupo de Emulsiones y Fenómenos Interfaciales, David, Alberto, Miguel y Daniel por su compañía y por el ánimo transmitido en todo momento.

A todos los compañeros, tanto de la sala de becarios como del Departamento, por ser estupendos tanto a nivel personal como de trabajo, y por todos los buenos ratos que hemos pasado.

Agradecer finalmente a mi familia y a mi pareja por apoyarme en todo momento.

# INDEX

ABSTRACT.....	1
RESUMEN.....	III
1. INTRODUCTION.....	1
1.1. ANTIOXIDANT COMPOUNDS.....	2
1.2. EMULSIONS.....	4
1.2.1. <i>Stabilizers</i> .....	5
1.2.2. <i>Pickering emulsions</i> .....	8
1.2.3. <i>High Internal Phase Emulsions (HIPEs)</i> .....	10
1.2.4. <i>Double emulsions</i> .....	10
1.3. MEMBRANE EMULSIFICATION.....	13
1.3.1. <i>Direct membrane emulsification</i> .....	14
1.3.1.1. <i>Droplet formation mechanism</i> .....	15
A. <i>Shear-based mechanism</i> .....	15
B. <i>Spontaneous emulsification</i> .....	16
1.3.2. <i>Premix emulsification</i> .....	18
2. OBJECTIVES.....	19
3. RESULTS.....	21
I. EMULSIFICATION WITH CERAMIC MICROFILTRATION MEMBRANES: A DIFFERENT APPROACH TO DROPLET FORMATION MECHANISM.....	22

II.	PREPARATION AND ENCAPSULATION PROPERTIES OF DOUBLE PICKERING EMULSIONS STABILIZED BY QUINOA STARCH GRANULES.....	41
III.	PREPARATION OF WATER-IN-OIL-IN-WATER ( $W_1/O/W_2$ ) DOUBLE EMULSIONS CONTAINING <i>TRANS</i> -RESVERATROL.....	50
IV.	PREPARATION OF HIPES WITH CONTROLLED DROPLET SIZE CONTAINING LUTEIN.....	63
4.	GENERAL CONCLUSIONS.....	85
5.	CONCLUSIONES GENERALES.....	87
6.	REFERENCES.....	89

## ABSTRACT

The objective of this thesis is the preparation of simple and double emulsions of interest in food, pharmaceutical and cosmetic industries, containing bioactive compounds with antioxidant capacity both of lipophilic (*lutein*) and hydrophilic character (*resveratrol*). Several technologies were used, such as, mechanical agitation, membrane emulsification and vacuum evaporation.

Taking into consideration the importance of the droplet size control in this type of emulsions, a fundamental study of the membrane emulsification process was carried out. Flat and tubular ceramic microfiltration membranes were used to prepare oil-in-water (O/W) emulsions. The performed experiments enabled to understand the effect of operation parameters on droplet size distributions, and to determine the droplet formation mechanism and the optimal operation conditions. Stable monodisperse emulsions were obtained with very low span values. A spontaneous emulsification mechanism is proposed for both flat and tubular membranes as the continuous phase shear stress had little influence on the oil droplet size.

Based on previous studies, which showed the extreme stability of simple oil-in-water (W/O) Pickering emulsions stabilized with starch granules from Quinoa, the feasibility of preparing double water-in-oil-in-water ( $W_1/O/W_2$ ) emulsions was studied. The initial encapsulation efficiency was higher than 98.5% immediately after emulsification process, and the encapsulation stability remained over 90% after 21 days for all systems formulated.

Food-grade water-in-oil-in-water ( $W_1/O/W_2$ ) double emulsions to encapsulate *trans*-resveratrol were formulated and prepared by mechanical agitation and membrane emulsification. A technique based on RP-HPLC to determine *trans*-resveratrol concentration in the external aqueous phase with UV-vis and fluorescence detectors was developed to measure the encapsulation efficiency (EE) and the encapsulation stability (ES). Several stabilizers were used, both in the oily phase and in the external aqueous phase, to achieve the optimal formulation.

Finally, highly concentrated oil-in-water (O/W) emulsions, also called high internal phase emulsions (HIPEs), containing lutein were formulated and prepared by two-step technique, combining either membrane emulsification or mechanical agitation with vacuum evaporation. The oil droplet size distribution and viscosity were measured to assess the vacuum evaporation performance. Oil-in-water (O/W) emulsions with an internal phase concentration up to 90% (v/v) were prepared by

mechanical agitation and evaporation. Emulsions obtained by membrane emulsification showed higher monodispersity but they could only be concentrated up to 75% (v/v) of internal phase. An appropriate formulation led to lutein encapsulation efficiency up to 97%.

## RESUMEN

En el presente trabajo, se han preparado emulsiones simples y dobles, de interés en la industria alimentaria, farmacéutica y cosmética, conteniendo biocompuestos con capacidad antioxidante, tanto de carácter lipófilo (*luteína*), como hidrófilo (*resveratrol*). Para ello, se utilizaron diferentes tecnologías, como agitación mecánica, emulsificación con membranas y evaporación a vacío.

Teniendo en cuenta la importancia del control del tamaño de gota en este tipo de emulsiones, se llevó a cabo un estudio fundamental del proceso de emulsificación con membranas. Se utilizaron membranas cerámicas de microfiltración con formato plano y tubular y se prepararon emulsiones aceite-agua (O/W). Los experimentos programados permitieron comprender el efecto de los parámetros de operación sobre la distribución de tamaños de gota, así como determinar el mecanismo de formación de gotas que tiene lugar y establecer las condiciones de operación óptimas. Se obtuvieron emulsiones monodispersas estables que presentaban valores muy bajos de span. Asimismo, se propuso un mecanismo espontáneo para la formación de las gotas de fase dispersa, al constatar la escasa influencia del esfuerzo cortante ejercido por la fase continua sobre el tamaño de gota obtenido

Basándonos en estudios previos, en los cuales se había demostrado la elevada estabilidad de emulsiones simples aceite-agua (O/W) tipo *Pickering*, con gránulos de almidón procedentes de la Quinoa como estabilizantes, se analizó si resultaba viable la preparación de emulsiones dobles agua-aceite-agua (W<sub>1</sub>/O/W<sub>2</sub>). Los resultados indicaban que el valor de la eficacia de encapsulación inicial, inmediatamente después del proceso de emulsificación, era del 98.5%. Además, la estabilidad de encapsulación se mantenía, después de 21 días, en un valor del orden del 90% para todos los sistemas formulados.

A continuación, se formularon y prepararon emulsiones dobles agua-aceite-agua (W<sub>1</sub>/O/W<sub>2</sub>) de grado alimentario para encapsular *trans-resveratrol*, empleando agitación mecánica y emulsificación con membranas. Se desarrolló un protocolo para analizar la concentración de *trans-resveratrol* en la fase acuosa externa, utilizando cromatografía líquida de alta resolución de fase inversa (RP-HPLC) con detectores UV-VIS y de fluorescencia, con el fin de determinar la eficacia de encapsulación (EE) y la estabilidad de encapsulación (ES). Se estudió el comportamiento de varios tipos de estabilizantes, tanto en la fase aceitosa, como en la fase acuosa externa, lo que permitió establecer una formulación óptima.

Finalmente, se formularon y prepararon emulsiones aceite-agua (O/W), con elevada proporción de fase interna (HIEPs) y conteniendo luteína, empleando una técnica en dos etapas, que combinaba emulsificación con membranas o agitación mecánica con evaporación a vacío. Para evaluar el rendimiento de la evaporación a vacío, se midió la distribución de tamaño de las gotas de aceite y la viscosidad de las emulsiones. Se obtuvieron emulsiones aceite-agua (O/W) con una concentración de fase interna que llegaba hasta el 90% (v/v), mediante agitación mecánica y evaporación. Las emulsiones obtenidas mediante emulsificación con membranas mostraban un superior carácter monodisperso, aunque con concentraciones máximas de fase interna del 75% (v/v). Una adecuada selección de los componentes de la formulación permitió alcanzar una eficacia de encapsulación de luteína del 97%.

# **INTRODUCTION**

The current way of life and the high sensibility towards health, creates the need to develop functional foods containing biological active components (such as vitamins, fatty acids, antioxidants, minerals, etc). These components supplement the nutritional characteristics of food, and contribute to health improvement and decrease the risk of diseases.

The main disadvantage is that most of the antioxidants are lipophilic, with none or very low solubility in water, and processes such as emulsification and/or microencapsulation allow to supply the bioactive compounds in stable structures, such as colloidal systems, of well-defined size. Some of the most common colloidal systems are emulsions.

Encapsulation techniques have been developed basically in the pharmaceutical and cosmetic industries and they are of different nature depending on the type of the bioactive compound and the application purpose. Food emulsions require the use of ingredients of food degree, such as natural components, which form structures (proteins, carbohydrates, lipids or their mixtures, polycarbonates, etc.), or ingredients functionalized in physical or enzymatic form.

The aim of this thesis is to contribute to the preparation of emulsions containing natural bioactive compounds (lutein and resveratrol) for food, pharmaceutical and cosmetic applications.

### **1.1. Bioactive compounds**

Bioactive compounds are defined as *essential and nonessential compounds (e.g., vitamins or polyphenols) that occur in nature, are part of the food chain, and can be shown to have an effect on human health* (Biesalski *et al.*, 2009).

Bioactive substances present as natural constituents in food provide health benefits beyond the basic nutritional value of the product. Until recently, vitamins and other micronutrients have been recommended just to avoid deficiency symptoms . Nowadays, the most extensively studied compounds are antioxidants, which prevent the risk of chronic diseases including cancer and cardiovascular disorders (Biesalski *et al.*, 2009).

Antioxidant compounds, such as carotenoids, polyphenols, phytosterols, omega-3 fatty acids, etc., protect the cells from the oxidative stress caused by the action of free radicals, and they are being used as active ingredients in several food products.

Carotenoids are compounds soluble in lipids (lipophilic antioxidants) and are responsible for the colour of fruits and vegetables. Among the most important for the organism are:  $\beta$ -carotenes,  $\alpha$ -carotenes, lycopene, cryptoxanthin, lutein and zeaxanthin.

**Lutein** is a natural yellow carotenoid that can be found in many fruits and vegetables, in some algae and in egg-yolk. Foods with a high content in lutein are: peas, leeks, broccoli, spinach, spinach beet, cabbage, corn, parsley, celery, squash, bananas and oranges. This compound is a dihydroxylated derivative of  $\alpha$ -carotene, belonging to the xanthophylls group, which is also of great interest for its antioxidant properties, since it prevents macular degeneration, avoiding the progress of cataracts and glaucoma that lead to the loss of vision. Lutein is also found naturally in human skin, where it acts as a potential antioxidant maintaining skin health by reducing UV-induced erythema and inflammation. Because of the link between UV radiation (particularly its UVB component) exposure and skin cancer, lutein may play a protective role against skin cancer. It has been demonstrated that topical treatment with 50 mg/L lutein twice a day induces immediate increase in skin surface lipids and a significant reduction in skin lipid peroxidation, improving the photoprotective activity and also the skin elasticity and hydration (Mitri *et al.*, 2011).

Lutein addition in food and cosmetic formulations is limited by its instability towards oxygen, light and temperature, and hence the use of oil droplets as lutein carriers is considered a suitable technique (Mitri *et al.*, 2011; Qv *et al.*, 2011).

Polyphenols are a typical example of hydrophilic antioxidants of food interest, as it is the case of **resveratrol** (trans-3,4',5-trihydroxystilbene), a phytoalexin present in dried fruits and in the grape skin where from it goes into the red wines, with a solubility up to 0.03 g/L in water and 50 g/L in ethanol. It has beneficial effects for human health, such as anti-oxidant, anti-inflammatory, cardioprotective and anti-tumour properties.

However, the applications of *trans*-resveratrol are limited because it is an easily oxidizable and extremely photosensitive compound, with low water solubility, short biological half-life, and rapid metabolism and elimination (Peng *et al.*, 2010; Amri *et al.*, 2012; Saiko *et al.*, 2008).

Encapsulation studies have been carried out to protect *trans*-resveratrol from degradation and to mitigate effectively these limitations (Fang and Bhandari, 2010; Amri *et al.*, 2012). Several methods for the encapsulation of polyphenols have been reported: spray drying, coacervation, liposome or niosome entrapment (Caddeo *et al.*,

2008; Fabris *et al.*, 2008; Kristl *et al.*, 2009; Pando *et al.*, 2013a; Pando *et al.*, 2013b; Wang *et al.*, 2011), inclusion complexation (Lucas-Abelán *et al.*, 2007), cocrystallization, nanoencapsulation (Shao *et al.*, 2010; Teskac and Kristl, 2010), freeze drying and emulsification (Fang and Bhandari, 2007; Donsi *et al.*, 2011).

In general, all the former compounds show strong antioxidant activity that helps to prevent cancer and delay aging. Furthermore, some of them offer specific clinical demonstrated benefits, as the anti-obesity effect of resveratrol or the protection of the macula of retina by lutein. Many of these antioxidants are available as a dietetic supplement, which is taken orally as tablets, capsules or suspensions, and they are sold in dietetic products shops, herbal and drugstores.

## 1.2. Emulsions

An emulsion is defined as a two-phase system consisting of two immiscible liquids of different composition, one of which is in the shape of drops, dispersed in the other one. The liquid in drop shape is called the *dispersed phase* or *inner phase*, whereas the liquid in which these drops are suspended is called *continuous phase* or *external phase*. The most common situation corresponds to an emulsion formed by a hydrophilic liquid (water) and another one hydrophobic (oil).

The structure of an emulsion depends to a great extent on the volume fraction of water, oil and a third component called *emulsifying agent* or *emulsifier*, as well as the nature of the interfacial film.

Emulsions play an important role in the formulation of foods for production of oil-in-water (O/W) emulsions (*e.g.* dressings or artificial milks) as well as for the preparation of some water-in-oil (W/O) emulsions (*e.g.* margarine and low fat spreads). Some emulsions are final products (*e.g.* coffee creamers) and other emulsions can be used as ingredients, which help in forming the structures of more complex products (*e.g.* yoghurts that must interact with other food ingredients, but that must not be destabilized in the process). However, emulsion droplets can also create new structures in the product (*i.e.*, ice-creams) where being emulsion destabilization required for this purpose (Charcosset, 2009).

Two special types of emulsions are microemulsions and nanoemulsions, with droplet sizes below 100 nm (Mason *et al.*, 2006). The appearance of these emulsions is translucent due to the fact that the light can penetrate through the emulsion without being scattered if the droplet sizes in the emulsion are below about 100 nm. The main difference is that nanoemulsions require specialized equipment to be produced, while

microemulsions are spontaneously formed by solubilizing oil molecules with a mixture of stabilizers (surfactants, co-surfactants, and co-solvents) (Mason *et al.*, 2006).

However, in most cases emulsions are inherently unstable and, therefore, do not tend to form spontaneously. An energy input is required to form an emulsion being the most common industrial emulsification processes: high pressure homogenizers, rotor stator devices and static mixers.

### 1.2.1. Stabilizers

The main kind of emulsifiers are *surfactants*. A surfactant, a contraction of the term **surface-active agent**, is a substance that, at low concentration in a system, has the property of adsorbing onto the surfaces or interfaces altering the associated free energies. The term *interface* refers to the boundary between two immiscible phases. The interfacial free energy is the minimum amount of work required to create that interface (Rosen J. Milton, 2004).

The interfacial free energy per unit of area is the interfacial tension between two phases. A surfactant is therefore a substance that at low concentration adsorbs at the interfaces in a system and significantly reduces the work required to expand the interfaces.

Surfactants have an *amphiphilic* molecular structure consisting of a structural group that has very little attraction for the solvent, and other group that has strong attraction for the solvent. The hydrophilic part is referred as the *head group* and the hydrophobic part as the *tail*.

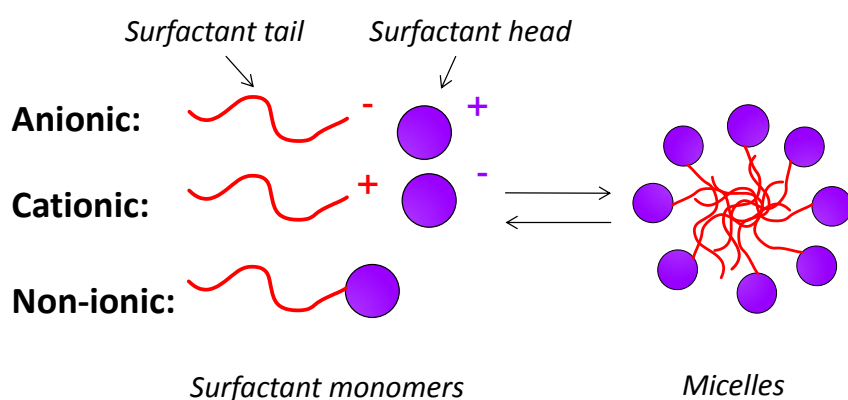


Fig. 1. Schematic illustration of the reversible monomer-micelle thermodynamic equilibrium. Head groups and tails of surfactants are respectively represented by circles and curved lines

Depending on the nature of the hydrophilic group, surfactants can be classified as:

1. *Anionic*. The surface-active portion of the molecule has a negative charge. Carboxylate, sulfate, sulfonate and phosphate are the polar group of this type of surfactants.
2. *Cationic*. The surface-active portion has a positive charge, and the nitrogen atom usually has the cationic charge. Amine and quaternary ammonium-based products are common groups, e.g.,  $\text{RN}(\text{CH}_3)_3^+\text{Cl}^-$  (quaternary ammonium chloride).
3. *Zwitterionic*. Both positive and negative charges may be present in the surface-portion. Whereas the positive charge is almost invariably ammonium, the source of negative charge may vary, although carboxylate is the most common.
4. *Non-ionic*. The surface-active portion has no apparent ionic charge with a polyether or a polyhydroxyl unit as the polar group.

The physical, chemical and electrical properties of matter confined to phase boundaries are often quite different from those of the same matter in bulk. For many systems (e.g., emulsions, foams and dispersions of solids) where a substantial fraction of the total mass is located at the boundaries (interfaces or surfaces), being relatively large with respect to the total volume of the system, surfactants are expected to play an important role.

Another fundamental property of surfactants is that monomers in solution tend to form aggregates called *micelles*. Surfactants molecules have very different behavior when they are present in micelles instead of free monomers in solution. Only surfactants monomers contribute to surface and interfacial tensions reduction and dynamic phenomena (e.g., wetting and foaming) are governed by the concentration of free monomers in solution.

Surfactants are among the most versatile products of the chemical industry and the world production is of several millions of metric tons. Some of their main applications are related to cosmetic, food and pharmaceutical industries (Myers, 2006).

Cosmetic and personal care products make up a multi-billion-dollar market worldwide. Most of these products are formulated at least with a small amount of surfactant (e.g. tints, lipsticks, hair dyes, mascara, etc.). Although the possible adverse

effects of surfactants in cosmetics and personal care products are an important aspect that must be studied in depth for safety reasons, due to the interaction of cosmetic formulation components with the human skin, membranes and other tissues or organs.

The presence of surfactants is crucial for obtaining products with specific characteristics in the food industry. Some examples are foam or sponge cakes, bread mayonnaise, salad dressing and ice creams. The surfactants used in these cases are identical to surfactants present in animal and vegetable systems (mono- and diglycerides derived from fats and oils, phospholipids, such as lecithin, glycerides with natural lactic and fruits acids, etc.).

The pharmaceutical industry uses surfactants extensively in spite of the strong regulatory standards of toxicity, allergenicity and collateral effects. They play an important role in formulation of solutions, emulsions, dispersions, gel capsules or tablets with delivery of active ingredients, such as timed-release medications or transdermal dosage.

The hydrophilic-lipophilic balance (HLB) of a surfactant is a measure of the degree to which it is hydrophilic or lipophilic, determined by calculating values for the different regions of the molecule, which ranges from 1 to 20. Its value can be used to determine final product that it is going to be obtained, as shown in Table 1 :

*Table 1. HLB scale used to classify the surfactants*

---

<b>HLB</b>	<b>GENERAL APPLICATION</b>
1-3	Antifoaming
3-6	Water-in-oil emulsions
7-9	Dispersants
8-18	Oil-in-water emulsions
13-15	Detergents
15-18	Solubilization

---

Bancroft's rule suggests that the type of emulsion is dictated by the type of emulsifier and that it should be soluble in the continuous phase (Bancroft, 1913; Bancroft, 1915). This empirical observation can be rationalised by considering the interfacial tension at oil-surfactant and water-surfactant interfaces. Moreover, W/O emulsions are usually formed when the water volume fraction is low, whereas O/W emulsions are formed when a small oil volume fraction is dispersed in a large amount of water. On the other hand, in systems formulated with the same fraction of oil and water, a bicontinuous emulsion is likely to exist. A theoretical ternary phase diagram of an emulsion is shown in Fig. 2.

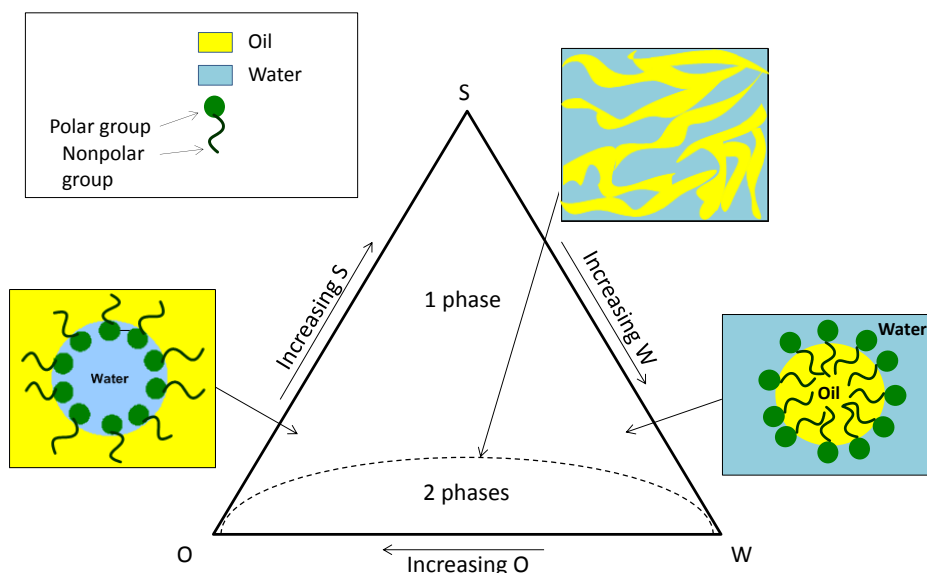


*Fig. 2. Theoretical ternary phase diagram of an emulsion. O, oil component, W, water component, S, amphiphilic component (surfactant)*

### 1.2.2. Pickering emulsions

Particle stabilized emulsions, known as Pickering emulsions, were originally observed independently by Ramsden (Ramsden, 1903) and Pickering (Pickering, 1907). This type of emulsion show special features due to its high degree of stability.

The use of particles to stabilize emulsions has received substantial and increasing research interest during the last decades due to their distinctive characteristics and promising technological applications in a wide range of fields (Binks, 2002; Tcholakova *et al.*, 2008) including foods.

Properties such as hydrophobicity, shape, particle size can affect the emulsion stability. The particle contact angle to the interface (droplet surface) is a characteristic of its hydrophobicity. Particles that are partially hydrophobic (*i.e.* contact angle of approximately 90°) are better stabilizers due to their partial dual wettability. This allows the spontaneous accumulation of particles at the oil-water interface with the subsequent stabilization against coalescence by volume exclusion and steric hindrances (Aveyard *et al.*, 2003), *i.e.* particles prevent oil-water interfaces of oil droplets from coming in to direct physical contact. Thus, Pickering emulsions are extremely stable against coalescence and Ostwald ripening compared to systems stabilized by surfactants.

Reduced use of surfactants via development of surfactant free particle stabilized emulsions is especially attractive due to their strong regulatory standards of toxicity, allergenicity, collateral effects and for safety reasons. The possible adverse effects of surfactants in topical formulations of personal care and cosmetics are due to the interaction of the components of the formulation with the human skin (*i.e.* irritation), membranes and other tissues or organs with which it will come into contact.

A high number of food-grade particles for stabilizing Pickering type emulsions have been reported in the literature, such as fat crystals, globular proteins and aggregated hydrocolloids (Dickinson, 2010), insoluble flavonoid particles (Luo *et al.*, 2011), cellulose-ethyl cellulose complexes for stabilizing emulsions and foams (Murray *et al.*, 2011), freeze fractured starch granules and protein mixtures (Murray *et al.* 2011; Yusoff *et al.*, 2011), and chitin-nano crystals stabilized emulsions (Tzoumaki *et al.*, 2011).

Starch is one of the most common food ingredients and it has been proved to be a suitable stabiliser for food grade Pickering emulsions. In previous studies intact starch granules isolated from Quinoa were modified hydrophobically with Octenyl Succinic Anhydride (OSA) and used to produce Pickering emulsions with excellent stability and barrier properties (Timgren *et al.*, 2010; Rayner *et al.* 2012). They could be suitable for applications such as encapsulation of sensitive, bioactive, or valuable ingredients in food and pharmaceutical products with starch particles acting as a barrier controlling release properties.

### **1.2.3. High internal phase emulsions (HIPEs)**

Another emulsions that play an important role in pharmaceutical, food and cosmetic applications are the High Internal Phase Emulsions (HIPEs) or gels. This type of emulsions can be used as a primary step to prepare microcapsules for drug delivery

systems (Lissant, 1966; Galvin *et al.*, 2001; Muschiolik, 2007; Augustin and Hemar, 2009; Dubensky and Reed, 2010; Pilcer and Amighi, 2010) or as reaction media, because of their high interfacial area (Solans *et al.*, 2003).

HIPES contain typically more than 74% (v/v) of oil (internal phase), which corresponds to the Ostwald critical volume, and 26% (v/v) of external phase filling the free space between them (Lissant, 1970; Princen, 1979; Princen *et al.*, 1980; Tyrode *et al.*, 2005; Rondón-González *et al.*, 2006; Rondón-González *et al.*, 2008; Liu and Friberg, 2009). Thus, an appropriate stabilizer selection is crucial to prepare this kind of emulsions.

The use of HIPES as carriers offers clear advantages from the transport point of view, making creams one of the most common drug delivery systems used for topical application.

HIPES have been widely investigated in the last years and their preparation arouses great interest, as some recent studies point out (Princen and Kiss, 1986; Esquena *et al.*, 2003; Mishchuk *et al.*, 2004; Márquez *et al.*, 2007; Lim *et al.*, 2009; Matsumoto *et al.*, 2009; Reynolds *et al.*, 2009; Alvarez *et al.*, 2010; Tcholakova *et al.*, 2011; Campbell *et al.*, 2012). However, although several techniques have been applied, their drop size has not yet been controlled in a proper and easy way. Monodisperse emulsions can be obtained with microfluidic devices (Priest *et al.*, 2006), but their major limitations are the large droplet size obtained and the process scale-up.

#### **1.2.4. Double emulsions**

Multiple emulsions are another type of emulsion which was first reported in 1925 by Seifriz (Seifriz, 1924). The simplest multiple emulsions are double emulsions, ternary systems where the dispersed droplets contain smaller droplets of a different phase. They have either a water-in-oil-in-water ( $W_1/O/W_2$ ) or an oil-in-water-in-oil ( $O_1/W/O_2$ ) structure (Aserin, 2008), as shown schematically in Fig. 3.

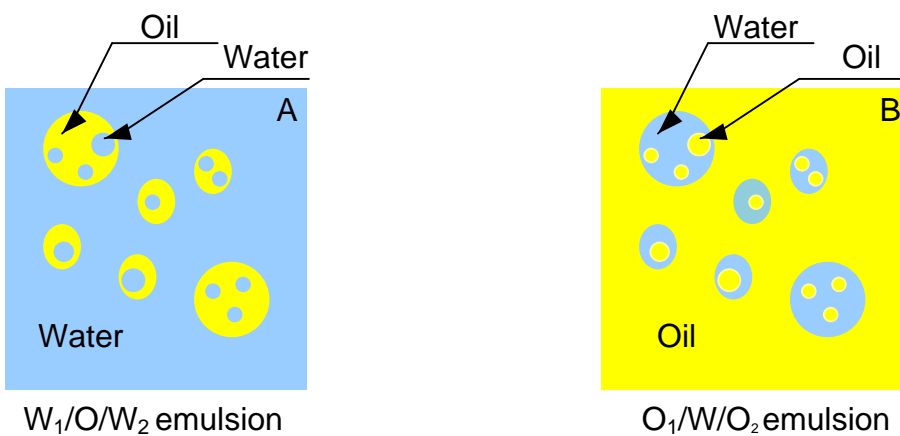


*Fig. 3. Structure of double emulsions: a) water-in-oil-in-water emulsion ( $W_1/O/W_2$ ) and b) oil-in-water-in-oil emulsion  $O_1/W/O_2$*

Due to their complex structure multiple emulsions can be viewed as systems that control the transport of molecules from an external to an internal phase or vice versa. Their major potential is in pharmaceutical, food and cosmetic applications (Garti *et al.*, 1997b; Okochi and Nakano, 1997; Krog, 1977; van der Graaf *et al.*, 2005; de los Reyes and Charcosset, 2010; Márquez *et al.*, 2010; Schmidts *et al.*, 2010; Frasch-Melnik *et al.*, 2010a; Frasch Melnik *et al.*, 2010b; Dickinson, 2011).

For treatments that require repeated administration, via ingestion or injection, and for compounds with very short half-life, the possibility of a single administration followed by a slow and controllable release is an improvement on the usual forms of drug delivery, protecting it from alterations caused by external environment (oxidation, light, enzymatic degradation) or during food digestion (Rosen, 2004; Aserin, 2008).

However, their use has been restricted by the fact that they are unstable thermodynamic systems due to an excess of free energy associated with the emulsion droplets surface (Garti, 1997a; Aserin, 2008).

To formulate a  $W_1/O/W_2$  double emulsion at least two stabilizers are introduced in the system: one lipophilic, to form the primary  $W_1/O$  emulsion and other hydrophobic, to form the final multiple emulsion.

In case that surfactants are the stabilizers chosen for both emulsions (internal and external) the “weighted hydrophilic-lipophilic balance (weighted HLB)” value serves as a good approximation to evaluate the best mixture of emulsifiers selected to prepare a double emulsion with an optimal droplet size and a maximum yield of formation of double emulsion droplets.

$$\text{Weighted HLB} = \frac{\text{HLB}_{(I)}\phi_{(W_1/O/W_2)} + \text{HLB}_{(II)}C_{(I)}}{\phi_{(W_1/O/W_2)} C_{(I)} + C_{(II)}}$$

where  $\text{HLB}_{(I)}$  is the hydrophobic emulsifier HLB value,  $\phi$  is the inner  $W_1/O$  emulsion fraction of the final  $W_1/O/W_2$ ,  $C_{(I)}$  is the hydrophobic emulsifier weight percent of the starting  $W_1/O$  emulsion,  $\text{HLB}_{(II)}$  is the hydrophilic emulsifier HLB value, and  $C_{(II)}$  is the hydrophilic emulsifier weight percent of the final  $W_1/O/W_2$ . When this value is lower or close to 10 the  $W_1/O/W_2$  reverses into an O/W emulsion. Other authors confirmed that best yields are obtained when the weighted HLB is between 2 to 20.

Progress in the development of stable double emulsions as food ingredients depends on replacing small-molecule emulsifiers and synthetic polymeric stabilizing agents by food-grade components (Dickinson, 2011).

In pharmaceutical, cosmetic and food formulations non-ionic surfactants are preferred due to their good emulsion properties and their relatively low toxicity. Among the most common nonionic surfactants used in pharmaceutical systems formulation are sucrose esters (Thevenin *et al.*, 1996), polyoxyethylene hydrogenated castor oil (Kunieda *et al.*, 1996), poly glycerol fatty acid esters (Ho *et al.*, 1996). Due to their biocompatible nature, some systems based on zwitterionic phospholipids, particularly lecithin, have been also investigated (Shinoda *et al.*, 1991; Saint Ruth *et al.*, 1995).

The most pharmaceutically common accepted cosurfactants are ethanol (Park *et al.*, 1999), medium chain mono and diglycerides (Constantinides, 1995; Constantinides *et al.*, 1996), 1,2-alkenoids (Kahlweit *et al.*, 1995; Kahlweit *et al.*, 1996) and sucrose ethanol mixtures (Joubran *et al.*, 1994), alkyl monoglucosides and geraniol (Stubenrauch *et al.*, 1997). The most significant problem associated with the formulation of pharmaceutical emulsions is related to excipients compatibility and acceptability. Pharmaceutically acceptable systems should be prepared using at least safe and ideally pharmaceutically grade ingredients, *i.e.*, the ones already approved by regulatory bodies for pharmaceutical use and without undesirable effects.

Hydrophilic macromolecules, such as bovine serum albumin (BSA) (Garti *et al.* 1994), amino acids, carboxyvinyllic compounds and cellulose and its analogues, introduced in the internal aqueous phase may increase emulsion stability (Dickinson, 2011). This stability increase can be attributed to a complexation between macromolecule and emulsifier at the  $W_1/O$  interface.

The addition of thickening agents (like gelatin (Sapei *et al.* 2012), xanthan gum, guar gum, Arabic gum (Su *et al.* 2006), carboxyvinyllic compounds, cellulose and its

derivatives) to increase emulsion viscosity and consequently emulsion stability has also been reported (Dickinson, 2011).

The oil nature has great influence on final emulsions properties, such as viscosity, density and polarity, which will determine their final applications. The oil phases most frequently used to form double emulsions are hydrocarbons (*i.e.* liquid paraffin), triglycerides (most of them are vegetable oils), and fatty acid esters such as myristate, isopropyl palmitate and ethyl oleate, and medium-chain triglycerides. Nowadays, medium-chain triglycerides are widely used because they are lighter, which allows obtaining emulsions with an oily external phase less viscous and greasy (Fanun, 2009).

A common water-in-oil emulsifying agent used in food formulations is polyglycerol polyricinoleate (PGPR) (Wilson *et al.*, 1998). It has been demonstrated to be highly effective for stabilizing this type of emulsions (Márquez *et al.*, 2010).

Active species or markers can be included in the internal phase. Typical markers used are dyes, sugars, fluorescence agents or electrolytes which are most often used to control the osmotic gradient between both aqueous phases, to increase emulsion stability (due to salt-out effects) and to monitor the rate of break-down.

### 1.3. Membrane emulsification

Emulsions must fulfil certain conditions of stability once they are formulated to keep their functional properties. Therefore, it is very important to study the properties and phenomena that may lead to destabilization. The problem with most emulsions, as the ones used in food, pharmaceutical and cosmetic industries, is that the droplets of the dispersed phase do not have a uniform size, bringing up problems of stability and loss of functional properties, as well as limitations in their applications. Conventional manufacturing processes used to produce these emulsions, such as high pressure homogenizers, rotor-stator systems, colloid mills, ultrasonics and microfluidizers, do not allow to obtain emulsions with a uniform droplet size. These techniques rely on the application of a high shear stress that deforms an interface generating polydisperse droplet size distributions and may damage shear-sensitive molecules, lead to phase inversion (Groeneweg *et al.*, 1998), and have lower efficiency in terms of energy density requirements (Vladisavljevic *et al.*, 2005).

Droplet size and droplet size distribution may determine the final properties of an emulsion. In some applications, such as drug delivery systems, a good control on droplet size and a narrow distribution are required to ensure a proper activity. Therefore, it becomes necessary to develop new manufacturing methods.

Techniques for membrane emulsification (ME) may be classified into two groups (Suzuki *et al.*, 1996; Kawakatsu *et al.*, 1997): (1) *Direct ME*, when a dispersed phase is injected through the membrane into the continuous phase; (2) *Premix ME*, when a coarse emulsion is pressed through the membrane to reduce the droplet size.

### 1.3.1. Direct membrane emulsification

ME was developed for the first time in Japan at the beginning of 1990s and it has been widely studied for the last two decades. This technique consists of injection of a dispersed phase through the membrane pores while continuous phase moves over the membrane surface enhancing droplet detachment. It gives high control on droplet size, since droplet diameter is in the range of 2-10 times the membrane pore diameter. Moreover, in ME the strain on liquid phases is reduced, and droplet size can be narrowly distributed with less shear stress and energy consumption.

Two membrane disposition are mainly used: (i) cross-flow membrane emulsification with tubular membranes in which dispersed phase is injected from the outer part of the membrane while continuous phase flows through the membrane lumen (Abrahamse *et al.*, 2001; De Luca *et al.*, 2008; Timgren *et al.*, 2010), and (ii) flat membranes where dispersed phase is injected from the bottom side of the membrane and continuous phase is placed in the upper part (Abrahamse *et al.*, 2002; Aryanti and Williams, 2009; Pathak, 2011).

Other membrane disposition more recently investigated can be also found in the literature (Pawlak and Norton, 2012; Vladisavljevic and Williams, 2006; Yuan *et al.*, 2009) in which rotating and vibrating membranes are used remaining the continuous phase static, while the membrane is continuously moving enhancing droplet detachment.

Several factors influence in mean droplet size and droplet size distribution when using membrane emulsification: emulsion formulation, membrane characteristics, equipment and operating parameters.

Membranes of several materials have been tested and reported in the literature. *Shirasu Porous Glass (SPG)* membranes were widely used in production of emulsions and emulsification chemical reactions (Kukizaki, 2009; Kukizaki and Goto, 2009; Vladisavljevic *et al.*, 2005; Vladisavljevic *et al.*, 2006ab; Yasuno *et al.* 2002), other types of membranes, such as filtration membranes (Williams *et al.* 1998; Shröder *et al.*, 1999) or hollow fibre modules (Vladisavljevic *et al.* 2002) have been used more recently for this purpose.

Dispersed phase can be gently dosed by means of a pump or a pressurized vessel. Droplet detachment usually takes place because of shear acting on membrane surface, which is often provided by the continuous phase flow, as shown in Fig. 4.

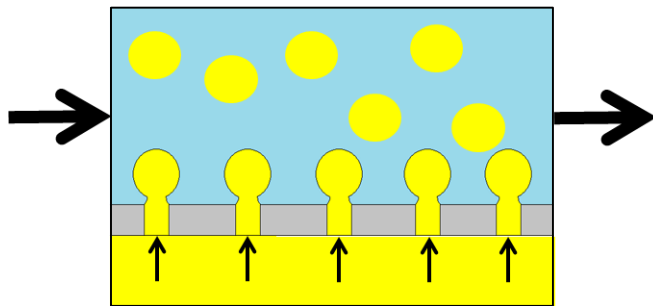


**Fig. 4. Schematic diagram of membrane emulsification**

Another achievement in ME was the design of silicon microengineered devices to promote droplet detachment in emulsions preparation. They have a wide variety of shapes and some of them (straight-through microchannels) have some similarities with membranes (Kobayashi *et al.*, 2003). Microchannel emulsification is not considered a membrane emulsification technique because of the different emulsification principle. However, tailor-made microchannels have been useful in understanding droplet formation mechanisms in direct membrane emulsification (van der Graaf *et al.*, 2005b; Eisner, 2007; Steegmans *et al.*, 2009) and in premix emulsification (van der Zwan *et al.*, 2006).

Several reviews have reported the state-of-the-art of membrane emulsification (Joscelyne and Trägårdh, 2000; Charcosset *et al.*, 2004; Gijbertsen-Abrahamse *et al.*, 2004; Lambrich and Schubert, 2005; Vladisavljevic and Williams, 2005; Yuan *et al.*, 2010; Suárez *et al.*, 2012). Furthermore, specific reviews on multiple emulsions formation (van der Graaf *et al.*, 2005a), premix membrane emulsification (Nazir *et al.*, 2011) and spontaneous emulsification (Maan *et al.*, 2011) have been also published.

### **1.3.1.1. Droplet formation mechanisms**

#### *a. Shear-based mechanism*

Fig. 5 shows a simple scheme of the forces acting on a droplet during crossflow emulsification. Interfacial tension force,  $F_\gamma$ , is the adhesion force of the droplet around the pore opening edge, being the main retaining force during droplet formation, but static pressure force ( $F_{ST}$ ), caused by dispersed phase flow moving through the capillary, makes the droplet grow. Drag force,  $F_D$ , is caused typically by the shear stress produced by cross-flowing continuous phase over the membrane surface. It acts on

the droplet, stretching it and is the main force that causes detachment (Timgren *et al.*, 2009). Dynamic lift force ( $F_{DL}$ ) is a result of the asymmetric velocity profile in continuous phase near the droplet (Rayner and Trägårdh, 2002). Additionally, buoyancy force ( $F_B$ ) is caused by the density difference between two phases and it is affected by the droplet volume, it helps detachment if dispersed phase density is lower than continuous phase density.

All the aforementioned forces that affect droplet size have been defined by simple algebraic expressions (Rayner and Trägårdh, 2002; Kosvintev *et al.*, 2005; Xu *et al.*, 2005; Peng and Williams, 1998) and also by more complex force balances (De Luca and Drioli, 2006; Christov *et al.*, 2008).

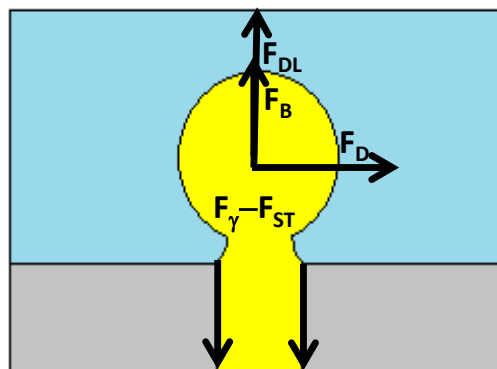


*Fig. 5. Schematic diagram of forces acting on a droplet in membrane emulsification*

This mechanism based on the shear rate allows to control the droplet size just by changing operating conditions and it is commonly used in metallic membranes.

Direct emulsification has been modelled according to force (Peng and Williams, 1998; Schröder and Schubert, 1999; De Luca and Drioli, 2006) and torque balances (Xu *et al.*, 2005; Hao *et al.*, 2008). A comparison of droplet size prediction by both models has been performed (De Luca *et al.*, 2008). Computational fluid dynamics (CFD) has also been used in modelling shear-based membrane emulsification (Abrahamse *et al.*, 2001; Timgren *et al.*, 2009; Timgren *et al.*, 2010).

Flow simulation for a single capillary microchannel has been used by several authors to study the effect of different operating parameters on droplet formation (Abrahamse *et al.*, 2001; Meyer and Crocker, 2009; Timgren *et al.*, 2009). These models are based either on image analysis (Abrahamse *et al.*, 2002; van der Graaf *et al.*,

2005; Meyer and Crocker, 2009) or simulations (Timgren *et al.*, 2009; Pathak, 2011). Devices in which shear is produced by membrane movement have been also modelled by force balances (Aryanti *et al.*, 2009; Holdich *et al.*, 2010).

### *b. Spontaneous emulsification*

Sugiura (Sugiura *et al.*, 2002) found that droplets could be spontaneously formed in microchannels. Moreover, when ME process with SPG membranes was optically monitored (Christov *et al.*, 2002; Yasuno *et al.*, 2002) it was observed that small droplets were formed under certain conditions, even in absence of shear. These results showed that droplet formation mechanism might be different than expected; this effect is mainly found in systems with slotted or tortuous pores (Kobayashi *et al.*, 2004).

It has been suggested that spontaneous emulsification is a result of surface free energy minimization. When dispersed phase flows through a tortuous pore or an oblong slot, the deformation makes the flow energetically non-favourable, so that it splits in droplets in order to minimize the surface free energy (Christov *et al.*, 2002; Sugiura *et al.*, 2002; Kobayashi *et al.*, 2004; Kukizaki, 2009).

Emulsions prepared by this mechanism are extremely monodisperse, with span factors of 0.3-0.4 (Vladisavljevic *et al.*, 2005). Spontaneous emulsification has been also reported in experiments in which droplet size is smaller than the predicted value by the force or torque balance models or even when no conversion is reached in theoretical dynamic balances (Hao *et al.*, 2008). Spontaneous mechanism can be coupled with shear-based in the same membrane, resulting in larger droplets (Christov *et al.*, 2002).

Emulsification membrane under shear and non-shear conditions (Kukizaki and Goto, 2009) has been studied using SPG membranes. It was observed that monodisperse emulsions were obtained without shear. This might be related to the mass transfer of surfactant to the droplet, as it has been demonstrated in models based on mass transfer (Rayner *et al.*, 2004; Rayner *et al.*, 2005). Spontaneous emulsification has been modelled using the force balance (Danov *et al.*, 2007; Christov *et al.*, 2008).

### **1.3.2. Premix emulsification**

A coarse emulsion is previously prepared by conventional methods (*i.e.* rotor-stator homogenizer, colloid mill) and then it is forced through the pores of a

membrane, as shown in Fig. 6. This refinement step can be repeated several times, and after several cycles the droplet size cannot be further decreased (Vladisavljevic *et al.* 2004).

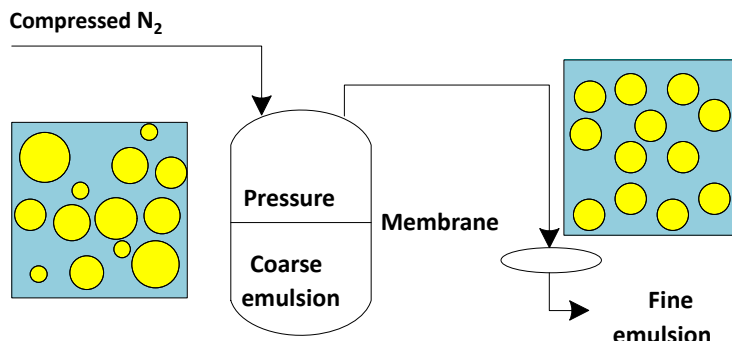


*Fig. 6. Schematic diagram of premix emulsification*

In this case the membrane determines droplet size, but it is not as critical as in direct emulsification and the final droplet size does not depend so much on operating parameters. The main disadvantage is that first conventional emulsification step can alter organic shear-sensitive molecules.

Premix devices have been described in several studies (Nazir *et al.*, 2010) and their performance differs slightly from conventional direct ME. Emulsions stabilized with macromolecules have been produced by premix membrane emulsification with organic (Trentin *et al.*, 2009; Rossier-Miranda *et al.*, 2010; Trentin *et al.*, 2010; Trentin *et al.*, 2011), SPG (Vladisavljevic *et al.*, 2004; Vladisavljevic *et al.*, 2006b; Surh *et al.*, 2008) and metallic (Nazir *et al.*, 2011) membranes. Premix emulsification is widely used nowadays for the preparation of microcapsules (Sawalha *et al.*, 2008; Yang *et al.*, 2010, Ramakrishnan *et al.*, 2012; Ramakrishnan *et al.* 2013).

## **OBJECTIVES**

In this work, membrane emulsification, mechanical agitation and vacuum evaporation have been used individually or in combined form to prepare simple and double emulsions containing bioactive compounds (*i.e.* lutein and resveratrol). The following specific objectives have been pursued:

- Preparation of oil-in-water (O/W) emulsions by membrane emulsification (ME) using common ceramic microfiltration (MF) membranes. Influence of operation parameters on droplet size distribution, determination of droplet formation mechanism and optimal operation conditions.
- Preparation of double Pickering emulsions stabilized by starch granules isolated from Quinoa and modified with octenyl succinic acid (OSA). Study of the encapsulation stability and the effect of lipophilic emulsifier content and salt concentration in the inner aqueous phase.
- Formulation of food-grade water-in-oil-in-water ( $W_1/O/W_2$ ) double emulsions to encapsulate trans-resveratrol, and preparation by mechanical agitation and membrane emulsification (ME).
- Formulation and preparation of emulsions with high proportion of internal phase, containing lutein (a lipophilic antioxidant), combining mechanical agitation or ME with vacuum evaporation.

# **RESULTS**

## I. Emulsification with microfiltration ceramic membranes: a different approach to droplet formation mechanism

Because of the high cost of some membranes used in membrane emulsification processes, such as *Shirasou Porous Glass* (SPG), the possibility of using microfiltration ceramic membranes was considered. The main disadvantage of this type of membranes is that the pore size distribution is not so well controlled. Membrane emulsification was carried out using flat membranes in a 1 liter stirred tank. Subsequently, experiments were performed at larger scale (5 liters) using tubular membranes in a continuous system. Furthermore, the droplet formation mechanism was observed in both systems and the obtained results were compared.

**Article 1. M. Matos, M.A. Suárez, G. Gutiérrez, J. Coca and C. Pazos.** "Emulsification with microfiltration ceramic membranes: a different approach to droplet formation mechanism".

**Journal of Membrane Science** 444 (2013) 345-358.

### **Personal contribution to work**

This work was undertaken with Dr. Miguel Ángel Suárez. Information was gathered regarding the *state of the art* and the droplet formation mechanisms reported in the literature. I also conducted flat ceramic membranes experiments, wrote most of the manuscript and drew the figures.

## I. Emulsificación con membranas cerámicas de microfiltración: una visión diferente del mecanismo de formación de gota

El elevado coste de las membranas más comúnmente utilizadas en procesos de emulsificación, caso de las membranas *Shirasou Porous Glass* (SPG), nos hizo plantearnos la posibilidad de utilizar membranas cerámicas de microfiltración con el mismo propósito. La principal desventaja de este tipo de membranas es que su distribución de tamaños de poro no es tan estrecha. Para ello, programamos diversos experimentos, empleando membranas planas en un tanque agitado de 1 litro de capacidad. A continuación, realizamos experimentos a mayor escala (5 litros) empleando membranas tubulares en un sistema que operaba en continuo. Adicionalmente, estudiamos el mecanismo de formación de gota en ambos dispositivos y comparamos los resultados obtenidos.

**Artículo 1. M. Matos**, M.A. Suárez, G. Gutiérrez, J. Coca y C. Pazos.  
“Emulsification with microfiltration ceramic membranes: a different approach to droplet formation mechanism”.

**Journal of Membrane Science** 444 (2013) 345-358.

### Aportación personal al trabajo

Durante su desarrollo, compartí con mi compañero Miguel Ángel Suárez la tarea de recopilar la información acerca del estado del arte y sobre los diferentes mecanismos de formación de gota descritos en la bibliografía. Asimismo, llevé a cabo los experimentos realizados con membranas cerámicas planas, redacté la mayor parte del manuscrito y elaboré las figuras que lo acompañan.



## Emulsification with microfiltration ceramic membranes: A different approach to droplet formation mechanism

M. Matos, M.A. Suárez, G. Gutiérrez, J. Coca, C. Pazos\*

Department of Chemical and Environmental Engineering, University of Oviedo, C/Julián Clavería 8, 33006 Oviedo, Spain



### ARTICLE INFO

#### Article history:

Received 1 April 2013

Received in revised form

17 May 2013

Accepted 18 May 2013

Available online 27 May 2013

#### Keywords:

Membrane emulsification

Microfiltration ceramic membranes

Spontaneous emulsification

Membrane pore activation

### ABSTRACT

Oil-in-water (O/W) emulsions were prepared by membrane emulsification (ME) in a large scale stirred tank with a submerged cell using flat membranes, and in a cross-flow tubular unit. Results obtained with flat and tubular membranes devices were compared. Common ceramic microfiltration (MF) membranes ( $ZrO_2$  supported on  $TiO_2$ ) were used in both cases. The main advantage of these membranes is their low cost compared to others frequently used in ME (SPG membranes), which implies a reduction up to 60%. The effect of operation parameters on droplet size distributions was studied to understand the droplet formation mechanism that takes place in both devices.

Monodisperse O/W emulsions were obtained using flat membranes with a droplet-to-pore diameter ratio ( $D_d/D_p$ ) in the range 2.1–2.9. Span values of 0.58, 0.66 and 0.81 corresponded to membrane pore diameters of 0.45, 0.80, and 1.4  $\mu m$ , respectively, being the active pores fraction in the range of 27–36%. The cross-flow tubular unit allowed for production of monodisperse O/W emulsions but with larger droplet sizes, having droplet-to-pore diameter ratios ( $D_d/D_p$ ) in the range 3.9–4.7. It was observed a major influence of pore activation by dispersed phase pressure on droplet size distribution.

Shear stress had little influence on the droplet size, with both flat and tubular membranes. This suggested that droplet formation mechanism was not shear stress-based. A spontaneous emulsification mechanism was proposed.

© 2013 Elsevier B.V. All rights reserved.

### 1. Introduction

Producing emulsions by dispersion of a liquid into another immiscible liquid is an area of interest in pharmaceutical, chemical, cosmetic and food industries. Current industrial emulsification processes, such as high pressure homogenizers, rotor stator devices (e.g., colloid mills), and static mixers techniques, can produce small droplets but with a high strain on the liquids, causing activity loss in compounds. Furthermore, droplet size is difficult to control and, therefore, usually polydisperse emulsions are obtained. In membrane emulsification (ME) the strain on the liquid phases is reduced, and droplet size can be narrowly distributed with less shear stress and energy consumption [1–6]. Although ME is technically simpler and needs less surfactant, the production of highly monodisperse emulsions requires the use of membranes with well-controlled pore size distribution [7].

Techniques for ME may be classified into two groups [8,9]: (1) Direct ME: The dispersed phase is injected through the membrane into the continuous phase; (2) Premix ME: A coarse emulsion is pressed through the membrane to reduce the droplet size.

Membranes frequently used in ME processes have been manufactured specifically for this purpose, such as, Shirasu Porous

Glass (SPG) membranes, which have a narrow pore size distribution [10–12]. The most common processes involve cross-flow systems where the shear stress required for the droplet detachment is induced by the continuous phase flow, although rotating devices can also be used [13].

There have been several studies using tubular, microporous membranes made of SPG,  $\alpha-Al_2O_3$  or  $ZrO_2$  [2,3,14–21]. Some of them used asymmetric, tubular-ME membranes [2,3,14,19–21], which are more cost-effective and easier available than the SPG membranes. In these studies, the performance of ME was investigated with changes in the operation and composition parameters [2,3,14–21]. Several studies about the potential ME applications in producing high-value products were also performed [22–28].

Flat ceramic membranes have been used for ME with cross-flow systems [29–31]. In commercial cells with flat-disc metallic membranes, the shear stress required for the droplet detachment was provided by a simple paddle-impeller that was rotating over the membrane [1,32–35].

The effect of ME process parameters on droplet formation has been evaluated by relating them to the forces acting on the system [6,16,32,36,37]. Several mathematical models have been developed to explain ME performance. The simplest ones were based either on a force balance [6,14,16,20,32,38] or a torque balance [16,36,37]. More complex models were also developed by using the Navier-Stokes equation and computational fluid dynamics [38–40], while others were based on dynamic diffusion [41,42].

\* Corresponding author. Tel.: +34 985103509; fax: +34 985103434.

E-mail address: [cpazos@uniovi.es](mailto:cpazos@uniovi.es) (C. Pazos).

In this work, we investigated the performance of commercially available microfiltration (MF) flat-disc ceramic membranes in a tailor-made emulsification cell. Several membrane pore diameters were selected for batch emulsification in a high-capacity stirred tank.

The effect of operation parameters such as impeller rotational speed, transmembrane pressure, continuous phase viscosity and geometric parameters on droplet size distribution was studied to determine the optimal operation conditions. The stability of the emulsions obtained by the ME and conventional agitation was monitored and compared.

Experimental results were compared with predicted values by a droplet size estimation model and with the force balance, to understand the emulsification performance and droplet formation mechanism. Experiments were also carried out using a cross-flow emulsification equipment with the MF tubular ceramic membranes at the same pore diameter, to understand the actual mechanism of the droplet formation in the process.

One advantage of MF membranes for ME is their low cost compared to SPG membranes. The cost of these membranes is around 0.17 €/cm<sup>2</sup> while the estimated cost for conventional MF membranes is around 0.07 €/cm<sup>2</sup>, roughly a reduction of 60%.

## 2. Theoretical background

### 2.1. Pressure and dispersed phase flux

In order to produce droplets, the pressure on the dispersed phase should overcome the interfacial tension to permeate through the membrane pores [43]. The minimum value required is the critical pressure ( $P_c$ ) and may be expressed by

$$P_c = \frac{4\gamma \cos \theta}{D_p} \quad (1)$$

where  $\gamma$  is the interfacial tension,  $\theta$  is the contact angle between the dispersed phase and the membrane surface and  $D_p$  is the nominal membrane pore diameter. The driving force for dispersed phase flow through the pores is the transmembrane pressure ( $\Delta P$ ):

$$\Delta P = P_d - P_0 \quad (2)$$

where  $P_d$  and  $P_0$  are the pressures at the dispersed phase side and at the continuous phase side, respectively. For a flat membrane module  $P_0$  is the pressure on the membrane surface.

It is desirable to have a higher flux rate of dispersed phase for the industrial-scale emulsion production using membranes [15,44]. The dispersed phase flux ( $J_d$ ) increases as the mean pore diameter and/or the transmembrane pressure ( $\Delta P$ ) increases [2,3,12]. The flux,  $J_d$ , is given as a function of  $\Delta P$  by Darcy's law [14]:

$$J_d = \frac{\Delta P}{\mu_d R_m} \quad (3)$$

where  $\mu_d$  is the viscosity of the dispersed phase (Pa s) and  $R_m$  is the intrinsic membrane resistance (m<sup>-1</sup>). It may be experimentally determined by measuring pure water flux at different  $\Delta P$  values since the resistance depends only on membrane characteristics, such as pore size, porosity and tortuosity.

### 2.2. Fraction of membrane active pores

Droplets are produced by only a fraction of membrane pores in the emulsification process using ceramic and SPG membranes. The fraction of active pores determines the flow in every pore and thus the dispersed phase velocity.

There have been several mathematical models for estimating the fraction of active pores ( $K$ ), most of them based on dispersed phase flux data. Vladisavljevic and Schubert developed a simple model

correlating the fraction of active pores ( $K$ ) with the membrane hydraulic resistance ( $R_m$ ) and the dispersed phase flux ( $J_d$ ):

$$K = \frac{J_d \mu_d R_m}{\Delta P} \quad (4)$$

where  $\mu_d$  is the viscosity of the dispersed phase [18].

A similar model was proposed by Lepercq et al. [21] in their study of the droplet coalescence on ceramic membranes. Flow through the membrane is explained in terms of flow through a packed bed using the Carman-Kozeny equation [21]. This model, however, uses a theoretical parameter that does not take into account certain membrane characteristics (e.g., tortuosity) that are related to the hydraulic resistance.

Coalescence of droplets is an undesirable phenomenon in the emulsion process. It takes place on the surface of a ceramic membrane when two droplets are formed very close to each other. The fraction of active pores should be kept below a maximum value to avoid coalescence. Vladisavljevic and Schubert proposed an equation to estimate this maximum fraction [18]. Assuming that the active pores were in a square-array on the membrane surface and that there is no coalescence at the membrane pore openings, the maximum fraction value ( $K_{max}$ ) can be expressed as

$$K_{max} = \left( \frac{\pi}{4\varepsilon} \right) \left( \frac{D_d}{D_p} \right)^{-2} \quad (5)$$

where  $D_d$  is the droplet diameter,  $D_p$  is the pore diameter and  $\varepsilon$  is the membrane porosity.

Droplet formation time ( $t_f$ ) can be calculated with the ratio of the droplet volume ( $V_d$ ) and the volumetric flow rate through a single pore ( $Q_{dp}$ ). This can then be rearranged as shown in the following equation:

$$t_f = \frac{V_d}{Q_{dp}} = \frac{\frac{\pi}{6} D_d^3}{\frac{\pi}{4} D_p^2 \frac{J_d}{K}} = \frac{2\varepsilon K D_d^3}{3 D_p^2 J_d} \quad (6)$$

where  $K$  is the fraction of active pores. The droplet formation time is also affected by the dynamic interfacial tension, and therefore, the type of the emulsifier [14,43].

### 2.3. Shear stress

For an emulsification cell in a stirred tank, droplet detachment is caused by the shear stress. The phenomenon can be modelled well by conventional hydrodynamics [1,32–35]. A liquid moving in a stirred tank may be in a regime of either free or forced vortex [45]. The free vortex regime is influenced by the tank walls. Shear stress decreases in proximity to the wall. The forced vortex regime develops around the rotation axis and, there, the liquid moves as a rigid body. The distance of the boundary between the two regions from the axis is called the *critical radius* ( $r_c$ ). The shear stress expression for the each region can be expressed by Eqs. (7) and (8), in the forced and free vortex regions, respectively [32]:

$$\tau = 0.825(2\pi)^{1.5} \rho_c^{0.5} \mu_c^{0.5} N^{1.5} r \quad (7)$$

$$\tau = 0.825(2\pi)^{1.5} \rho_c^{0.5} \mu_c^{0.5} N^{1.5} r_c^{1.6} r^{0.6} \quad (8)$$

where  $\rho_c$  and  $\mu_c$  are the density and viscosity of the continuous phase, respectively,  $N$  is the impeller rotational speed and  $r$  the distance to the rotation axis. These equations may be applied if droplet diameter is smaller than the boundary layer thickness. It is a modification of Nagata's model [45] using a correction factor of 0.825 based on experimental data obtained with an impeller-to-tank diameter ratio of 0.8 [46].

These expressions for the shear stress differ from the one for tubular membranes ( $\tau$ ), which is based on the pressure drop due to

the continuous phase flow ( $\Delta P_0$ ):

$$\tau = \frac{\Delta P_0 D_m}{4L_m} \quad (9)$$

Furthermore, the shear stress depends on membrane parameters such as the length ( $L_m$ ) and the internal diameter ( $D_m$ ).

#### 2.4. Force balance

Modelling droplet formation in membrane emulsification has been specifically undertaken, and the importance of process parameters in each case has been reported. Intensive work including numerical approaches has been performed for a better understanding of membrane emulsification mechanisms and to predict membrane performance. Although several models based on force balance have been reported, it is not clear how well they fit the data [6,16,38,43]. Most of these models have been developed for tubular membranes operating in cross-flow. To have a better understanding of the forces involved in the process, all forces involved in droplet formation at the membrane surface during the membrane emulsification are listed in Table 1 [16,36,37,43,47].

The drag force,  $F_D$ , is caused by the cross-flowing continuous phase over the membrane surface. It is usually defined by the Stokes equation (Eq. (10)) because droplet formation is assumed to take place within the laminar sub-layer [16]. Depending on the model, this force is expressed either as a function of the velocity or shear stress. In both cases, the wall correction factor  $k_s$  is a key parameter for determining the magnitude of the force [48]. The configuration of the system (tubular or flat) also influences the shear stress.

The interfacial tension force,  $F_\gamma$ , is the adhesion force of the droplet around the edge of the pore opening, being the main retaining force during droplet formation. It depends on interfacial tension ( $\gamma$ ) and pore diameter ( $D_p$ ), as Eq. (11) indicates.

The static pressure difference force,  $F_{ST}$ , corresponds to the pressure difference between the drop and the surrounding continuous phase at the membrane surface. It is determined by the interfacial tension, pore diameter and the ratio of the diameter of the neck, which connects the droplet and the pore, and the droplet diameter. However, this neck diameter is often assumed to be equal to the pore diameter [36] as shown in Eq. (12).

The dynamic lift force,  $F_{DL}$ , results from the asymmetric velocity profile of the continuous phase near the droplet. It depends on shear stress and droplet size (Eq. (13)).

The buoyancy force,  $F_B$ , is caused by the density difference between the two phases and it is affected by the droplet volume (Eq. (14)).

The last force listed in Table 1 is the inertial force, which is associated with a mass of the fluid flowing out from the opening of the pore (Eq. (15)).

The relative magnitude of the forces involved in the process [41,43] changes as the droplet size increases. The size of the droplet grows until the detachment forces ( $F_{ST}$ ,  $F_{DL}$ ,  $F_B$  and  $F_D$ ) exceed the retaining forces. Peng and Williams [16] found that

**Table 1**  
Forces acting on a droplet during membrane emulsification process.

Force	Expression
Drag	$F_D = \frac{3}{2} \pi k_s D_d^2 \tau$ (10)
Interfacial tension	$F_\gamma = \pi \gamma D_p$ (11)
Static pressure	$F_{ST} = \pi T \frac{D_p^2}{D_d}$ (12)
Dynamic lift	$F_{DL} = 0.761 \frac{\tau^{1.5} D_p^{0.5}}{\rho_c}$ (13)
Buoyancy	$F_B = \frac{4}{3} \Delta \rho g D_d^3$ (14)
Inertial	$F_I = \frac{\pi}{4} \rho_d v_d^2 D_p^2$ (15)

their model of the torque balance among drag, buoyancy and interfacial tension forces fit well for the cross-flow velocity in the range 0.1–0.4 m/s. In their work with droplets formed with a 0.45 μm diameter capillary, they reported that buoyancy effects become more important at the droplet size scale of 200 μm. However, for the smallest droplets in the micron scale, the inertial and buoyancy forces are of 9 and 6 orders of magnitude smaller than the drag and interfacial tension forces, respectively [6,47].

A force balance model taking into account only interfacial tension and drag forces has been proposed by Kosvintsev et al., for flat metallic membranes in a commercial stirred tank emulsification unit with a simple paddle impeller. The droplet diameter is given by [30]

$$D_d = \frac{1}{3\tau} \sqrt{\frac{9}{2} \tau^2 D_p^2 + 2 \sqrt{\frac{81}{16} \tau^4 D_p^4 + (\gamma \tau D_p)^2}} \quad (16)$$

In this force balance, the shear stress corresponds to the shear stress produced by the continuous phase flowing on the membrane surface given by Eqs. (7) and (8).

## 3. Experimental

### 3.1. Materials

Emulsions were prepared with a food-grade extra virgin olive oil ( $\mu_d = 51$  mPa s,  $\rho_d = 886$  kg/m<sup>3</sup>, refractive index = 1.4677, at 25 °C, and an acid value lower than 0.8) as dispersed phase. The non-ionic surfactant added to the continuous aqueous phase was Tween® 20 at 2% (w/v) along with a viscosity modifier, medium viscosity sodium carboxymethylcellulose with polymerization degree 1100 (CMCNa), at 0.01–1.0% (w/v), both supplied by Sigma Aldrich (USA).

Commercially available, ceramic MF membranes (Tami Industries, France) at pore diameters of 0.45, 0.80 and 1.4 μm were used. The membrane active layer consists of microporous zirconia ( $ZrO_2$ ) supported on titania ( $TiO_2$ ). The flat-disc membranes (Inside DisRam™) have dimensions of 47 mm diameter and thickness of 2.5 mm, with a diameter of 31.5 mm for the effective area. Tubular membranes (Inside CéRam™) have a 10 mm external diameter, with a length of 20 mm for the effective area and a thickness of 2 mm. Both types of membranes were supplied from TAMI Industries (France).

### 3.2. Methods

#### 3.2.1. Emulsion characterization

Droplet size distributions were determined by laser light scattering with a long bench Mastersizer S (Malvern instruments Ltd., UK). Three replicates were obtained for each emulsion and results were reported as the typical droplet size distribution in microns. The width of the droplet size distribution is expressed in terms of the span, defined according to the following equation:

$$span = \frac{D(v, 0.9) - D(v, 0.1)}{D(v, 0.5)} \quad (17)$$

where  $D(v, 0.5)$ ,  $D(v, 0.1)$  and  $D(v, 0.9)$  are standard percentile readings from the analysis.  $D(v, 0.5)$  is the size in microns at which 50% of the sample is smaller and 50% is larger.  $D(v, 0.1)$  and  $D(v, 0.9)$  are the size of the droplets below 10% and 90%, respectively, of the sample lies.

The emulsion stability was determined with a Turbiscan Lab Expert (Formulaction Co., France) by the static, multiple light scattering (MLS), which consists of sending a light beam through a cylindrical glass cell containing the sample. Emulsions were placed, without dilution, in the test cells and the transmitted and backscattered lights were monitored as a function of time and cell height for 2 days at 30 °C. The profiles

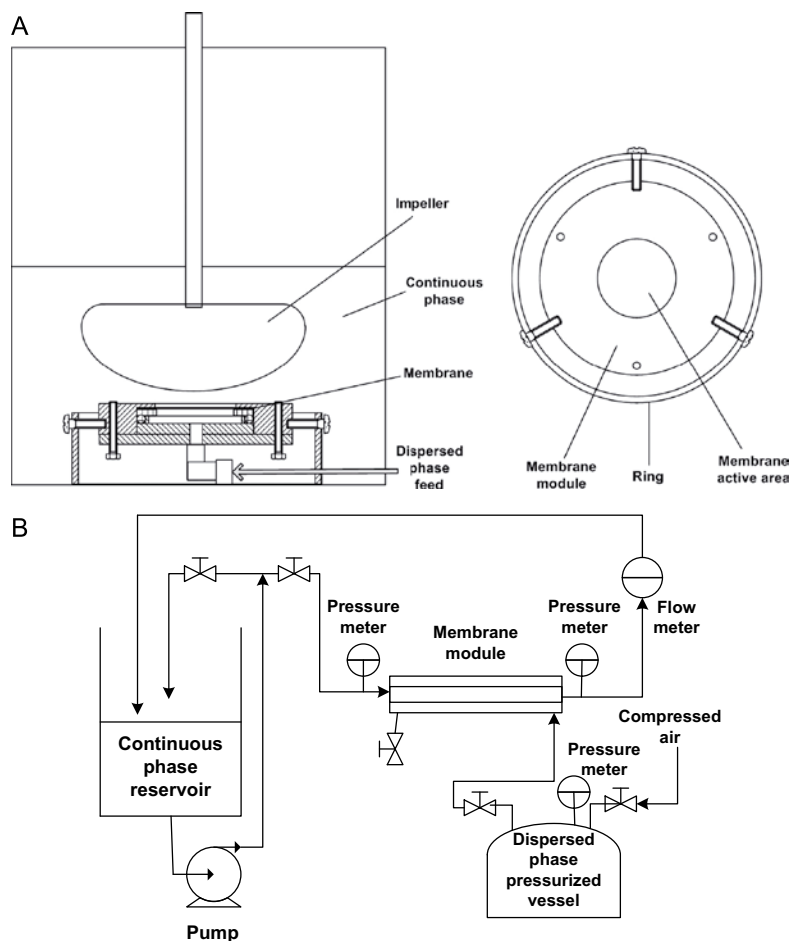


**Fig. 1.** Schematic diagrams of (A) the emulsification cell in a stirred tank [48,49] and (B) the cross-flow emulsification unit.

obtained build up a macroscopic fingerprint of the sample at a given time.

The viscosity of the continuous phase was measured by an Ubbelohde type viscometer PSL-Rheotek (Poulten Selfe & Lee Ltd, UK) at 25 °C.

The flow rate of the dispersed phase was determined by measuring the dry oil matter of the emulsion. Emulsion samples were collected at known time ranges. Samples were placed in porcelain cells, pre-dried at 110 °C and cooled under vacuum to avoid adsorbing moisture. The cells were weighed before and after placing the sample and they were immediately placed in an oven at 110 °C for 24 h. The cells were again weighed and the dry oil matter content in the emulsion was determined. Each sample was measured a minimum of three times.

### 3.2.2. Membrane characterization

The intrinsic resistance of the membrane was determined by measuring the flux of deionized water through it at various transmembrane pressures.

The scanning electron microscopy (SEM) of the membrane cross sections was performed using a MEB JEOL-6100 microscope (Japan).

The Atomic Force Microscopy (AFM) was performed using Nanotec Cervantes System (Nanotec Electrónica S.L., Spain), which was operated in the dynamic mode using Olympus OMCL-RC800PSA Silicon Nitride ( $\text{Si}_3\text{N}_4$ ) point probes ( $k=0.76 \text{ N/m}$ ,  $\omega_0=76 \text{ kHz}$ , UK) at 25 °C.

### 3.2.3. Emulsion preparation

Membrane emulsification experiments were performed using two experimental devices: a flat membrane module, specially designed for our study (Fig. 1A) [48,49] and a cross-flow emulsification device (Fig. 1B).

The flat membrane module was submerged in the continuous phase. The dispersed phase was fed from a pressurized vessel and pushed through the membrane pores into the continuous phase, where a rotating flow was produced by a paddle impeller. Droplets were formed and detached from the membrane surface. The dimensions of the device used in the experiments are described in Table 2. This emulsification device was tailor-made and has been previously used with metallic membranes [48,49].

Emulsion was also prepared by high shear mixing (Silent-Crusher M., rotor model 22 G, Heidolph, Germany) at 10,000 rpm for 5 min in order to compare both techniques.

**Table 2**  
Geometric parameters of the stirred tank emulsification unit.

Geometric parameter	Value (m)
Impeller diameter ( $D_i$ )	0.06–0.09
Tank diameter ( $D_T$ )	0.12
Continuous phase height ( $H$ )	0.09–0.12
Distance from impeller to membrane surface ( $Z$ )	0.005
Membrane active-area diameter ( $D_{mf}$ )	0.0315

For the experiments using the tubular membranes, the dispersed phase was fed from the pressurized vessel and then pushed through the membrane pores into the continuous phase, which was recirculated using a screw pump (PCM, France). The droplets formed on the membrane surface were detached by the movement of the continuous phase.

### 3.2.4. Membrane cleaning

The flat membranes were cleaned at 50 °C in a flat filtration Millipore (France) module at  $\Delta P=100$  kPa, using a basic detergent (P3-Ultrasil-10), supplied by Ecolab (USA), at 0.5 wt%. Cleaning was conducted for 20 min and the membranes were rinsed twice with distilled water at 50 °C after the cleaning step.

The importance of proper membrane cleaning in the membrane emulsification has been previously discussed by researchers. It was reported that sonication in a washing solution provides good results for cleaning of tubular ceramic membranes used for emulsification [2]. However, the active layer was damaged when sonication was applied to the membrane with a basic cleaning solution.

A similar washing procedure was applied to the cross-flow device. First, the tubular membrane was cleaned with water until no turbidity was observed. Then, the membrane was washed with the same basic detergent solution used for the flat membranes. The solution was pumped and recirculated for 30 min. Then the circuit was rinsed with tap water several times. Finally, the membrane was rinsed with distilled water before soaking into the continuous phase.

## 4. Results and discussion

### 4.1. Emulsification with flat ceramic membranes

The first part of the study was to determine the parameters affecting the emulsification process in the designed device, such as transmembrane pressure, impeller rotational speed, continuous phase viscosity and geometric parameters. The mean droplet size in terms of  $D(v,0.5)$  and span values was compared. The effect of membrane pore size was also studied using membranes with 0.45, 0.80, and 1.4 μm pore diameters. The stability of the emulsions was monitored with Turbiscan Lab Expert equipment and compared to the emulsion obtained by conventional mechanical agitation.

#### 4.1.1. Membrane characterization

4.1.1.1. Water flux. Membranes with pore diameters of 0.45, 0.80 and 1.4 μm were characterized by water flux at several transmembrane pressures. Results are shown in Fig. 2. There is a linear relation between  $J_w$  and  $\Delta P$ , with increasing slope as the mean pore diameter increases.

$R_m$  values were determined applying Eq. (3) for individual membranes. The following values were obtained for 0.45, 0.80 and 1.4 μm membranes, respectively:  $1.24 \times 10^{11}$ ,  $1.03 \times 10^{11}$  and  $0.45 \times 10^{11} \text{ m}^{-1}$ .

4.1.1.2. SEM. The length and the shape of the pores are two important parameters in the ME process [50–52]. The microstructure of the cross

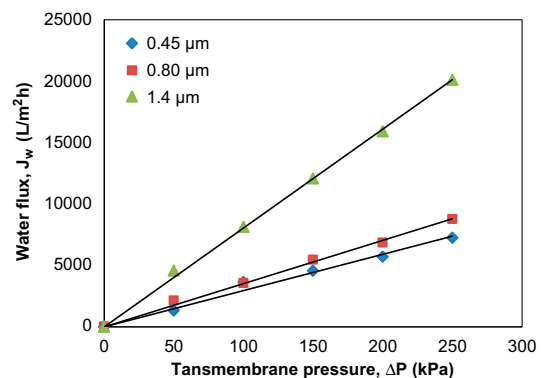


Fig. 2. Influence of transmembrane pressure on water flux through new flat ceramic membranes of different pore diameters.

sections of the dry membranes was studied by scanning electronic microscopy (SEM) in order to learn more about the membranes used in this study.

The images revealed that these types of membranes have two distinct microstructures when they are dried (Fig. 3). The active top layer consists of closely packed nodules. The porous support layer where the packed nodules are interconnected shows a less dense packing than the active layer of the membrane surface. Thus, the thickness of the active layer can be obtained from these images being 80–100 μm for the three membranes analysed.

4.1.1.3. AFM. Images of the membranes were taken using atomic force microscopy (AFM) (Fig. 4) to better characterize their surface micro-morphology.

The AFM images, Fig. 4, show the representative three-dimensional surface morphologies of the 0.45 μm and 0.80 μm pore diameter membranes. The nodules are readily observed along the active layer of the membrane surface according to the SEM images.

#### 4.1.2. Effect of operation parameters

The geometric parameters applied for these experiments were as follows: impeller diameter ( $D_i$ ), 0.09 m, impeller-to-tank diameter ratio ( $D_i/D_T$ ), 0.75, and ratio between the continuous phase height and the tank diameter ( $H/D_T$ ), 0.7, and volume of continuous phase ( $V_c$ ), 1L.

4.1.2.1. Effect of transmembrane pressure. The critical pressure ( $P_c$ ) was calculated with Eq. (1) and the following values were obtained: 28, 16 and 9 kPa for 0.45, 0.80 and 1.4 μm pore diameter membranes, respectively.  $\Delta P$  from Eq. (2) must be higher than the critical pressure in order to produce droplets. In the experimental device used, the pressure on the membrane surface ( $P_0$ ) can be assumed equal to the atmospheric pressure, because the column of liquid above the membrane surface is negligible, as a result of the vortex formation caused by stirring.

Experiments were carried out at different  $\Delta P$  values, from 50 kPa to 200 kPa with 50 kPa step increases. The dispersed phase flux was determined by measuring the dry oil matter content of the resulting emulsions. The fraction of active pores ( $K$ ) was estimated with Eq. (4). Droplet formation time ( $t_f$ ) was calculated with Eq. (6). Parameters for these experiments are listed in Table 3. The impeller rotational speed ( $N$ ) was 400 rpm.

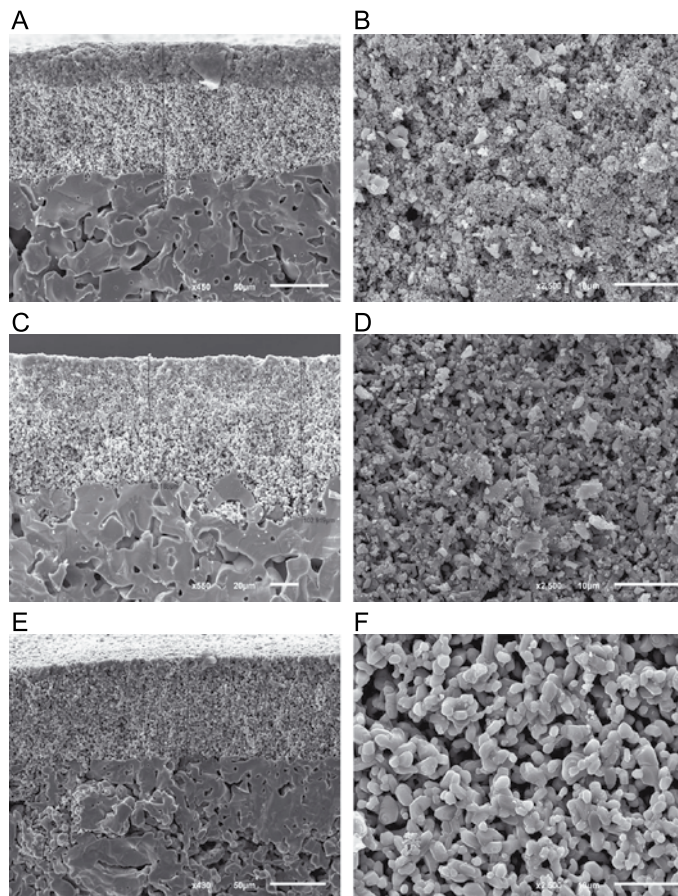


**Fig. 3.** SEM images of a cross-section of the 0.45, 0.80 and 1.4  $\mu\text{m}$  flat ceramic membranes showing: (A),(C),(E) overall microstructure, (B),(D),(F) the active layer.

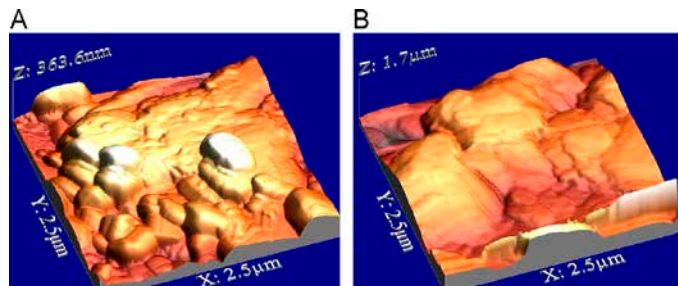


**Fig. 4.** AFM images of 0.45  $\mu\text{m}$  (A) and 0.80  $\mu\text{m}$  (B) flat ceramic membranes at the scan size  $2.5 \mu\text{m} \times 2.5 \mu\text{m}$ .

The mean droplet diameter slightly changes with the dispersed phase flux as shown in Table 3. Normally at higher fluxes the mean droplet size tends to increase because of faster droplet growth and coalescence at the membrane surface [15].

Vladisavljevic et al. [2,3] found that the influence of  $\Delta P$  on the mean droplet size was dependent on the wall shear stress and the  $\Delta P/P_c$  ratio. At high ratios ( $\Delta P/P_c > 4$ ) the shear stress in the continuous phase should be high enough to produce a monodisperse emulsion with a small mean droplet size, while at

$\Delta P/P_c < 2$  the mean droplet size is only slightly affected by the wall shear stress [2].

In the present work, the ratio  $\Delta P/P_c$  was higher than 4 in most of the experiments (3.1–12.5 range) which could explain the slight differences observed in the droplet diameter values given in Table 3.

The fraction of active pores plays, at the same time, an important role in droplet size. Smaller droplets are obtained with higher fluxes because this fraction is higher. In this study, higher  $K$

**Table 3**

Mean droplet diameter, span value, fraction of active pores and droplet formation time, as a function of dispersed phase flux and transmembrane pressure, for emulsions prepared with flat ceramic membranes of different pore diameters in the emulsification cell.  $N=400$  rpm.

$\Delta P$ (kPa)	$J_d$ (L/m <sup>2</sup> h)	$D$ (v,0.5) ( $\mu\text{m}$ )	span value	$K$	$t_f \times 10^2$ (s)
<b><math>D_p=0.45 \mu\text{m}</math></b>					
200	30.8	1.24 ± 0.01	0.58 ± 0.01	0.271	3.97
150	20.5	1.27 ± 0.01	0.78 ± 0.01	0.241	5.69
100	10.3	1.30 ± 0.02	0.77 ± 0.02	0.180	9.15
50	3.85	1.65 ± 0.02	1.93 ± 0.02	0.135	37.4
<b><math>D_p=0.80 \mu\text{m}</math></b>					
200	49.0	1.63 ± 0.03	0.57 ± 0.02	0.357	2.37
150	35.6	1.73 ± 0.01	0.70 ± 0.01	0.346	3.78
100	22.4	1.71 ± 0.01	0.69 ± 0.01	0.327	5.47
50	10.5	1.78 ± 0.01	0.64 ± 0.01	0.306	12.3

values were obtained at higher dispersed phase fluxes, corresponding to the high  $\Delta P$  (200 kPa), as it can be observed in Table 3.

Moreover, the span value is the parameter used to measure the width of the distribution: The narrower the distribution, the smaller the span. Best span values were obtained, with both types of membranes, with higher values of the dispersed phase flux, which agrees to the higher values of  $K$ . Thus, this value of transmembrane pressure (200 kPa) was selected for all subsequent experiments.

The span values obtained are also similar to those previously reported in the literature. Vladisavljevic et al. [2] obtained spans of 0.45 and 0.59 for 0.4 and 0.5  $\mu\text{m}$  pore diameter membranes, respectively, using tubular SPG and  $\text{Al}_2\text{O}_3$  membranes. Williams et al. [17] obtained a span of 0.83 with a 0.5  $\mu\text{m}$   $\alpha\text{-Al}_2\text{O}_3$  pore diameter membrane, and a dispersed phase flux of 8 L/m<sup>2</sup> h. Larger values were reported by Joscelyne and Trägårdh [15] with spans of 1.12–1.51 using tubular ceramic membranes of a mean pore diameter of 0.5  $\mu\text{m}$ , and operating at a dispersed phase flux of approximately 200 kg/m<sup>2</sup> h and 20 kPa of  $\Delta P$ . In this work, best results were obtained at fluxes of 12 L/m<sup>2</sup> h with a span of 0.58 using 0.45  $\mu\text{m}$  pore diameter membrane, and 0.57 for the 0.80  $\mu\text{m}$  pore diameter membrane at 22.01 L/m<sup>2</sup> h of dispersed phase flux.

The maximum fraction of active pores ( $K_{max}$ ) was calculated for 0.45 and 0.80  $\mu\text{m}$  pore diameters membranes, at 200 kPa, with Eq. (5) using the porosity value provided by the manufacturer ( $\epsilon=0.20$ ). Values were 51.9% and 94.4%, respectively. The fractions of active pores (Table 3) were in the range 14–27% for 0.45  $\mu\text{m}$  pore diameter membrane and 31–36% for 0.80  $\mu\text{m}$  pore diameter membrane. Thus no coalescence in principle should take place on the membrane surface. For SPG membranes the percentage of active pores must be lower than 2–25% to ensure that no coalescence occurs at the membrane surface [18]. Vladisavljevic and Schubert obtained monodisperse emulsions with droplets 3.5 times larger than the mean pore diameter, when 2% of the pores were active, at a transmembrane pressure slightly exceeding the capillary pressure and a dispersed phase flux in the 0.7–7 L/m<sup>2</sup> h range.

To estimate droplet formation time, it was assumed that no coalescence occurred at the membrane surface. Under these conditions, the droplet formation time should become shorter with increasing  $\Delta P$ , as it is shown in Table 3. Values obtained are lower compared to those reported by Schröder and Schubert, around 1–1.5 s, using Tween 20 as emulsifier and an  $\text{Al}_2\text{O}_3$  membrane [14]. However, in that case, the emulsifier concentration was significantly lower (0.1 wt%), as well as the  $\Delta P$  (70, 150 kPa) and the fraction of active pores (0.03). This implies a slow reduction of the interfacial tension at the droplet surface requiring longer times for droplet formation. In addition, under the same experimental conditions

**Table 4**

Mean droplet diameter and span value, as a function of impeller rotational speed, angular velocity and shear stress, for emulsions prepared with flat ceramic membranes of different pore diameters in the emulsification cell.  $\Delta P=200$  kPa.

$N$ (rpm)	$\omega$ (rad/s)	$\tau$ (Pa)	$D_p=0.45 \mu\text{m}$		$D_p=0.80 \mu\text{m}$	
			$D(v,0.5)$ ( $\mu\text{m}$ )	span value	$D(v,0.5)$ ( $\mu\text{m}$ )	span value
200	20.94	0.65	1.23 ± 0.01	0.55 ± 0.01	1.63 ± 0.01	0.59 ± 0.02
300	31.42	1.20	1.22 ± 0.01	0.55 ± 0.01	1.64 ± 0.02	0.48 ± 0.01
400	41.89	1.85	1.24 ± 0.01	0.58 ± 0.01	1.63 ± 0.01	0.57 ± 0.01

lower droplet formation times were reported for the same authors (0.04–0.09 s) when 2 wt % SDS was used as emulsifier.

**4.1.2.2. Effect of impeller rotational speed.** Experiments at optimal  $\Delta P$  were conducted for three impeller rotational speeds (200, 300 and 400 rpm), which generate the shear stress on the membrane surface. Shear stresses can be estimated with aforementioned Eqs. (7) and (8) for the experiments carried out in the ME cell. However, in this study the critical radius was always larger than the membrane active-area radius, which means that the experiments were performed in the forced vortex region [45]. Thus, the average shear stress was calculated using Eq. (7). Results are shown in Table 4.

Very low span values were obtained with both types of membranes as appreciated in Table 6. It was also observed that there was no influence on the mean droplet diameter with the shear stress.

The mean droplet size usually decreases sharply as the shear stress increases until a maximum value is reached. Once this maximum is exceeded, the continuous phase velocity has no influence on the droplet size. Schröder and Schubert [14] reported values of 30 and 2 Pa for microporous tubular  $\text{Al}_2\text{O}_3$  membranes with pore diameters of 0.80 and 0.10  $\mu\text{m}$ , respectively. The same authors found that the effect of the wall shear stress on droplet size reduction depended on the membrane pore size, being more effective for membranes with smaller pores. Joscelyne and Trägårdh [15] using 0.50  $\mu\text{m}$   $\alpha\text{-Al}_2\text{O}_3$  tubular membranes found also that the influence was much greater for wall shear stresses below 30 Pa.

Shear stress values shown in Table 6 are in range 0.65–1.85. Therefore, the shear stress required for droplet detachment is quite lower than values reported by other authors using tubular ceramic membranes.

It has also been reported that monodisperse emulsions can be prepared in shearless systems by spontaneous emulsification [53]. This mechanism is different than the conventional shear stress-based. Although it has been mainly observed in microchannel emulsification [51,54–56], it also occurred in membranes with tortuous pores, like SPG [50,53,56,57]. Droplets formed by spontaneous emulsification mechanism are not much affected by shear stress.

**4.1.2.3. Effect of continuous phase viscosity.** According to Eq. (7), the shear stress increases with the impeller rotational speed, but also by increasing the continuous phase viscosity. Experiments were performed varying the viscosity of the continuous phase by raising the concentration of CMCNa to the range 0.01–1% (w/v). Droplet size distributions are plotted as a function of the continuous phase viscosity in Fig. 5. It can be observed that the width of the droplet size distributions gets worse for higher continuous phase viscosities obtaining the best span value at 0.01% (w/v) of CMCNa. Thus, this concentration was considered enough to yield stable monodisperse emulsions.

These results can be explained by the diffusional hindrance of the surfactant [42,58], which might cause coalescence on membrane surface, as the proportion of large droplets increases with increasing viscosity. A similar behaviour was observed for flat metallic membranes in the same stirred tank emulsification unit [48].

**4.1.2.4. Effect of membrane pore diameter.** There is a close connection between the membrane pore diameter of and the emulsion droplet size when using ME. The diameter of the droplets produced is approximately between 2 and 10 times the diameter of the membrane pore and the droplet size increases proportionally to the increase in pore size [6,59]. Thus, the effect of membrane pore diameter was studied after the optimal operation conditions were established, using membranes with 0.45, 0.80, and 1.4 µm pore diameters. Droplet size distributions are shown in Supporting Information Fig. S1, and mean diameters and span values are listed in Table 5.

In addition, 1 L of emulsion was prepared with a rotor-stator homogenizer operating at 10,000 rpm for 5 min in order to analyse the differences in droplet size distributions compared to a conventional method of homogenization.

As observed in Table 5, the relationship between the average droplet diameter of the emulsions ( $D_d$ ), expressed as  $D(v,0.5)$ , and the mean pore diameter of the membranes ( $D_p$ ) corresponds to a  $D_d/D_p$  ratio in the range 2.1–2.9. These results are in good agreement with those reported by Williams et al., who obtained a  $D_d/D_p$  ratio of 2.80–2.83 for  $\alpha\text{-Al}_2\text{O}_3$  membranes with  $D_p=0.2\text{--}0.5\text{ }\mu\text{m}$  [17]. They also agree with results reported by Vladisavljevic et al. using SPG membranes, who obtained span values of 0.45 and 0.30, respectively, for 0.4 and 1.4 µm membrane pore diameters [18]. These authors also determined 0.6–0.7 s droplet formation time values with 0.4–1.4 µm

membrane pore diameters when using SPG membranes, which present a relatively higher porosity value of 0.58. The formation times obtained in this work were lower (0.02–0.05 s) due to the smaller membrane porosity ( $\epsilon=0.20$ ).

They additionally reported that the fraction of active pores ( $K$ ) was higher when comparing  $\alpha\text{-Al}_2\text{O}_3$  membranes (29%) with SPG membranes (8.5%). The maximum fraction of active pores ( $K_{max}$ ) was also higher, due to the smaller porosity of the active layer and the smaller  $D_d/D_p$  ratio for  $\alpha\text{-Al}_2\text{O}_3$  membranes [2].  $K$  values shown in Table 5 were in the range of 27–36% remaining below the maximum values aforementioned under the experimental conditions used in this work.

The emulsion prepared with the rotor-stator homogenizer showed a wide droplet size distribution (Supporting Information Fig. S1) with a mean droplet diameter of 11 µm. The stability of this emulsion was determined from the Turbiscan light backscattering profile obtained for 2 days. It was compared with those obtained for emulsions prepared by ME (Supporting Information Fig. S2).

There was no significant backscattering variation with time for all the emulsions. This is an indication that the droplet size was unchanged and coalescence did not occur, remaining the emulsions stable. This fact can be explained by the formulation of the emulsion, which has more influence in emulsion stability than the droplet size. At the same time, clarification and creaming zones were observed because the oil droplets tended to go to the top of the Turbiscan cell due to their lower density. There was only a slight difference in the clarification layer for the emulsion shown in Supporting Information Fig. S2C which was thicker due to the larger size of the oil droplets.

**4.1.2.5. Effect of geometric parameters.** It was found in previous studies using the same batch emulsification cell with flat metallic membranes, that the droplet size distribution of emulsions was influenced by geometric parameters [49]. Thus, experiments were performed at several geometric ratios to check whether they affected droplet size distributions achieved with the flat ceramic membranes used.

The geometric parameters studied were those used by Suarez et al. [49] for metallic membranes, who determined that the optimal conditions were as follows: impeller diameter,  $D_i=0.06\text{ m}$ , impeller-to-tank diameter ratio,  $D_i/D_T=0.5$  and ratio between the continuous phase height and the tank diameter,  $H/D_T=1.0$ , being the volume of continuous phase 1.4 L. Experiments were performed at 450 rpm and 600 rpm, and results are shown in Fig. 6.

No significant change in droplet size distribution was found for different geometric ratios, using the membranes of 0.45 µm and 0.80 µm pore diameters. This result suggests that droplet size is not affected by the geometric parameters, which are related to shear stress [49]. It is important to remark that under the selected conditions the vortex was different than with geometric dimensions used in previous sections. As a consequence, for the experiments carried out in this study with the flat ceramic membranes the vortex did not affect the droplet size.

#### 4.1.3. Droplet formation mechanism

It has been reported that Eq. (16) is suitable to fit ME data obtained with flat metallic membranes [32,48]. It was selected to predict mean droplet diameters of the emulsions and to compare them with the experimental ones. The shear stress was estimated with Eq. (7), as the membrane lay within the forced vortex region. The predicted mean droplet diameters were compared to the experimental results (Table 6). Predicted values were 7, 5 and 4 times higher than the actual mean droplet diameters, for the flat ceramic membranes with pore diameters of 0.45, 0.80 and 1.4 µm, respectively, with relative errors up to 600%.

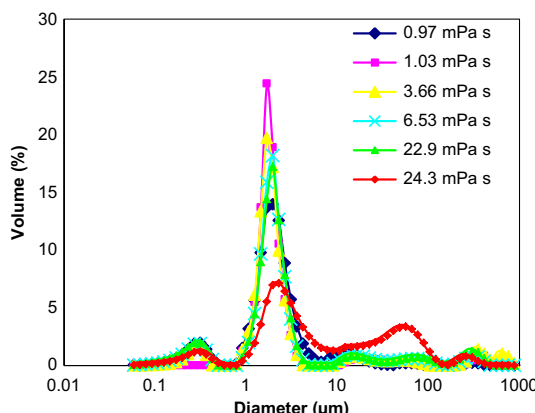


**Fig. 5.** Influence of continuous phase viscosity on droplet size distribution of emulsions prepared with a flat ceramic membrane (0.45 µm pore diameter) in the emulsification cell ( $N=400$  rpm,  $\Delta P=200$  kPa).

**Table 5**

Mean droplet diameter, span value, dispersed phase flux, membrane intrinsic hydraulic resistance, fraction of active pores and droplet formation time for emulsions prepared with flat ceramic membranes of different pore diameters in the emulsification cell.  $\Delta P=200$  kPa,  $\tau=1.85$  Pa.

$D_p$ (µm)	$D(v,0.5)$ (µm)	span value	$J_d$ (L/m <sup>2</sup> h)	$R_m \times 10^{-11}$ (m <sup>-1</sup> )	$K$	$t_f \times 10^2$ (s)
0.45	$1.24 \pm 0.01$	$0.58 \pm 0.01$	30.81	1.24	0.271	3.97
0.80	$1.63 \pm 0.03$	$0.66 \pm 0.02$	49.01	1.03	0.358	2.37
1.40	$4.10 \pm 0.03$	$0.81 \pm 0.02$	113.7	0.45	0.361	5.36

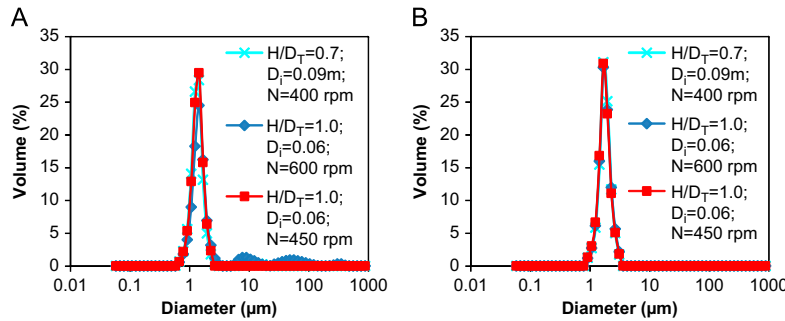


**Fig. 6.** Droplet size distributions of emulsions prepared with flat ceramic membranes of  $0.45\text{ }\mu\text{m}$  (A) and  $0.80\text{ }\mu\text{m}$  (B) pore diameter in the stirred tank emulsification unit with different geometric parameters ( $\Delta P=200\text{ kPa}$ ).

**Table 6**

Mean droplet diameter predicted by Kosvintsev et al. model [32] for emulsions prepared with flat ceramic membranes of different pore diameters in the emulsification cell.  $\gamma=0.0045\text{ N/m}$ ,  $\tau=1.85\text{ Pa}$  and  $\Delta P=200\text{ kPa}$ .

D <sub>p</sub> ( $\mu\text{m}$ )	Predicted D <sub>d</sub> ( $\mu\text{m}$ )	Experimental D <sub>d</sub> ( $\mu\text{m}$ )	Relative error (%)
0.45	8.70	1.24	602
0.80	11.5	2.10	448
1.4	15.3	4.10	273

Rayner compared experimental data obtained for SPG membranes with five different pore sizes to the mean droplet diameters predicted from the force balance model (using  $k_x=1.7$ ) [50]. She concluded that the force balance badly predicted droplet size with relative errors in the range 100–800%.

Rayner also compared these experimental results with the obtaining ones from an innovative model developed to quantify droplet formation in ME. This model involves Gibbs free energy and uses the Surface Evolver General equation (SEG). When the SEG-equation including the mass transfer-expansion ratio (MER) was applied, she obtained much better results in predicting droplet diameter values, as relative errors ranged from 0.4% to 22% and the average value was 9.3%. She concluded that droplets were spontaneously formed without significant effect of the continuous phase cross-flow due to the oblong shape of the SPG membranes pores.

The forces involved in ME, listed in Table 1, were estimated using the experimental data to perform the force balance. These parameters were calculated to determine the droplet formation mechanism that was taking place. These forces were estimated using the average shear stress from Eq. (7), and  $k_x=3$  in Eq. (10), as they had provided the best fit for experimental data in cells immersed in stirred tanks [32,48,49]. Values for these forces are indicated in Table 7.

It can be seen that dynamic lift, buoyancy and inertial forces are much lower than other ones. So, they can be neglected and the force balance expressed as

$$F_D + F_{ST} = F_Y \quad (18)$$

However, from the data in Table 9 it is observed that this force balance does not converge because the drag force is much lower than interfacial tension and static pressure forces. The theoretical value should be  $4.05 \times 10^{-9}\text{ N}$ , which is more than 100 times higher than the experimental value. This result agrees with the difference found in droplet size estimation with Eq. (16) and it suggests that a different mechanism than shear stress should be responsible for droplet detachment. It has been suggested that spontaneous emulsification may explain the behaviour of ME when no force or torque balance is applied [37].

**Table 7**

Forces acting on a droplet (Eqs. (10)–(15)) for emulsions prepared with flat ceramic membranes of different pore diameters in the emulsification cell.  $\gamma=0.0045\text{ N/m}$ ,  $\tau=1.85\text{ Pa}$ ,  $\Delta P=200\text{ kPa}$ .

Force	Membrane pore diameter		
	0.45 $\mu\text{m}$	0.80 $\mu\text{m}$	1.40 $\mu\text{m}$
F <sub>D</sub> (N)	$3.26 \times 10^{-11}$	$9.35 \times 10^{-11}$	$3.56 \times 10^{-10}$
F <sub>r</sub> (N)	$6.36 \times 10^{-9}$	$1.13 \times 10^{-8}$	$1.98 \times 10^{-8}$
F <sub>ST</sub> (N)	$2.31 \times 10^{-9}$	$4.31 \times 10^{-9}$	$6.76 \times 10^{-9}$
F <sub>DL</sub> (N)	$7.17 \times 10^{-14}$	$3.48 \times 10^{-13}$	$2.59 \times 10^{-12}$
F <sub>B</sub> (N)	$4.31 \times 10^{-16}$	$2.09 \times 10^{-15}$	$1.56 \times 10^{-14}$
F <sub>I</sub> (N)	$3.52 \times 10^{-18}$	$1.61 \times 10^{-17}$	$2.61 \times 10^{-16}$

Spontaneous emulsification usually occurs in microchannels with oblong shape [51,54,55] and membranes with tortuous pores [53,56,57]. Consequently, additional experiments were carried out in order to check whether shear stress had no influence in droplet formation. These experiments were performed at very low rotational speed (60 rpm,  $\tau=0.20\text{ Pa}$ ) or even with no agitation, and compared with those aforementioned at 400 rpm. Results are shown in Fig. 7.

Similar values were found for experiments at 60 and 400 rpm with the membrane of  $0.45\text{ }\mu\text{m}$  pore diameter, obtaining mean droplet diameters of  $1.29$  and  $1.24\text{ }\mu\text{m}$  and span values of  $0.60$  and  $0.58$ , respectively. A slight increase in the mean droplet diameter was obtained for the experiment carried out at  $0\text{ rpm}$ , obtaining a mean droplet diameter of  $1.44\text{ }\mu\text{m}$  and a span value of  $1.06$ . No differences were observed for the mean droplet diameters obtained with the  $0.80\text{ }\mu\text{m}$  pore diameter membrane. The mean droplet diameters were  $1.57$ ,  $1.64$  and  $1.63\text{ }\mu\text{m}$ , with span values of  $1.37$ ,  $1.23$  and  $0.57$ , at  $0$ ,  $60$  and  $400\text{ rpm}$ , respectively. This suggests that droplets were not formed by a shear stress-based mechanism.

In order to get an additional confirmation of the droplet formation mechanism, experiments were carried out with tubular ceramic membranes.

#### 4.2. Emulsification with tubular ceramic membranes

##### 4.2.1. Membrane characterization

4.2.1.1. Water flux. Specific membrane resistances,  $R_m$ , were determined from  $J_w$  vs.  $\Delta P$  data for deionized water. The following values were obtained for membranes of  $0.45$ ,  $0.80$  and  $1.4\text{ }\mu\text{m}$ , respectively:  $5.94 \times 10^{10}$ ,  $6.74 \times 10^{10}$ ,  $3.90 \times 10^{10}\text{ m}^{-1}$ .

The  $R_m$  values for tubular membranes are between 1.2 and 2.1 times smaller than the corresponding values for flat membranes.

**4.2.1.2. SEM.** The SEM images shown in Fig. 8 reveal that tubular membranes have a similar structure to the one observed with flat membranes.

However, the thickness of the active layer is smaller being 60  $\mu\text{m}$  for membranes of 0.45  $\mu\text{m}$  and 0.80  $\mu\text{m}$  pore diameters, and 80  $\mu\text{m}$  for membranes of 1.4  $\mu\text{m}$  pore diameter.

#### 4.2.2. Effect of operation parameters

ME experiments were performed in the cross-flow equipment shown in Fig. 2, and results were compared with those obtained with flat membranes.

**4.2.2.1. Effect of continuous phase flow.** The influence of continuous phase flow ( $Q_c$ ) on droplet size distribution at values of 150, 300,

450 and 600 L/h, was studied for 0.45 and 0.80  $\mu\text{m}$  membrane pore diameters. An increase of the cross-flow velocity of the continuous phase raised the pressure drop (Eq. (9)) and the wall shear stress.

As continuous phase pressure ( $P_0$ ) changes with the flow rate, experiments were conducted in two ways: (i) keeping constant the dispersed phase pressure ( $P_d=100 \text{ kPa}$ ), as shown in Fig. 9, and (ii) keeping constant  $\Delta P$  ( $\Delta P=40 \text{ kPa}$ ), as shown in Fig. 10.

For tubular membranes  $\Delta P$  is expressed as

$$\Delta P = \frac{(P_d - P_{01}) + (P_d - P_{02})}{2} \quad (19)$$

As shown in Fig. 9, there is no significant change in droplet size distribution with shear stress, being always higher than 30 Pa

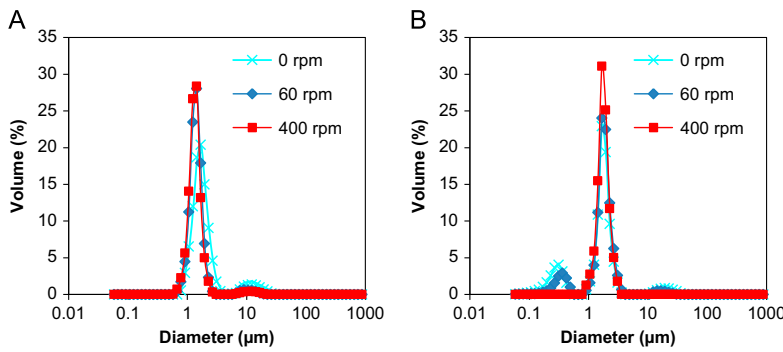


**Fig. 7.** Droplet size distributions of emulsions prepared with flat ceramic membranes of 0.45  $\mu\text{m}$  (A) and 0.80  $\mu\text{m}$  (B) pore diameter in the stirred tank emulsification unit using different impeller rotational speeds ( $\Delta P=200 \text{ kPa}$ ).

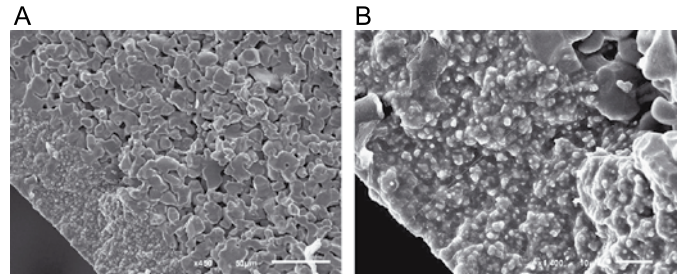


**Fig. 8.** SEM images of a cross-section of the 0.45  $\mu\text{m}$  tubular ceramic membrane showing: (A) overall microstructure and (B) the active layer.

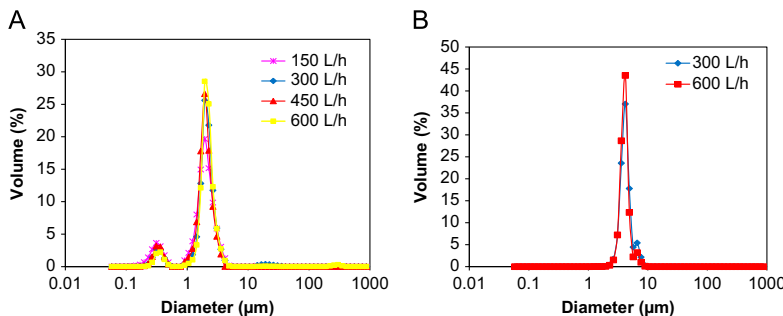


**Fig. 9.** Droplet size distributions of emulsions prepared with tubular ceramic membranes of 0.45  $\mu\text{m}$  (A) and 0.80  $\mu\text{m}$  (B) pore diameter in the cross-flow emulsification unit ( $P_d=100 \text{ kPa}$ ).

[14,15], and as high as 115 Pa.  $\Delta P/P_c$  ratios were in the range 2–4 in most cases and no significant effect of the shear stress was observed, in the range investigated. This is in good agreement with results reported by Vladisavljevic et al. [2,3] and with those obtained with flat membranes.

Table 8 also shows that for the 0.45  $\mu\text{m}$  membrane, spans values were in the range 0.68–1.35, similar to those obtained with flat membranes, and also similar to the results reported by Williams et al. [17] (0.83) and Joscelyne and Trägård [15] (1.12–1.51), although these authors used higher dispersed phase fluxes ( $8 \text{ L/m}^2 \text{ h}$  and  $200 \text{ kg/m}^2 \text{ h}$ ) than those used in this work ( $0.57$ – $1.08 \text{ L/m}^2 \text{ h}$ ).

The fraction of active pores was in the range 1–9%, being lower than the fraction obtained for flat membranes probably due to the higher values of dispersed phase fluxes used in those cases.

Span values for the 0.80  $\mu\text{m}$  membrane were similar to those obtained with flat ceramic membranes (0.48–0.58), and even with SPG membranes, being the droplet formation times in the range of those observed by Vladisavljevic et al. [18] (0.6–0.7 s). It was observed that the fraction of active pores was higher (5–6%) and the span values were significantly lower in comparison with 0.45  $\mu\text{m}$  pore diameter membranes.

Fig. 10 shows that droplet size distributions changed when  $P_d$  and  $Q_c$  were varied, keeping  $\Delta P$  constant. Under these conditions,  $P_d$  was lower for low  $Q_c$  values, resulting in lower fractions of active pores, as it is observed in Table 9.

It was observed that the droplet size distributions were affected by shear stress although the shear stresses were high. However,  $\Delta P/P_c$  was constant and lower than 2, which implied that shear rates slightly affected the resulting droplet diameter [2]. For experiments performed at  $Q_c=150$ – $300 \text{ L/h}$  the mean droplet diameters, given in Table 9, are

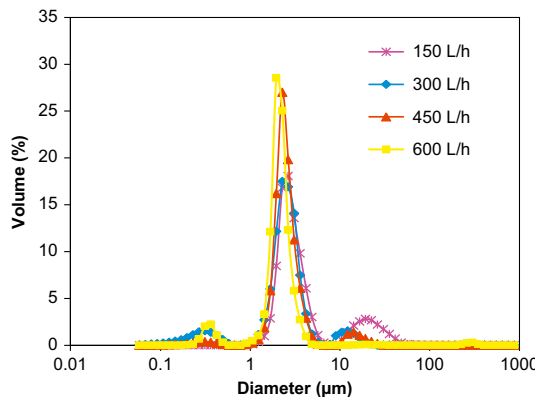


**Fig. 10.** Droplet size distributions of emulsions prepared with a tubular ceramic membrane (0.45  $\mu\text{m}$  pore diameter) in the cross-flow emulsification unit ( $\Delta P=40 \text{ kPa}$ ).

not meaningful. They were altered by a small fraction of large droplets, as Fig. 10 shows, yielding high span values. This can be explained because the fraction of active pores was lower as  $P_d$  decreased and the presence of large droplets increased, having a huge influence on span value. Large droplets yield lower  $K_{max}$  values, according to Eq. (5). Therefore, these droplets might result from droplet coalescence on the membrane surface.

However, when  $Q_c$  was in the range 450–600  $\text{L/h}$ , better span values than those reported by Joscelyne and Trägård [15] (1.12–1.51), who kept  $\Delta P=20 \text{ kPa}$  but with a lower shear stress, were obtained. Most data reported in the literature were acquired keeping  $\Delta P$  constant, but with fractions of active pores higher than those listed in Table 9.

**Table 9**

Mean droplet diameter, span value, dispersed phase flux, dispersed phase pressure and fraction of active pores, as a function of continuous phase flow, axial velocity and shear stress, for emulsions prepared with a tubular ceramic membrane of 0.45  $\mu\text{m}$  pore diameter in the cross-flow emulsification unit.  $\Delta P=40 \text{ kPa}$ .

$Q_c$ ( $\text{L/h}$ )	$v$ ( $\text{m/s}$ )	$\tau$ ( $\text{Pa}$ )	$D(v,0.5)$ ( $\mu\text{m}$ )	span value	$J_d$ ( $\text{L/m}^2 \text{ h}$ )	$P_d$ ( $\text{kPa}$ )	$K$
150	1.47	29	$2.71 \pm 0.13$	$6.1 \pm 2.4$	0.17	20	0.004
300	2.95	38	$2.27 \pm 0.09$	$1.5 \pm 1.5$	0.27	50	0.006
450	4.42	77	$2.23 \pm 0.06$	$0.83 \pm 0.04$	0.43	80	0.009
600	5.89	115	$1.93 \pm 0.01$	$0.68 \pm 0.02$	0.57	100	0.012

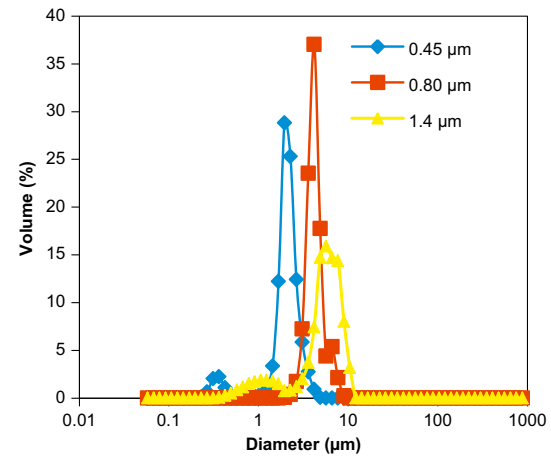


**Fig. 11.** Droplet size distributions of emulsions prepared with tubular ceramic membranes of different pore diameters (0.45, 0.80 and 1.4  $\mu\text{m}$ ) in the cross-flow emulsification unit ( $Q_c=600 \text{ L/h}$ ,  $P_d=100 \text{ kPa}$ ).

**Table 8**

Mean droplet diameter, span value, dispersed phase flux, fraction of active pores and droplet formation time, as a function of the continuous phase flow, axial velocity, shear stress and transmembrane pressure, for emulsions prepared with tubular ceramic membranes of different pore diameters in the cross-flow emulsification unit.  $P_d=100 \text{ kPa}$ .

$D_p$ ( $\mu\text{m}$ )	$Q_c$ ( $\text{L/h}$ )	$v$ ( $\text{m/s}$ )	$\tau$ ( $\text{Pa}$ )	$\Delta P$ ( $\text{kPa}$ )	$D(v,0.5)$ ( $\mu\text{m}$ )	span value	$J_d$ ( $\text{L/m}^2 \text{ h}$ )	$K$	$t_f \times 10^2$ ( $\text{s}$ )
0.45	150	1.47	29	90	$1.75 \pm 0.03$	$1.35 \pm 0.13$	9.62	0.087	11.5
0.45	300	2.95	38	83	$1.90 \pm 0.04$	$0.91 \pm 0.04$	1.08	0.011	16.6
0.45	450	4.42	77	61	$1.78 \pm 0.03$	$1.14 \pm 0.03$	0.80	0.011	18.4
0.45	600	5.89	115	42	$1.93 \pm 0.01$	$0.68 \pm 0.02$	0.57	0.012	35.9
0.80	300	2.95	38	83	$3.85 \pm 0.02$	$0.55 \pm 0.07$	4.34	0.050	49.3
0.80	600	5.89	115	42	$3.75 \pm 0.01$	$0.36 \pm 0.03$	2.61	0.059	89.4

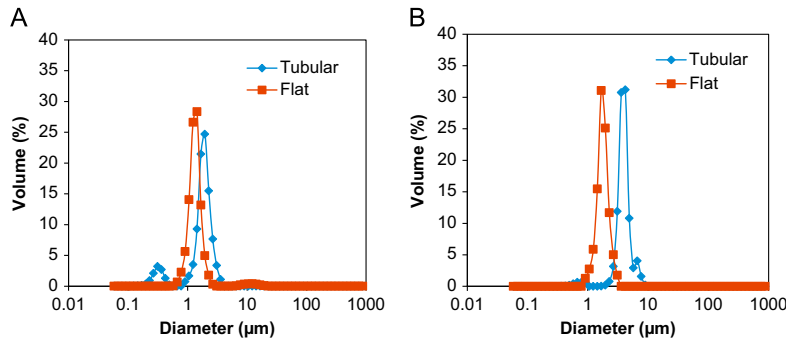


**Fig. 12.** Droplet size distributions of emulsions prepared with tubular and flat ceramic membranes of  $0.45\text{ }\mu\text{m}$  (A) and  $0.80\text{ }\mu\text{m}$  (B) pore diameter in the cross-flow emulsification unit ( $Q_e=600\text{ L/h}$ ), and in the stirred tank emulsification unit ( $N=400\text{ rpm}$ ,  $P_d=200\text{ kPa}$ ).

**4.2.2.2. Effect of membrane pore diameter.** Droplet size distributions of the emulsions prepared with tubular membranes of  $0.45$ ,  $0.80$  and  $1.4\text{ }\mu\text{m}$  pore diameters were measured. They are shown in Fig. 11. As expected, the pore diameter had again an important influence on droplet size although the droplet to pore diameter ratio was higher, being in the range of  $3.9$ – $4.7$ .

However, it was also observed that the  $1.4\text{ }\mu\text{m}$  pore diameter membrane yielded an emulsion with a wider droplet size distribution.

**4.2.2.3. Comparison of flat and tubular ME units.** The performance of both flat and tubular membranes with the same pore diameters ( $0.45\text{ }\mu\text{m}$  and  $0.80\text{ }\mu\text{m}$ ) and dispersed phase pressure ( $200\text{ kPa}$ ) was compared as Fig. 12 shows.

Similar span values were obtained for both membranes and both pore diameters. However, droplet size distributions were different. Larger droplets were obtained with the tubular device, even though the shear stress was extremely high in the cross-flow tubular equipment ( $>100\text{ Pa}$  compared to  $<1\text{ Pa}$ ). These results confirmed the conclusion drawn from Fig. 9 that the droplet formation mechanism was not driven by shear stress.

Droplets were likely formed by a spontaneous emulsification mechanism. This mechanism was previously reported for SPG membranes [53,56,57], which have tortuous pores, and for microchannels with oblong shape [54]. The main advantage of this mechanism is the low span values. SEM images, Figs. 3 and 8, reveal that the internal structure of the membranes possesses tortuous pores.

The pores on the membrane surface have a complex structure, as shown in Fig. 4, and their shape is not circular. These characteristics support the fact that droplets could be formed by spontaneous emulsification.

Besides their shapes, flat and tubular membranes differed in membrane resistances and thicknesses of active and support layers. Geometric dimensions have been reported to affect spontaneous droplet formation in microchannels [51,52]. Thus, the internal membrane morphology might also affect droplet formation in ceramic membranes and it could explain the differences observed in the mean droplet diameters for both types of membranes.

Moreover, considerable differences in the fraction of active pores were observed, being significantly higher for flat membranes, yielding smaller droplets. Therefore, the droplet size could also be affected by the fraction of active pores.

## 5. Conclusions

- Good results were obtained with very low span values when stable monodisperse O/W emulsions were prepared using

commercial available microfiltration flat and tubular ceramic membranes. The main advantage of these membranes is their low cost compared to others commonly used in membrane emulsification, as SPG membranes.

- Typical operation ME parameters had slight influence on mean droplet diameter and size distribution, what suggested that the droplet formation mechanism was not shear stress-based. Therefore, spontaneous emulsification was proposed for both types of membranes as droplet formation mechanism.
- Droplet size differences observed with both types of membranes were related to pore activation which was influenced by dispersed phase pressure. These differences seemed to be also related to membrane intrinsic parameters, as a result of different thicknesses of the support and active layers.

## Acknowledgements

This work was supported by the MICINN, Spain, under the grant CTQ2007-65348 and CTQ2010-20009-C02-01. M. Matos acknowledges receipt of a graduate fellowship from FPI Program (MECD, Spain). M.A. Suárez acknowledges receipt of a graduate fellowship from FPU Program (MECD, Spain), co-funded by European Social Fund. This study was co-financed by the Consejería de Educación y Ciencia del Principado de Asturias (PCTI Asturias 2006-2009, Ref. EQP06-024). The authors thank Profs. Kyung Kang (University of Louisville, KY) and Morris Schoenberg (University of Wisconsin, WI) for fruitful discussions.

## Appendix A. Supporting information

Supplementary data associated with this article can be found in the online version at <http://dx.doi.org/10.1016/j.memsci.2013.05.033>.

### Nomenclature

$D_d$	droplet diameter ( $\mu\text{m}$ )
$D_i$	impeller diameter ( $\mu\text{m}$ )
$D_m$	internal diameter of the tubular membrane (m)
$D_{mf}$	flat membrane active-area diameter (m)
$D_p$	membrane pore diameter ( $\mu\text{m}$ )
$D_T$	tank diameter (m)
$D(v,0.1)$	diameter for which 10% of volume distribution have smaller size ( $\mu\text{m}$ )

$D(v,0.5)$	diameter for which 50% of volume distribution have smaller size ( $\mu\text{m}$ )	[1] E. Egidi, G. Gasparini, R.G. Holdich, G.T. Vladisavljevic, S. Kosvintsev, Membrane emulsification using membranes of regular pore spacing: droplet size and uniformity in the presence of surface shear, <i>J. Membr. Sci.</i> 323 (2008) 414–420.
$D(v,0.9)$	diameter for which 90% of volume distribution have smaller size ( $\mu\text{m}$ )	[2] G.T. Vladisavljevic, U. Lambrich, M. Nakajima, H. Schubert, Production of O/W emulsions using SPG membranes, ceramic-aluminium oxide membranes, microfluidizer and a silicon microchannel plate-a comparative study, <i>Colloids Surf. A: Physicochem. Eng. Aspects</i> 232 (2004) 199–207.
$F_B$	buoyancy force (N)	[3] G.T. Vladisavljevic, H. Schubert, Preparation of emulsions with a narrow particle size distribution using microporous $\alpha$ -alumina membranes, <i>J. Dispersion Sci. Technol.</i> 24 (2003) 811–819.
$F_D$	drag force (N)	[4] S.M. Joscelyne, G. Trägård, Membrane emulsification-a literature review, <i>J. Membr. Sci.</i> 169 (2000) 107–117.
$F_{DL}$	dynamic lift force (N)	[5] C. Charcosset, Preparation of emulsions and particles by membrane emulsification for food processing industry, <i>J. Food Eng.</i> 92 (2009) 241–249.
$F_i$	inertial force (N)	[6] M. Rayner, G. Trägård, Membrane emulsification modelling: how can we get from characterisation to design? <i>Desalination</i> 145 (2002) 165–172.
$F_{ST}$	static pressure force (N)	[7] M. Nakajima, M.A. Neves, I. Kobayashi, Novel Microchannel Emulsification Technology for Monodisperse Emulsions, WCCEB Program Book, 516e, 2009.
$F_\gamma$	interfacial tension force (N)	[8] U. Lambrich, H. Schubert, Emulsification using microporous systems, <i>J. Membr. Sci.</i> 257 (2005) 76–84.
$g$	gravity constant (9.81 $\text{m/s}^2$ )	[9] M.A. Suárez, J. Coca, C. Pazos, Membrane emulsification: factors influencing the size and distribution of the drops, <i>Ing. Quim.</i> 505 (2012) 58–73.
$H$	continuous phase height (m)	[10] T Nakashima, M. Shimizu, M. Kukizaki, Membrane emulsification by micro-porous glass, <i>Key Eng. Mater.</i> 61&62 (1991) 513–516.
$J$	flux ( $\text{m}^3/\text{m}^2\text{s}$ )	[11] T Nakashima, M. Shimizu, M. Kukizaki, Particle control of emulsion by membrane emulsification and its applications, <i>Adv. Drug Delivery Rev.</i> 45 (2000) 47–56.
$k_x$	wall correction factor for a simple sphere touching an impermeable wall	[12] R. Katoh, Y. Asano, A. Furuya, K. Sotoya, M. Tomita, Preparation of food emulsions using a membrane emulsification system, <i>J. Membr. Sci.</i> 113 (1996) 131–135.
$K$	fraction of membrane active pores	[13] A.K. Pawlik, I.T. Norton, Encapsulation stability of duplex emulsions prepared with SPG cross-flow membrane, SPG rotating membrane and rotor-stator techniques-A comparison, <i>J. Membr. Sci.</i> 415–416 (2012) 459–468.
$K_{max}$	maximum fraction of membrane active pores	[14] V. Schröder, H. Schubert, Production of emulsions using microporous ceramic membranes, <i>Colloids Surf. A: Physicochem. Eng. Aspects</i> 152 (1999) 103–109.
$L_m$	tubular membrane length (m)	[15] S.M. Joscelyne, G. Trägård, Food emulsions using membrane emulsification: conditions for producing small droplets, <i>J. Food Eng.</i> 39 (1999) 59–64.
$N$	impeller rotational speed (rps)	[16] S.J. Peng, R.A. Williams, Controlled production of emulsions using a crossflow membrane: Part I: droplet formation from a single pore, <i>Chem. Eng. Res. Des.</i> 76 (1998) 894–901.
$P_c$	capillary pressure (Pa)	[17] R.A. Williams, S.J. Peng, D.A. Wheeler, N.C. Morley, D. Taylor, M. Whalley, D. W. Houldsworth, Controlled production of emulsions using a crossflow membrane. Part II: industrial scale manufacture, <i>Chem. Eng. Res. Des.</i> 76 (1998) 902–910.
$P_d$	dispersed phase pressure (Pa)	[18] G.T. Vladisavljevic, H. Schubert, Preparation and analysis of oil-in-water emulsions with narrow droplet size distribution using Shirasu-porous glass (SPG) membranes, <i>Desalination</i> 144 (2002) 167–172.
$P_0$	continuous phase pressure on the membrane surface (Pa)	[19] Q. Yuan, R.A. Williams, N. Aryanti, Innovations in high throughput manufacturing of uniform emulsions and capsules, <i>Adv. Powder Technol.</i> 21 (2010) 599–608.
$Q_{dp}$	dispersed phase flow in a pore ( $\text{m}^3/\text{s}$ )	[20] E. Lepercq-Bost, M.L. Giorgi, A. Isambert, C. Arnaud, Use of the capillary number for the prediction of droplet size in membrane emulsification, <i>J. Membr. Sci.</i> 314 (2008) 76–89.
$r$	distance to the rotation axis (m)	[21] E. Lepercq-Bost, M.L. Giorgi, A. Isambert, C. Arnaud, Estimating the risk of coalescence in membrane emulsification, <i>J. Membr. Sci.</i> 357 (2010) 36–46.
$r_c$	critical radius (m)	[22] I. Limayem Blouza, C. Charcosset, S. Sfar, H. Fessi, Preparation and characterization of spironolactone-loaded nanocapsules for paediatric use, <i>Int. J. Pharm.</i> 325 (2006) 124–131.
$R_m$	membrane intrinsic hydraulic resistance ( $\text{m}^{-1}$ )	[23] M. Ebrahimi, G. Lavi, T. Schmidts, F. Runkel, P. Czermak, Development and production of oil-in-water vehicles-sub-micron emulsion using tubular ceramic membranes, <i>Desalination</i> 224 (2008) 40–45.
$t$	time (s)	[24] J.S. de los Reyes, C. Charcosset, Preparation of water-in-oil and ethanol-in-oil emulsions by membrane emulsification, <i>Fuel</i> 89 (2010) 3482–3488.
$t_f$	droplet formation time (s)	[25] C. Charcosset, H. Fessi, Preparation of nanoparticles with a membrane contactor, <i>J. Membr. Sci.</i> 266 (2006) 115–120.
$v$	axial velocity ( $\text{m/s}$ )	[26] N. Sheibat-Othman, T. Burne, C. Charcosset, H. Fessi, Preparation of pH-sensitive particles by membrane contactor, <i>Colloids Surf. A: Physicochem. Eng. Aspects</i> 315 (1–3) (2008) 13–22.
$v_d$	dispersed phase velocity ( $\text{m/s}$ )	[27] R. Mazzei, E. Drioli, L. Giorno, Biocatalytic membrane reactor and membrane emulsification concept combined in a single unit to assist production and separation of water unstable reaction products, <i>J. Membr. Sci.</i> 352 (1–2) (2010) 166–172.
$V$	volume ( $\text{m}^3$ )	[28] L. Giorno, E. D'Amore, R. Mazzei, E. Piacentini, J. Zhang, E. Drioli, R. Cassano, N. Picci, An innovative approach to improve the performance of a two separate phase enzyme membrane reactor by immobilizing lipase in presence of emulsion, <i>J. Membr. Sci.</i> 295 (1–2) (2007) 95–101.
$Z$	distance from impeller to membrane surface (m)	[29] N.A. Wagdare, A.T.M. Marcelis, O. Boen, Ho, R.M. Boom, C.J.M. van Rijn, High throughput vegetable oil-in-water emulsification with a high porosity micro-engineered membrane, <i>J. Membr. Sci.</i> 347 (2010) 1–7.
<b>Greek letters</b>		
$\gamma$	interfacial tension ( $\text{N/m}$ )	[30] M.J. Geerken, R.G.H. Lammerink, M. Wessling, Interfacial aspects of water drop formation at micro-engineered orifices, <i>J. Colloid Interface Sci.</i> 312 (2007) 460–469.
$\epsilon$	membrane porosity	[31] A.J. Gijssbertsen-Abrahams, A. van der Padt, R.M. Boom, Influence of membrane morphology on pore activation in membrane emulsification, <i>J. Membr. Sci.</i> 217 (2003) 141–150.
$\Delta\rho$	density difference between dispersed and continuous phases ( $\text{kg/m}^3$ )	[32] S.R. Kosvintsev, G. Gasparini, R.G. Holdich, I.W. Cumming, M.T. Stillwell, Liquid-liquid membrane dispersion in a stirred cell with and without controlled shear, <i>Ind. Eng. Chem. Res.</i> 44 (2005) 9323–9330.
$\Delta P$	transmembrane pressure (Pa)	[33] S.R. Kosvintsev, G. Gasparini, R.G. Holdich, Membrane emulsification: droplet size and uniformity in the absence of surface shear, <i>J. Membr. Sci.</i> 313 (2008) 182–189.
$\theta$	contact angle ( $^\circ$ )	
$\mu$	dynamic viscosity ( $\text{Pa s}$ )	
$\rho$	density ( $\text{kg/m}^3$ )	
$\tau$	shear stress (Pa)	
$\omega$	angular velocity (rad/s)	
<b>Subscripts</b>		
c	continuous phase	
d	dispersed phase/droplet	
m	membrane	
p	pore	
w	pure water	

## References

- E. Egidi, G. Gasparini, R.G. Holdich, G.T. Vladisavljevic, S. Kosvintsev, Membrane emulsification using membranes of regular pore spacing: droplet size and uniformity in the presence of surface shear, *J. Membr. Sci.* 323 (2008) 414–420.
- G.T. Vladisavljevic, U. Lambrich, M. Nakajima, H. Schubert, Production of O/W emulsions using SPG membranes, ceramic-aluminium oxide membranes, microfluidizer and a silicon microchannel plate-a comparative study, *Colloids Surf. A: Physicochem. Eng. Aspects* 232 (2004) 199–207.
- G.T. Vladisavljevic, H. Schubert, Preparation of emulsions with a narrow particle size distribution using microporous  $\alpha$ -alumina membranes, *J. Dispersion Sci. Technol.* 24 (2003) 811–819.
- S.M. Joscelyne, G. Trägård, Membrane emulsification-a literature review, *J. Membr. Sci.* 169 (2000) 107–117.
- C. Charcosset, Preparation of emulsions and particles by membrane emulsification for food processing industry, *J. Food Eng.* 92 (2009) 241–249.
- M. Rayner, G. Trägård, Membrane emulsification modelling: how can we get from characterisation to design? *Desalination* 145 (2002) 165–172.
- M. Nakajima, M.A. Neves, I. Kobayashi, Novel Microchannel Emulsification Technology for Monodisperse Emulsions, WCCEB Program Book, 516e, 2009.
- U. Lambrich, H. Schubert, Emulsification using microporous systems, *J. Membr. Sci.* 257 (2005) 76–84.
- M.A. Suárez, J. Coca, C. Pazos, Membrane emulsification: factors influencing the size and distribution of the drops, *Ing. Quim.* 505 (2012) 58–73.
- T Nakashima, M. Shimizu, M. Kukizaki, Membrane emulsification by micro-porous glass, *Key Eng. Mater.* 61&62 (1991) 513–516.
- T Nakashima, M. Shimizu, M. Kukizaki, Particle control of emulsion by membrane emulsification and its applications, *Adv. Drug Delivery Rev.* 45 (2000) 47–56.
- R. Katoh, Y. Asano, A. Furuya, K. Sotoya, M. Tomita, Preparation of food emulsions using a membrane emulsification system, *J. Membr. Sci.* 113 (1996) 131–135.
- A.K. Pawlik, I.T. Norton, Encapsulation stability of duplex emulsions prepared with SPG cross-flow membrane, SPG rotating membrane and rotor-stator techniques-A comparison, *J. Membr. Sci.* 415–416 (2012) 459–468.
- V. Schröder, H. Schubert, Production of emulsions using microporous ceramic membranes, *Colloids Surf. A: Physicochem. Eng. Aspects* 152 (1999) 103–109.
- S.M. Joscelyne, G. Trägård, Food emulsions using membrane emulsification: conditions for producing small droplets, *J. Food Eng.* 39 (1999) 59–64.
- S.J. Peng, R.A. Williams, Controlled production of emulsions using a crossflow membrane: Part I: droplet formation from a single pore, *Chem. Eng. Res. Des.* 76 (1998) 894–901.
- R.A. Williams, S.J. Peng, D.A. Wheeler, N.C. Morley, D. Taylor, M. Whalley, D. W. Houldsworth, Controlled production of emulsions using a crossflow membrane. Part II: industrial scale manufacture, *Chem. Eng. Res. Des.* 76 (1998) 902–910.
- G.T. Vladisavljevic, H. Schubert, Preparation and analysis of oil-in-water emulsions with narrow droplet size distribution using Shirasu-porous glass (SPG) membranes, *Desalination* 144 (2002) 167–172.
- Q. Yuan, R.A. Williams, N. Aryanti, Innovations in high throughput manufacturing of uniform emulsions and capsules, *Adv. Powder Technol.* 21 (2010) 599–608.
- E. Lepercq-Bost, M.L. Giorgi, A. Isambert, C. Arnaud, Use of the capillary number for the prediction of droplet size in membrane emulsification, *J. Membr. Sci.* 314 (2008) 76–89.
- E. Lepercq-Bost, M.L. Giorgi, A. Isambert, C. Arnaud, Estimating the risk of coalescence in membrane emulsification, *J. Membr. Sci.* 357 (2010) 36–46.
- I. Limayem Blouza, C. Charcosset, S. Sfar, H. Fessi, Preparation and characterization of spironolactone-loaded nanocapsules for paediatric use, *Int. J. Pharm.* 325 (2006) 124–131.
- M. Ebrahimi, G. Lavi, T. Schmidts, F. Runkel, P. Czermak, Development and production of oil-in-water vehicles-sub-micron emulsion using tubular ceramic membranes, *Desalination* 224 (2008) 40–45.
- J.S. de los Reyes, C. Charcosset, Preparation of water-in-oil and ethanol-in-oil emulsions by membrane emulsification, *Fuel* 89 (2010) 3482–3488.
- C. Charcosset, H. Fessi, Preparation of nanoparticles with a membrane contactor, *J. Membr. Sci.* 266 (2006) 115–120.
- N. Sheibat-Othman, T. Burne, C. Charcosset, H. Fessi, Preparation of pH-sensitive particles by membrane contactor, *Colloids Surf. A: Physicochem. Eng. Aspects* 315 (1–3) (2008) 13–22.
- R. Mazzei, E. Drioli, L. Giorno, Biocatalytic membrane reactor and membrane emulsification concept combined in a single unit to assist production and separation of water unstable reaction products, *J. Membr. Sci.* 352 (1–2) (2010) 166–172.
- L. Giorno, E. D'Amore, R. Mazzei, E. Piacentini, J. Zhang, E. Drioli, R. Cassano, N. Picci, An innovative approach to improve the performance of a two separate phase enzyme membrane reactor by immobilizing lipase in presence of emulsion, *J. Membr. Sci.* 295 (1–2) (2007) 95–101.
- N.A. Wagdare, A.T.M. Marcelis, O. Boen, Ho, R.M. Boom, C.J.M. van Rijn, High throughput vegetable oil-in-water emulsification with a high porosity micro-engineered membrane, *J. Membr. Sci.* 347 (2010) 1–7.
- M.J. Geerken, R.G.H. Lammerink, M. Wessling, Interfacial aspects of water drop formation at micro-engineered orifices, *J. Colloid Interface Sci.* 312 (2007) 460–469.
- A.J. Gijssbertsen-Abrahams, A. van der Padt, R.M. Boom, Influence of membrane morphology on pore activation in membrane emulsification, *J. Membr. Sci.* 217 (2003) 141–150.
- S.R. Kosvintsev, G. Gasparini, R.G. Holdich, I.W. Cumming, M.T. Stillwell, Liquid-liquid membrane dispersion in a stirred cell with and without controlled shear, *Ind. Eng. Chem. Res.* 44 (2005) 9323–9330.
- S.R. Kosvintsev, G. Gasparini, R.G. Holdich, Membrane emulsification: droplet size and uniformity in the absence of surface shear, *J. Membr. Sci.* 313 (2008) 182–189.

- [34] M.T. Stillwell, R.G. Holdich, S.R. Kosvintsev, G. Gasparini, I.W. Cumming, Stirred cell membrane emulsification and factors influencing dispersion drop size and uniformity, *Ind. Eng. Chem. Res.* 46 (2007) 965–972.
- [35] M.M. Dragosavac, M.N. Sovili, S.R. Kosvintsev, R.G. Holdich, G.T. Vladisavljević, Controlled production of oil-in-water emulsions containing unrefined pumpkin seed oil using stirred cell membrane emulsification, *J. Membr. Sci.* 322 (2008) 178–188.
- [36] J.H. Xu, G.S. Luo, G.C. Chen, J.D. Wang, Experimental and theoretical approaches on droplet formation from a micrometer screen hole, *J. Membr. Sci.* 266 (2005) 121–131.
- [37] D.X. Hao, F.L. Gong, G.H. Hu, Y.J. Zhao, G.P. Lian, G.H. Ma, Z. Su, Controlling factors on droplets uniformity in membrane emulsification: experiment and modelling analysis, *Ind. Eng. Chem. Res.* 47 (2008) 6418–6425.
- [38] G. De Luca, F. Di Maio, A. Di Renzo, E. Drioli, Droplet detachment in cross-flow membrane emulsification: comparison among torque- and force-based models, *Chem. Eng. Process.* 47 (2008) 1150–1158.
- [39] K.D. Danov, D.K. Danova, P.A. Králčevský, Hydrodynamic forces acting on a microscopic emulsion drop growing at a capillary tip in relation to the process of membrane emulsification, *J. Colloid Interface Sci.* 316 (2007) 844–857.
- [40] A. Tingren, G. Trägård, C. Trägård, A model for drop size prediction during cross-flow emulsification, *Chem. Eng. Res. Des.* 88 (2) (2010) 229–238.
- [41] M. Rayner, G. Trägård, C. Trägård, The impact of mass transfer and interfacial tension expansion rate on droplet size in membrane emulsification processes, *Colloids Surf. A: Physicochem. Eng. Aspects* 266 (2005) 1–17.
- [42] M. Rayner, G. Trägård, C. Trägård, P. Dejmek, Using the surface evolver to model droplet formation processes in membrane emulsification, *J. Colloid Interface Sci.* 279 (2004) 175–185.
- [43] V. Schröder, O. Behrend, H. Schubert, Effect of dynamic interfacial tension on the emulsification process using microporous ceramic membranes, *J. Colloid Interface Sci.* 202 (1998) 334–340.
- [44] Q. Yuan, N. Aryanti, G. Gutiérrez, R.A. Williams, Enhancing the throughput of membrane emulsification techniques to manufacture functional particles, *Ind. Eng. Chem. Res.* 48 (2009).
- [45] S. Nagata, *Mixing. Principles and Applications*, John Wiley & Sons Inc., New York, 1975.
- [46] M. Ciofalo, Turbulent flow in closed and free surface unbaffled tanks stirred by radial impellers, *Chem. Eng. Sci.* 51 (14) (1996) 3557–3573.
- [47] G. Trägård, *Fundamentals and Applications in Membrane Emulsification*, NanoMemCourse Italy, 2010.
- [48] M.A. Suárez, G. Gutiérrez, J. Coca, C. Pazos, Stirred tank membrane emulsification using flat metallic membranes: a dimensional analysis, *Chem. Eng. Process.*, 69, 2013, 31–43.
- [49] M.A. Suárez, G. Gutiérrez, J. Coca, C. Pazos, Geometric parameters influencing production of O/W emulsions using flat metallic membranes and scale-up, *J. Membr. Sci.* 430 (2013) 140–149.
- [50] M. Rayner, Manufacturing Method of a Membrane and a Membrane Thereof, for Emulsification, Patent Application No. PCT/SE2007/000490, 2007.
- [51] S. Sugura, M. Nakajima, N. Kumazawa, S. Iwamoto, M. Seki, Characterization of spontaneous transformation-based droplet formation during microchannel emulsification, *J. Phys. Chem. B* 106 (2002) 9405–9409.
- [52] M.L.J. Steegmans, C.G.P.H. Schroën, R.M. Boom, Generalised insights in droplet formation at T-junction through statistical analysis, *Chem. Eng. Sci.* 64 (2009) 3042–3050.
- [53] M. Kukizaki, Shirasi porous glass (SPG) membrane emulsification in the absence of shear flow at the membrane surface: influence of surfactant type and concentration, viscosities of dispersed and continuous phases, and transmembrane pressure, *J. Membr. Sci.* 327 (2009) 234–243.
- [54] I. Kobayashi, S. Mukataka, M. Nakajima, Effect of slot aspect ratio on droplet formation from silicon straight-through microchannels, *J. Colloid Interface Sci.* 279 (2004) 277–280.
- [55] A.A. Maan, K. Schroën, R. Boom, Spontaneous droplet formation techniques for monodisperse emulsions—preparation—perspectives for food applications, *J. Food Eng.* 107 (2011) 334–346.
- [56] M. Yasuno, M. Nakajima, S. Iwamoto, T. Maruyama, S. Sugura, I. Kobayashi, A. Shono, K. Satoh, Visualization and characterization of SPG membrane emulsification, *J. Membr. Sci.* 210 (2002) 29–37.
- [57] N.C. Christov, D.N. Ganchev, N.D. Vassileva, N.D. Denkov, K.D. Danov, P.A. Králčevský, Capillary mechanisms in membrane emulsification: oil-in-water emulsions stabilized by Tween 20 and milk proteins, *Colloids Surf. A: Physicochem. Eng. Aspects* 209 (2002) 83–104.
- [58] Q. Yuan, R.A. Williams, S. Biggs, Surfactant selection for accurate size control of microcapsules using membrane emulsification, *Colloids Surf. A: Physicochem. Eng. Aspects* 347 (2009) 97–103.
- [59] G. Gutiérrez, M. Rayner, P. Dejmek, Production of vegetable oil in milk emulsions using membrane emulsification, *Desalination* 245 (2009) 631–638.

## **Supporting information**

### **Emulsification with microfiltration ceramic membranes: a different approach to droplet formation mechanism**

María Matos, Miguel Suárez, Gemma Gutiérrez, José Coca, Carmen Pazos\*

Department of Chemical and Environmental Engineering, University of Oviedo, Julián Clavería 8, 33006 Oviedo, Spain

\*Corresponding author: Prof. C. Pazos

Tel: +34 985103509;

Fax: +34 985103434

E-mail address: [cpazos@uniovi.es](mailto:cpazos@uniovi.es)

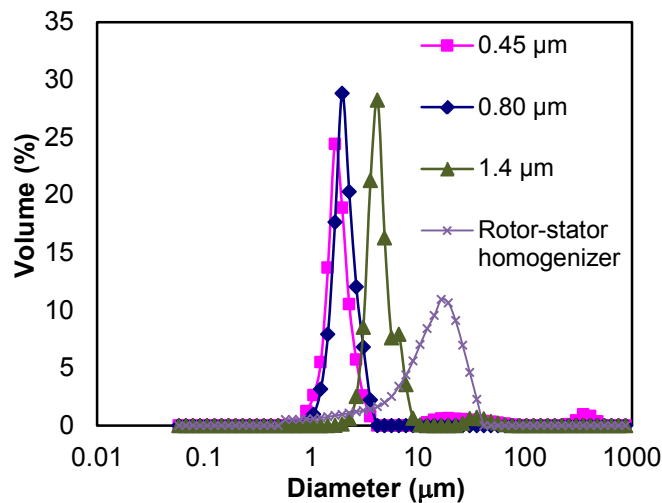


**Figure S1.** Droplet size distributions of emulsions prepared with flat ceramic membranes of different pore diameter (0.45, 0.80 and 1.4  $\mu\text{m}$ ) in the emulsification cell ( $N = 400$  rpm,  $\Delta P = 200$  kPa), and with a rotor-stator homogenizer ( $N = 10,000$  rpm)

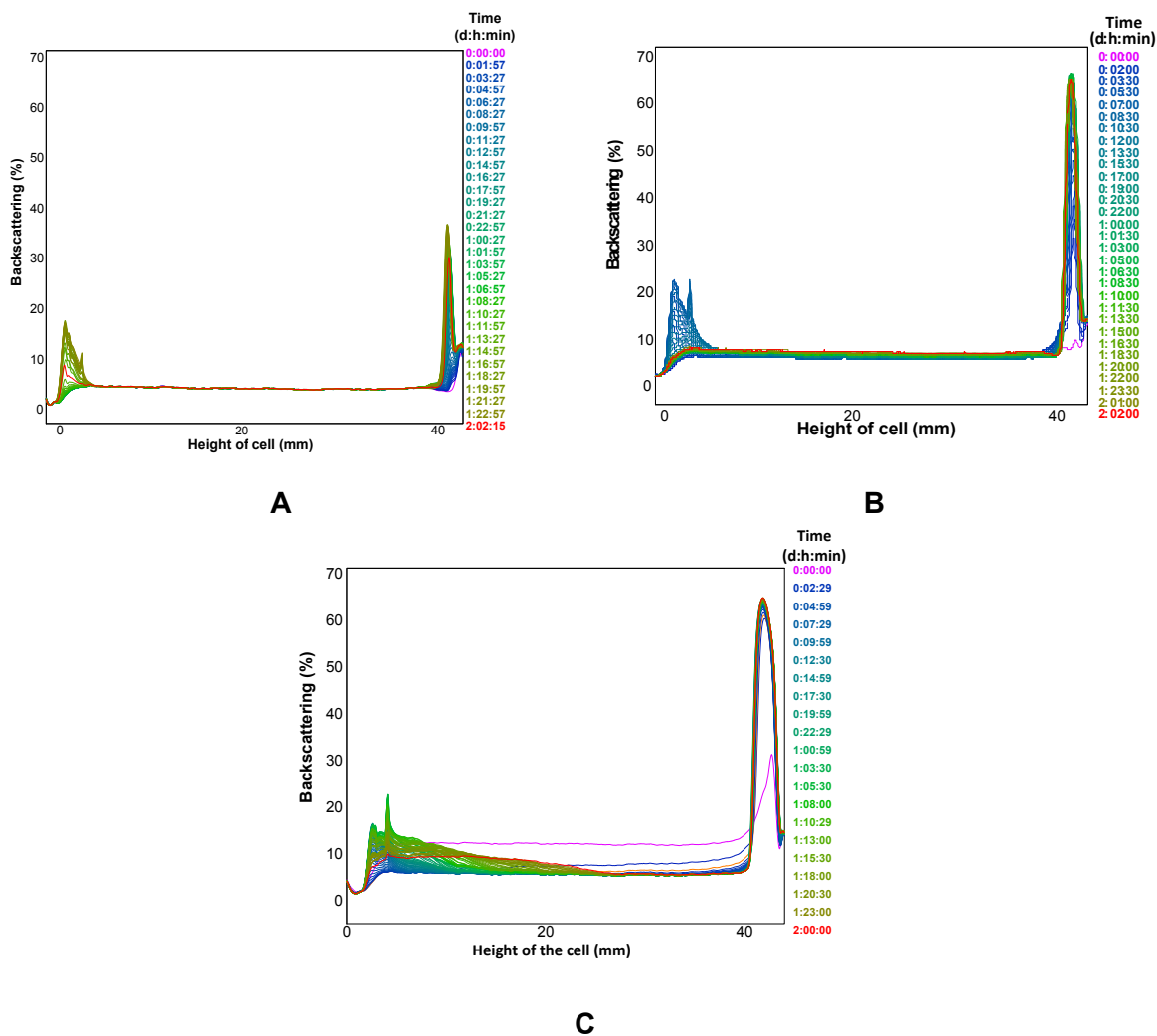


**Figure S2.** Light backscattering profiles of emulsions prepared with flat ceramic membranes of 0.45 µm (A) and 0.80 µm (B) pore diameter in the emulsification cell ( $N = 400$  rpm,  $\Delta P = 200$  kPa), and with a rotor-stator homogenizer (C) ( $N = 10,000$  rpm)

## **II. Preparation and encapsulation properties of double Pickering emulsions stabilized by Quinoa starch granules**

Progress in the development of stable double emulsions as food ingredients intends to replace small-molecule emulsifiers and synthetic polymeric stabilizing agents by food-grade components. One way to produce systems with high stability is using Pickering type emulsions. The use of particles to stabilize emulsions has received considerable attention and research has been conducted to determine their distinctive characteristics and technological applications in a variety of fields. There are several particles reported in the literature for stabilizing Pickering emulsions, being starch one of the most common ingredients in food applications. Starch shows novel and useful emulsifying properties after its hydrophobic modification. In previous studies starch granules isolated from Quinoa were modified with Octenyl Succinic Anhydride (OSA) and used to produce Pickering emulsions with excellent stability. So, we thought that a double emulsion could be a good choice to achieve encapsulation of hydrophilic ingredients. For this purpose, double Pickering emulsions stabilized with starch granules were prepared, and their encapsulation stability was determined.

**Article 2. M. Matos, A. Timgren, M. Sjöö, P. Dejmek and M. Rayner. "Preparation and encapsulation properties of double Pickering emulsions stabilized by Quinoa starch granules".**

**Colloids and Surfaces A: Physicochemical and Engineering Aspects** 423 (2013) 147-153.

### **Personal contribution to work**

This work was carried out during my stay at the Department of Food, Engineering and Nutrition of University of Lund (Sweden). After understanding double emulsions behaviour, I performed the experiments that led to the results included in this publication. Finally, I collaborated in the manuscript and figures preparation under Prof. Petr Dejmek's supervision.

## II. Preparación y propiedades de encapsulación de emulsiones dobles tipo Pickering estabilizadas mediante gránulos de almidón procedentes de la Quinoa

El avance en el desarrollo de emulsiones dobles estables con fines alimentarios depende de la sustitución de las pequeñas moléculas de emulsionantes y agentes estabilizantes poliméricos sintéticos por componentes de grado alimentario. Una forma de producir sistemas de elevada estabilidad es utilizar emulsiones tipo Pickering. El uso de partículas para estabilizar emulsiones ha recibido un interés considerable y creciente en los últimos tiempos, debido a sus características distintivas y a sus prometedoras aplicaciones tecnológicas en diversos ámbitos. En la bibliografía, se encuentran referencias a numerosos tipos de partículas capaces de estabilizar emulsiones tipo Pickering, siendo el almidón uno de los ingredientes alimentarios más comunes, el cual se ha demostrado que presenta buenas propiedades emulsionantes después de una modificación hidrófoba. En estudios anteriores, se modificaron gránulos de almidón aislados procedentes de la Quinoa con anhídrido octenil succínico (OSA) y se utilizaron para producir emulsiones tipo Pickering con excelente estabilidad. Por ello, pensamos que una emulsión doble de tipo agua-aceite-agua podría resultar un sistema adecuado para encapsular ingredientes de tipo hidrófilo. Para ello, se prepararon emulsiones dobles tipo Pickering estabilizadas con gránulos de almidón modificados y se determinó su estabilidad de encapsulación con el tiempo.

**Artículo 2. M. Matos, A. Timgren, M. Sjöö, P. Dejmek y M. Rayner. "Preparation and encapsulation properties of double Pickering emulsions stabilized by quinoa starch granules".**

**Colloids and Surfaces A: Physicochemical and Engineering Aspects** 423 (2013) 147-153.

### Aportación personal al trabajo

Llevé a cabo este trabajo durante mi estancia en el Departamento de *Food, Engineering and Nutrition* de la Universidad de Lund (Suecia). Allí me inicié en el conocimiento sobre emulsiones dobles y realicé la experimentación reflejada en este artículo. Finalmente, participé en la redacción del manuscrito y en la elaboración de las figuras en él incluidas, bajo la supervisión del Prof. Petr Dejmek.



## Preparation and encapsulation properties of double Pickering emulsions stabilized by quinoa starch granules



María Matos<sup>a</sup>, Anna Timgren<sup>b,1</sup>, Malin Sjöö<sup>b</sup>, Petr Dejmek<sup>b</sup>, Marilyn Rayner<sup>b,\*</sup>

<sup>a</sup> Department of Chemical Engineering and Environmental Technology, University of Oviedo, Spain

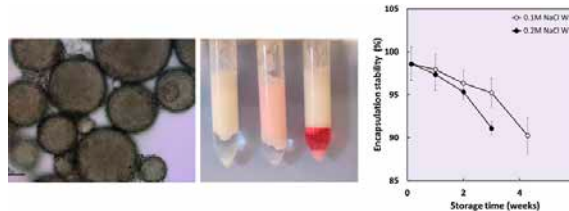
<sup>b</sup> Department of Food Technology, Engineering, and Nutrition, Lund University, Lund, Sweden

### HIGHLIGHTS

- Quinoa starch granule stabilized W/O/W double Pickering emulsions were prepared.
- Encapsulation stability of a hydrophilic inner water phase as a function of time was determined.
- Initial encapsulation efficiency was over 98.5% immediately after emulsification.
- The encapsulation stability remained over 90% after 21 days.

### GRAPHICAL ABSTRACT

Release of hydrophilic marker from Quinoa starch granule stabilized double emulsions.



### ARTICLE INFO

#### Article history:

Received 10 September 2012

Received in revised form 2 January 2013

Accepted 22 January 2013

Available online 8 February 2013

#### Keywords:

Double emulsions  
Starch granule  
Encapsulation  
Pickering emulsions

### ABSTRACT

Double emulsions have potential applications in the food, cosmetic and pharmaceutical industries as vehicles for encapsulation and delivery of nutrients during food digestion or for drug release. The major drawback of this type of emulsions is that they are often difficult to stabilize. Particle stabilized emulsions, known as Pickering emulsions, show special features, such as being extremely stable with respect to coalescence. Starch granules have proved to be a suitable stabilizer for food grade Pickering emulsions. In this work, starch double W<sub>1</sub>/O/W<sub>2</sub> Pickering emulsions were prepared and their encapsulation stability was studied as well as the impact of varying the lipophilic emulsifier (PGPR90) content and the salt concentration in the W<sub>1</sub> inner aqueous phase. Encapsulation properties were quantified by monitoring the release of a hydrophilic dye from the inner aqueous phase spectrophotometrically. Two double emulsion systems were studied, one with an inner aqueous phase with 0.1 M NaCl and the other with 0.2 M NaCl. The initial encapsulation efficiency was over 98.5% immediately after emulsification production. The encapsulation stability (ES) remained over 90% after 21 days for both systems studied, where 0.1 M NaCl W<sub>1</sub> emulsion had a ES of 95.2% and the 0.2 M NaCl W<sub>1</sub> emulsion had a ES of 91.1% respectively.

© 2013 Elsevier B.V. All rights reserved.

### 1. Introduction

The simplest multiple emulsions are called double emulsions and are ternary systems, having either a water-in-oil-in-water (W<sub>1</sub>/O/W<sub>2</sub>) or an oil-in-water-in-oil (O<sub>1</sub>/W/O<sub>2</sub>) structure, whereby the dispersed droplets contain smaller droplets of a different phase

[1] essentially an emulsion in an emulsion. Multiple emulsions have been studied since their first description in 1924 by Seifriz [2]. The structural properties of this kind of multiple emulsions allow a controlled release of a component from the inner to the outer phase which leads to a number of potential applications in the fields of medicine, pharmacy, cosmetics and separation processes [1,3–10]. Double emulsions have also applications in the food industry [4,9,11–16].

Water-in-oil-in-water (W<sub>1</sub>/O/W<sub>2</sub>) type emulsions considered in this study have several food applications such as in the formulation of reduced fat-food products (by replacing some of the volume of

\* Corresponding author. Tel.: +46 46 222 4743; fax: +46 46 222 4622.

E-mail address: marilyn.rayner@food.lth.se (M. Rayner).

<sup>1</sup> deceased Nov 12th, 2012

the oil droplets with entrapped water drops) and as vehicles for encapsulation and delivery of hydrophilic nutrients [12]. For example to fortify foods with water soluble vitamins [17–19] or minerals [20], to entrap poorly tasting bio-actives in taste-masking applications, and to protect probiotics against the harsh effects of bile acids and gastric juices [21]. Through designing W/O/W structure taste perception can be controlled modifying the release of internal aqueous phase which interacts with oral surfaces [12]. Sensory tests have indicated that there is a significant taste difference between W/O/W emulsions in which there is a delayed release of flavour and O/W emulsions containing the same ingredients [8].

The main reasons why  $W_1/O/W_2$  emulsions have not been yet widely used is that they are more complicated to produce because they have an additional internal surface (and the excess free energy associated with it) of the  $W_1/O$  emulsion which needs to be stabilized in addition to the surface of the secondary emulsion [1]. Furthermore homogenisation conditions must also be such that they can create the secondary emulsion but at the same time keep the primary  $W_1/O$  emulsion more or less intact. Progress in the development of stable double emulsions as food ingredients depends on replacing small-molecule emulsifiers and synthetic polymeric stabilizing agents by food-grade components. One way to produce emulsions with a high degree of stability is through the use of Pickering type emulsions. The use of particles to stabilize emulsions has received substantial and increasing research interest as of late due to their distinctive characteristics and promising technological applications in a range of fields including foods. The stabilization of emulsion droplets by particles is possible due to their partial dual wettability. This allows for the spontaneous accumulation of particles at the oil–water interface and stabilizing it against coalescence by volume exclusion and steric hindrance [22], i.e. the particles prevent oil–water interfaces of oil droplets from coming in to direct physical contact.

There are numerous varieties of particles reported in the literature for stabilizing Pickering type emulsions, and due to advances in nano technology and micro-manufacturing their availability and design ability will no-doubt increase in the future. Examples where food based/edible stabilizing particles have been studied have included: fat crystals, globular proteins and aggregated hydro-colloids [10], insoluble flavonoid particles [24], cellulose–ethyl cellulose complexes for stabilizing emulsions and foams [25], freeze fractured starch granules and protein mixtures [25,26], and chitin–nano crystals stabilized emulsions [27]. For comprehensive reviews on particle stabilized emulsions, applications and related theory please refer to [28], Aveyard et al. [22] Hunter et al. [29], and for food emulsion in particular see [23,30]. Recent work where Pickering type double emulsions have been studies include those using fat-crystals to stabilize the inner emulsion of a W/O/W emulsions [31] and combinations of fat-crystals and particles producing highly stable Pickering-in-Pickering double emulsions. This novel design enables food technologists to achieve a significant fat replacement in a way that is imperceptible to the consumer [32].

Starch is one of the most common food ingredients, and after hydrophobic modification intact starch granules has been shown to have novel and useful emulsifying properties [20,33–35]. In our previous studies starch granules isolated form quinoa were modified with octenyl succinic anhydride (OSA) and used to produce Pickering emulsions with excellent stability. Quinoa starch granules were chosen as Pickering agents because the granules are relatively small ( $0.5\text{--}3\ \mu\text{m}$  in diameter) with a unimodal size distribution. Small size is of interest as it reduces the amount required (mg starch per ml oil) to stabilize a given emulsion droplet interface. The size of the emulsion drops produced were a function of the starch to oil ratio used, but were independent of the overall dispersed phase content over a range of 7–33% v/v oil [37]. Furthermore these emulsions have shown an outstanding degree of

stability being un-changed after 2 years of storage under peri-kineti conditions [35]. By taking advantage of starches' distinctive physical–chemical characteristics and careful application of heat we have been able to increase the cohesively of the partially gelatinized starch layer to increase resistance to lipolysis by up to 70% [37]. Although the drop size of starch granule stabilized emulsions was relatively large, their excellent stability and barrier properties can prove suitable for applications such as encapsulation of various ingredients in food and pharmaceutical products with the starch particles controlling the release properties. In order to achieve encapsulation of hydrophilic ingredients a double emulsion system may be a good choice of system. Thus, in this study, starch granule stabilized double Pickering emulsions were prepared and their encapsulation stability of a hydrophilic inner water phase as a function of time was determined.

## 2. Materials

Starch was isolated form quinoa (Biofood-Biolivs AB, Sweden) by a wet-milling process and OSA-modified with a degree of substitution of 1.8% using the method described in Rayner et al. [33] (processed by Lyckeby-Culinair AB, Sweden). The external water phase of the double emulsions ( $W_2$ ) was a 5 mM phosphate buffer with 0.2 M NaCl. As internal water phase ( $W_1$ ) two (0.1 M and 0.2 M NaCl) solutions were used. The oil phase was the medium-chain triglyceride oil Miglyol 812, density  $945\ \text{kg/m}^3$  at  $20^\circ\text{C}$  (Sasol GmbH, Germany) was prepared containing several concentrations (1–5% w/v) of polyglycerol polyricinoleate PGPR 90 (Grinsted Danisco AS, Denmark). Polyglycerol polyricinoleate (PGPR) is a powerful water-in-oil emulsifying agent commonly used with limited concentrations in food formulations [9]. The encapsulation efficiency was determined with carmine, an approved pigment food colouring agent (E120). It is stable to heat and light but sensitive to low and high pH. At neutral pH it has a bright red colour with a maximum UV light absorption at 520 nm [38]. Carmine was purchased as commercial water-soluble red dye solution from the local supermarket (Ekströms röd hushållsfärg, Procordia Foods AB, Sweden).

## 3. Methods

### 3.1. Preparation of primary ( $W_1/O$ ) water in oil emulsions

Water in oil emulsions ( $W_1/O$ ), 20%  $W_1$  and 80% oil-phase with a total volume of 7 mL were prepared. The  $W_1$  disperse phase was deionized water containing carmine dye solution (4  $\mu\text{L}$  dye/mL deionised water) with the corresponding amount of NaCl added to obtain either 0.1 M or 0.2 M. The continuous oil phase consisted of Miglyol 812 with varying concentrations 1–5% (w/v) of PGPR90 as lipophilic surfactant dissolved into it by stirring the oil phase in a covered container at  $25\text{--}30^\circ\text{C}$  for 1 h at 240 rpm. The 5.6 mL of continuous and 1.4 mL of dispersed phase were emulsified in glass test tubes by high shear mixing in an Ystral X10 mixer (Ystral GmbH, Germany) with 6 mm dispersing tool at 24,000 rpm for 10 min.

### 3.2. Preparation of double $W_1/O/W_2$ emulsions

Double Pickering ( $W_1/O/W_2$ ) emulsions consisting of total phase volumes: 8.25% v/v internal aqueous phase containing carmine dye ( $W_1$ ), 33% v/v Miglyol 812 oil phase including 5% w/v PGPR (O), and 58.75% v/v outer aqueous phase ( $W_2$ ). The total dispersed phase fraction was 41.25%. A sodium phosphate buffer was used in the outer aqueous phase as it has been shown to enable the separation of oil droplets by centrifugation and also promotes a more accurate measurement of some polymeric dyes, used as

markers, in the recovered outer aqueous phase [39]. This is important us to be able to quantify the encapsulation efficiency and stability described in Section 3.4. The amount of granules (214 mg per ml of oil) was based on our previous studies on simple starch Pickering emulsions [37].

The preparations of the double emulsions are as follows: first 4.1 mL of  $W_2$  containing 5 mM phosphate buffer with pH 7.0 and 0.2 M NaCl in deionized water was added to a glass test tube with 494 mg of 1.8% OSA modified quinoa starch (214 mg/mL Miglyol 812 oil) and then thoroughly dispersed using a vortex mixer. Then 2.9 mL of the  $W_1/O$  primary emulsion prepared as described above was added to the  $W_2$  starch dispersion in the glass test tube and emulsified using an Ystral X10 mixer with 6 mm dispersing tool at 22,000 rpm for 30 s. All the emulsions were prepared in triplicate for each analysis time and stored at room temperature.

A sodium phosphate buffer was used as outer aqueous phase as it has been shown to enable the separation of oil droplets by centrifugation and also promotes a more accurate measurement of some polymeric dyes, used as markers, in the recovered outer aqueous phase [35]. This is important us to be able to quantify the encapsulation efficiency and stability described in Section 3.4.

### 3.3. Emulsion characterization

Particle size distributions of the emulsions prepared were measured by laser diffraction using a Malvern Particle Size Analyzer (Mastersizer 2000 S, Malvern Instruments Ltd. UK). For starch covered double emulsions dispersed in an aqueous phase a refractive index of 1.54 was used [40]. In case of the  $W_1/O$  emulsion the water refractive index was used and the samples were dispersed in paraffin oil (Petromax, Germany). Micrographs of the emulsions were obtained with a light microscope (Olympus BX50, Tokyo, Japan) with 10–100 $\times$  magnification and digital camera (DFK 41AF02, Imaging source, Germany) with the software ImageJ (NIH, version 1.42 m) one day after emulsification.

### 3.4. Determination of the recovery yield of the marker, encapsulation efficiency and stability of the double emulsion

The encapsulation efficiency is related to the initial amount of marker lost from the  $W_1$  phase into the  $W_2$  phase during the emulsification process creating the final double emulsions and the emulsification stability is a measure of how much of the marker leaks from the internal  $W_1$  phase into the outer continuous  $W_2$  phase during storage. It may be considered that a double emulsion has a good stability when the initial encapsulation efficiency is around 95% and after a few weeks of storage it is still around 70–80% [12,41].

In order to measure marker concentration in the external  $W_2$  phase in a spectrophotometer it has to be separated from the emulsion drops and free starch particles. Centrifugation is the most common and simple method of separation used for measuring the encapsulation stability of double emulsions, where the oily phase containing the small  $W_1$  droplets (cream phase) is separated from the outer aqueous phase ( $W_2$ ) [4,13,41].

In this study the samples were centrifuged for 10 min at 4000 rpm and the subnatant aqueous phase was then recovered carefully with a Pasteur pipette and filtered using a 0.2  $\mu\text{m}$  syringe filter of polyethersulfone (PES). To determine the concentration of the carmine dye used as a marker present in the external aqueous phase a calibration curve was prepared by measuring the absorbance values of several solutions of known concentration. The marker was dissolved in the same sodium phosphate buffer used as external phase (pH 7.0 and 0.2 M NaCl) and in the same concentrations as added to the inner aqueous phase. The absorbance values were determined using a UV-visible spectrophotometer (Hitachi

U-1500) at 520 nm. The calibration curve had a good correlation coefficient ( $r^2 = 1$ ) over the relevant range of concentrations measured.

To determine properly the encapsulation efficiency or encapsulation stability of a system it is necessary to know the recovery yield of the marker used after the separation of the external aqueous phase, in this case after isolating the subnatant after centrifugation and filtration. The reason being to ensure that if some of the marker interacts with the starch or oil or containers or is in some way lost during the separation and analysis it can be accounted for in the calibration curve. Thus by adding 100% of the inner phase to the outer aqueous phase, simulating as if the emulsion had completely lost its  $W_1$  phase to the outer continuous phase we create a standard to determine the recovery yield of the marker from the emulsion [12]. For this purpose a simple oil-in-water emulsion ( $O/W_2$ ) was prepared using the same oily phase ( $O$ ) and the same outer aqueous phase ( $W_2$ ) as in the double emulsions. Then the  $O/W_2$  emulsion was diluted with the same proportion of inner aqueous phase ( $W_1$ ) containing the red dye at the same concentrations used for the preparation of the double emulsions. The concentration of dye in the recovered aqueous phases was calculated from the absorbance values of the calibration curve. This concentration was then compared to the actual concentration initially added to the water phase used for dilution. To determine the value of the corresponding reference blank,  $O/W_2$  emulsions were prepared and diluted by adding the same proportion of  $W_1$  but without dye. Several standard samples ( $n = 11$ ) were prepared and the absorbance of the aqueous phases recovered by centrifugation and filtration were measured. Using the calibration absorbance curve the concentration of dye in the recovered water phase was determined ( $C_{\text{recovered}}$ ) and the recovery yield ( $R_y$ ) was calculated as:

$$R_y(\%) = \frac{C_{\text{recovered}} \times 100}{C_0} \quad (1)$$

where  $C_0$  is the expected concentration based on the amount of marker added.

The recovery yield of our marker after centrifugation and filtration is  $51\% \pm 2$  of the freshly prepared  $O/W_2$ . Although 51% could be considered as a rather low recovery yield, the method had a high degree of reproducibility over the concentrations tested.

The encapsulation efficiency of a double emulsion can be defined as the percentage of primary emulsion aqueous phase that is retained in the inner aqueous phase ( $W_1$ ) after the second emulsification step or manufacture of the  $W_1/O/W_2$ .

The encapsulation efficiency (EE) was then determined by measuring the concentration of dye present in the external water phase applying the described method but replacing  $O/W_2$  by  $W_1/O/W_2$ . The encapsulation efficiency was calculated using the following equations:

$$\text{EE}(\%) = 100 - \frac{C_{\text{recovered}} \times 100}{R_y C_0} \quad (2)$$

In Eq. (2) the encapsulation efficiency is related to the concentration initially added to the inner aqueous phase and includes the correction of the recovery yield of marker. The encapsulation stability (ES) can be defined as the amount of the aqueous phase marker which remains entrapped in the inner aqueous phase ( $W_1$ ) on storage or by exposure of the double emulsion to environmental stresses [41]. Thus, the encapsulation stability was calculated using the equation:

$$\text{ES}(\%) = 100 - \frac{C_t \times 100}{R_y C_0} \quad (3)$$

where  $C_t$  is the recovered phase concentration of marker after storage time,  $t$ . For determining the encapsulation stability with time samples were prepared and stored at room temperature. The

encapsulation stability was measured each week during one month and a triplicate of each sample was monitored.

#### 4. Results and discussion

##### 4.1. Effect of PGPR content on droplet size of W<sub>1</sub>/O emulsions

To produce a stable double emulsion the stability of the water-in-oil emulsion from which it is prepared should be ensured. The stability of the primary emulsion depends on droplet size (normally 1 μm), the amount of dispersed and continuous phase (the amount of water usually ranges between 20–30%) and the affinity of the emulsifier for both aqueous and oily phases (HLB value) [4,6,7,10,42]. Therefore, several water in oil emulsions were prepared varying the amount of PGPR 90 present in the oily phase from 1–5% (w/v) for both types of dispersed phase used (0.1 M and 0.2 M NaCl) and its droplet size distributions were measured. The addition of electrolytes to the aqueous phase increases the W/O emulsion stability because electrolytes lower the attractive force between the water droplets, decreasing the dielectric constant of the aqueous phase and reducing collision frequency. The presence of salts may also interfere with the adsorption density of PGPR at the interfacial film [13,16,31].

As expected, it was observed that the mean droplet size decreased as the amount of PGPR 90 was increased. This effect of PGPR content has been previously reported [16]. The mean diameters of the aqueous W<sub>1</sub> droplets and the corresponding standard error of their means ( $n = 3$ ) obtained from the particle size distributions (Malvern Mastersizer 2000) are shown in Table 1 as well as the mean diameters of the droplets determined using image analysis of digital micrographs using Image J. The micrograph images agree with the light scattering results, and the same trend was observed when increasing PGPR concentrations. The particle size distributions for the highest (5%) and lowest (1%) PGPR concentrations are shown in Fig. 1. All the W<sub>1</sub>/O emulsions prepared presented a mean droplet size  $d$  (0.5) under 1 μm. A small peak was observed around 0.1 μm likely because of the presence of PGPR90 micelles. However, no significant differences were observed between the two salt concentrations used.

The stability of the W<sub>1</sub>/O emulsions during storage at room temperature was also analysed. All the samples prepared presented an initially homogeneous structure and no phase separation was observed. After one month of storage a slight oil layer was observed at the top, which decreased with increasing amounts of PGPR. This can be explained because at increasing PGPR concentrations sedimentation of the aqueous W<sub>1</sub> droplets is less pronounced because of their smaller droplet size, but also likely due to the higher viscosity of the oil phase with higher levels of dissolved PGPR polymer.

Based on these results, 5% PGPR 90 (w/v) was chosen as the formulation for the primary W<sub>1</sub>/O emulsion used for the preparation

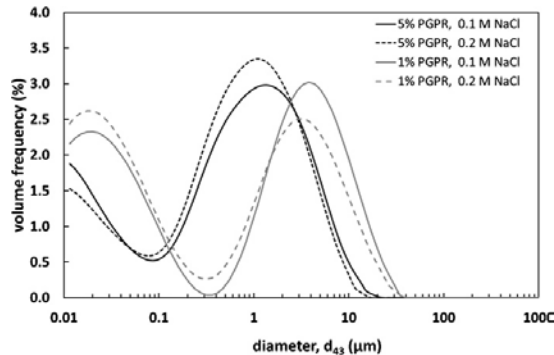


**Fig. 1.** Particle size distributions of the water-in-oil emulsions prepared using W<sub>1</sub> 0.1 M NaCl and 1% or 5% (w/v) of PGPR90 (grey and black solid lines respectively) and W<sub>1</sub> 0.2 M NaCl and 1% or 5% (w/v) of PGPR90 (grey and black dashed lines respectively).

double starch granule stabilized Pickering emulsions. In other studies the concentration of PGPR had a significant effect on the encapsulation efficiency (EE) of W<sub>1</sub>/O/W<sub>2</sub> emulsions. It has also been reported that the ionic environment created in buffered systems affects the emulsifying ability of PGPR. In non-buffered systems, the PGPR concentration could be reduced to 2% (w/v) to obtain an EE higher than 90%, whereas, in buffered systems, 4% (w/v) PGPR was required to maintain a similar EE [32].

##### 4.2. Droplet size and microstructure of W<sub>1</sub>/O/W<sub>2</sub> emulsions

Examples of the overall microstructure of the double starch Pickering emulsions are shown in Fig. 2. Images are focused at different depths using 50× magnification. The starch granules can be easily identified around the surface of the oil droplets while it was necessary to take several pictures at different heights to appreciate properly the inner water droplets. The mean size of the inner water droplets observed in the micrographs and measured using Image J was in the range 0.9–8.3 μm with an average diameter of  $3.1 \pm 1.5$  μm while the starch particles stabilized emulsion droplets are in the range 23–43 μm with an average diameter of  $33 \pm 7$  μm.

In Table 2 the mean droplet diameters and span values of the double Pickering emulsions measured by light scattering in the Malvern Mastersizer prepared using 0.1 M and 0.2 M NaCl as inner aqueous W<sub>1</sub> phases is presented. The diameter  $d$  (0.5) was 38 μm when an inner water phase of 0.1 M NaCl was used and 42 μm in the case of 0.2 M NaCl. This size is similar to the size reported in previous studies with simple starch granule stabilized

**Table 1**

Mean diameters measured by light scattering ( $D$  [4,3],  $D$  [3,2], and  $d$  (0.5)) of the water-in-oil emulsions prepared using as W<sub>1</sub> 0.1 M NaCl or W<sub>1</sub> 0.2 M NaCl with varying concentrations of PGPR (values are mean ± standard error of the means,  $n = 3$ ), and mean diameters from digital micrographs measured with Image J (mean ± standard deviation,  $n = 200+$ ).

Lipophilic emulsifier content salt conc. in W <sub>1</sub> phase	$D$ [4,3] (μm)	$D$ [3,2] (μm)	$d$ (0.5) (μm)	Diameter (μm)
5% PGPR90, 0.1 M NaCl	1.2 ± 0.1	0.22 ± 0.01	0.841 ± 0.08	0.7 ± 0.1
4% PGPR90, 0.1 M NaCl	1.18 ± 0.09	0.250 ± 0.016	0.93 ± 0.13	0.8 ± 0.2
3% PGPR90, 0.1 M NaCl	1.25 ± 0.06	0.25 ± 0.02	1.06 ± 0.04	0.82 ± 0.18
2% PGPR90, 0.1 M NaCl	1.32 ± 0.11	0.24 ± 0.03	1.1 ± 0.3	0.9 ± 0.2
1% PGPR90, 0.1 M NaCl	1.6 ± 0.2	0.233 ± 0.013	1.08 ± 0.07	0.89 ± 0.16
5% PGPR90, 0.2 M NaCl	1.1 ± 0.2	0.265 ± 0.013	0.86 ± 0.19	0.76 ± 0.14
4% PGPR90, 0.2 M NaCl	1.04 ± 0.09	0.27 ± 0.04	0.9 ± 0.4	0.81 ± 0.16
3% PGPR90, 0.2 M NaCl	1.3 ± 0.1	0.26 ± 0.02	1.10 ± 0.04	0.88 ± 0.17
2% PGPR90, 0.2 M NaCl	1.36 ± 0.04	0.24 ± 0.04	1.12 ± 0.08	0.9 ± 0.3
1% PGPR90, 0.2 M NaCl	1.28 ± 0.06	0.21 ± 0.03	1.15 ± 0.06	0.93 ± 0.09

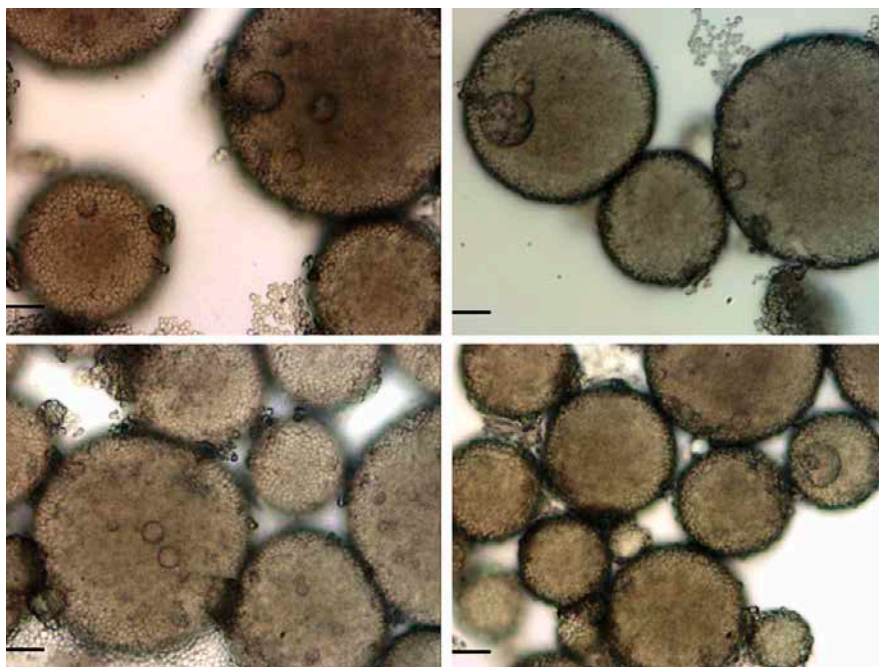


**Fig. 2.** Micrographs of the  $W_1/O/W_2$  emulsion ( $50\times$  magnification, scale bars represent 10 microns) focused at different depths.

**Table 2**  
Mean diameters of the double Pickering emulsions prepared measured by light scattering (mean  $\pm$  standard error of the means,  $n=3$ ).

	$D [4,3]$	$D [3,2]$	$d (0.5)$
0.1 M NaCl	$48 \pm 10$	$21 \pm 9$	$38 \pm 3$
0.2 M NaCl	$50 \pm 8$	$36 \pm 6$	$42 \pm 1$

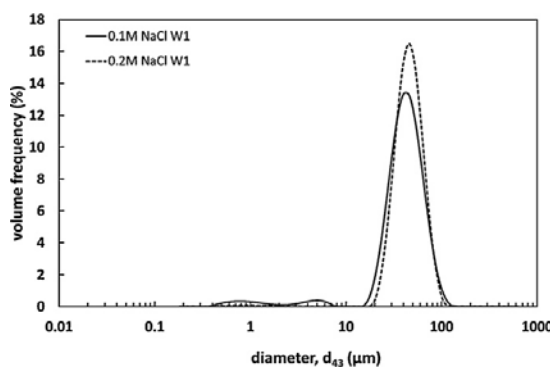


**Fig. 3.** Particle size distributions of double Pickering emulsions prepared using as  $W_1$  0.1 M (solid line) and 0.2 M NaCl (dashed line).

Pickering emulsions, where it was observed that an emulsion with 214 mg starch/ml oil typically consists of droplets with a volume mean diameter of 35–45  $\mu\text{m}$  [34]. Particle size distributions are shown in Fig. 3. In both cases low span values (1.4 and 1.3) were observed.

#### 4.3. Determination of recovery yield and encapsulation stability

Images of samples prepared for determining the encapsulation efficiency of the double emulsions are shown in Fig. 4. The three samples shown (i.e. blank, standard sample (0% EE) and  $W_1/O/W_2$  emulsion) have a creamy phase at the top and clear water phase at the bottom of the glass test tube. The blank and the standard sample (0% EE) shows a white cream phase while in the case of the double emulsion a pink colour is observed due to the presence of the carmine dye in the inner droplets dispersed in the oily phase ( $W_1$ ).

To determine the encapsulation stability over time, double emulsion samples and standards were prepared and stored at room temperature. The encapsulation stability was monitored each week

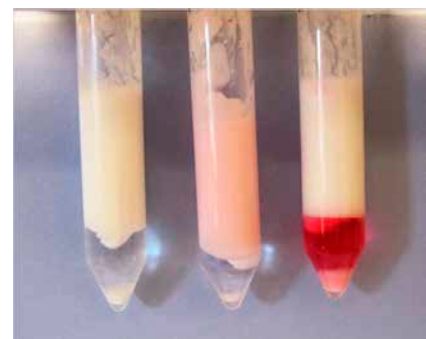


**Fig. 4.** Image of the reference blank (left), the  $W_1/O/W_2$  emulsion (middle) and the standard sample prepared used to determine the recovery yield of the marker 0% EE (right).

**Table 3**

Encapsulation stability of double Pickering emulsions prepared using as  $W_1$  0.1 M NaCl or 0.2 M NaCl, (values are means  $\pm$  standard deviation,  $n=3$ ).

t (days)	$W_1$ 0.1 M NaCl	$W_1$ 0.2 M NaCl
	ES (%)	ES (%)
0	98.6 $\pm$ 1.9	98.6 $\pm$ 1.9
7	97.9 $\pm$ 1.8	97.4 $\pm$ 1.9
14	96.3 $\pm$ 1.5	95.3 $\pm$ 0.9
21	95.2 $\pm$ 1.7	91.1 $\pm$ 0.8
30	90 $\pm$ 2	no data

during one month and each sample was prepared by triplicate. Results are shown in Table 3 with rather low variability with small standard deviation, and the values are plotted as a function of storage time in Fig. 5. The starch Pickering emulsions prepared had an initial encapsulation efficiency of more than 98.5% for both  $W_1$  concentrations of NaCl. After 30 days of storage the encapsulation stability still remained around 90% when 0.1 M NaCl was used as the  $W_1$  internal phase, and for the 0.2 M NaCl  $W_1$  phase the ES remained over 90% for 21 days. The measured encapsulation stability was slightly higher when 0.1 M NaCl was used as the aqueous  $W_1$  internal phase. A negative osmotic pressure,  $\Delta\pi$ , indicates that the concentration of solute is greater in  $W_2$  resulting in preferential water transport from  $W_1$  to  $W_2$  but in this case the osmotic pressure difference between both phases is quite low ( $\sim 2.4$  atm, calculated by the Van't Hoff equation). Furthermore some authors also indicated that it is not essential to exactly balance osmotic pressure to achieve good emulsion stability in particle stabilized double emulsions [31].

The ability of starch granule stabilized Pickering emulsions to retain the inner aqueous ( $W_1$ ) phase could be attributed to the observed overall stability of Pickering type emulsions. Pickering particles, in this case OSA modified quinoa starch granules, adsorbed at the oil-water interface create a physical barrier preventing contact between droplets. This is not essentially unlike the steric barrier created by other emulsifiers such as proteins and hydrocolloids however, in the case of Pickering emulsions, once particles absorb to the oil-water interface they are effectively trapped there, due to their large size and partial wettability [22]. In general, if particles have suitable wetting conditions at the oil-water interface and are larger than approximately 10 nm their adsorption at the oil water interface is virtually irreversible as the desorption energy per particle is several thousand times larger than the thermal energy,  $kT$  [26]. Here, the strong adsorption of hydrophobically modified quinoa starch granules at the interface can also explain the stability (even at large droplet sizes) over

extended periods of time observed in particle stabilized emulsions, both with respect to coalescence of oil droplets and the released internal aqueous phase. Based on droplet stability measurements of starch granule stabilized emulsion in a series of previous studies [33–37] and the surprisingly good retention to the inner aqueous phase marker (even after storage and centrifugation of samples), we believe that this phenomena is due largely to the strong and practically irreversible adsorption of the partially wetting granules at the oil water interface. This mechanism prevents both the coalescence of the oil drops (secondary emulsion) and the rupture of the interval  $W_1$  droplets into the external aqueous  $W_2$  phase, thereby explaining the low rate of loss of marker and the high encapsulation stability observed over the present storage study.

## 5. Conclusions

Stable water-in-oil emulsions were obtained using 5% of PGPR 90 (w/v) in the oily phase and an aqueous phase of 0.1 M–0.2 M NaCl with a medium droplet size in the range of 0.8–0.9  $\mu$ m.

A procedure to determine the encapsulation efficiency as a function of absorbance determination was established using centrifugation and filtration for  $W_2$  separation. The recovery yield of the marker used should be considered for determining the encapsulation efficiency and stability of the  $W_1/O/W_2$  prepared.

The double starch Pickering emulsions prepared showed high encapsulation efficiency and encapsulation stability after one month storage at room temperature. The initial encapsulation efficiency was more than 98.5% immediately after emulsification production and the encapsulation stability remained over 90% after 21 days for all systems studied. To put these figures in perspective, as we noted earlier, an accepted criteria for good double emulsion stability is a system having an initial encapsulation efficiency of approximately 95% and after a few weeks of storage of the order of 70–80% [12,41]. In this context, we believe that these results based on a double starch granule stabilized Pickering emulsion system, if expanded upon, may have an enduring impact in the progress of double emulsion techniques with applications in a variety food and pharmaceutical products.

## Acknowledgements

The study was supported by the Lund University Antidiabetic Food Centre, which is a VINNOVA Vinn Excellence Centre, and by the MICINN, Spain, under the grant CTQ2007-65348. M. Matos acknowledges receipt of a graduate fellowship from FPI Program (MEC, Spain).

## References

- [1] A. Aserin, in: *Multiple Emulsions: Technology and Applications*, Wiley-Interscience, Hoboken, NJ, 2008.
- [2] W. Seifriz, Studies in emulsions. III–V, *J. Phys. Chem.* 29 (6) (1924) 738–749.
- [3] Y. Mine, M. Shimizu, et al., Preparation and stabilization of simple and multiple emulsions using a microporous glass membrane, *Colloids Surf. B: Biointerfaces* 6 (4–5) (1996) 261–268.
- [4] S. Mun, Y. Choi, et al., Effects of enzymatically modified starch on the encapsulation efficiency and stability of water-in-oil-in-water emulsions, *Food Chem.* 128 (2) (2011) 266–275.
- [5] T. Nakashima, M. Shimizu, et al., Particle control of emulsion by membrane emulsification and its applications, *Adv. Drug Deliv. Rev.* 45 (1) (2000) 47–56.
- [6] H. Okochi, M. Nakano, Comparative study of two preparation methods of w/o/w emulsions: stirring and membrane emulsification, *Chem. Pharm. Bull. (Tokyo)* 45 (8) (1997) 1323–1326.
- [7] J. Silvestre De Los Reyes, C. Charcosset, Preparation of water-in-oil and ethanol-in-oil emulsions by membrane emulsification, *Fuel* 89 (11) (2010) 3482–3488.
- [8] S. Van Der Graaf, C.G.P.H. Schroën, et al., Preparation of double emulsions by membrane emulsification – a review, *J. Membr. Sci.* 251 (1–2) (2005) 7–15.
- [9] R. Wilson, B.J. Van Schie, et al., Overview of the preparation, use and biological studies on polyglycerol polyricinoleate (PGPR), *Food Chem. Toxicol.* 36 (9–10) (1998) 711–718.

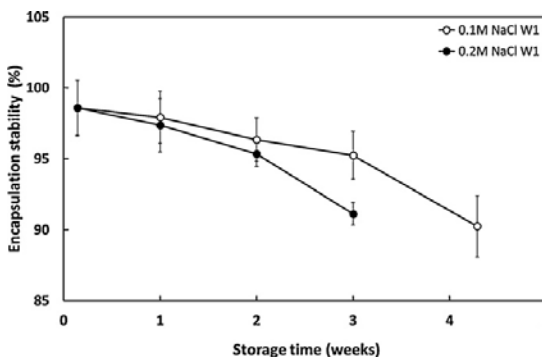


Fig. 5. Encapsulation stability of the double starch Pickering emulsions prepared using as  $W_1$  0.1 M NaCl (open circles) and 0.2 M NaCl (filled circles).

- [10] G.T. Vladisavljević, M. Shimizu, et al., Preparation of monodisperse multiple emulsions at high production rates by multi-stage premix membrane emulsification, *J. Membr. Sci.* 244 (1–2) (2004) 97–106.
- [11] C. Charcosset, Preparation of emulsions and particles by membrane emulsification for the food processing industry, *J. Food Eng.* 92 (3) (2009) 241–249.
- [12] E. Dickinson, Double emulsions stabilized by food biopolymers, *Food Biophys.* 6 (1) (2011) 1–11.
- [13] S. Frasch-Melnik, I.T. Norton, et al., Fat-crystal stabilised w/o emulsions for controlled salt release, *J. Food Eng.* 98 (4) (2010) 437–442.
- [14] N. Garti, Progress in stabilization and transport phenomena of double emulsions in food applications, *LWT – Food Sci. Technol.* 30 (3) (1997) 222–235.
- [15] N. Krog, Functions of emulsifiers in food systems, *J. Am. Oil Chem. Soc.* 54 (3) (1977) 124–131.
- [16] A.L. Márquez, A. Medrano, et al., Effect of calcium salts and surfactant concentration on the stability of water-in-oil (w/o) emulsions prepared with polyglycerol polyricinoleate, *J. Colloid Interface Sci.* 341 (1) (2010) 101–108.
- [17] A. Benichou, A. Aserin, et al., Double emulsions stabilized with hybrids of natural polymers for entrapment and slow release of active matters, *Adv. Colloid Interface Sci.* 108–109 (2004) 29–41.
- [18] A. Fechner, A. Knott, et al., Stability and release properties of double-emulsions stabilised by caseinate–dextran conjugates, *Food Hydrocolloids* 21 (5–6) (2007) 943–952.
- [19] H.J. Giroux, S. Constantineau, et al., Cheese fortification using W/O/W double emulsions as a carrier for water soluble nutrients, *Int. Dairy J.* (2012).
- [20] M. Bonnet, M. Cansell, et al., Release rate profiles of magnesium from multiple W/O/W emulsions, *Food Hydrocolloids* 23 (1) (2009) 92–101.
- [21] M. Shima, Y. Morita, et al., Protection of *Lactobacillus acidophilus* from the low pH of a model gastric juice by incorporation in a W/O/W emulsion, *Food Hydrocolloids* 20 (8) (2006) 1164–1169.
- [22] R. Aveyard, B.P. Binks, et al., Emulsions stabilised solely by colloidal particles, *Adv. Colloid Interface Sci.* 100–102 (2003) 503–546.
- [23] E. Dickinson, Food emulsions and foams: Stabilization by particles, *Curr. Opin. Colloid Interface Sci.* 15 (2010) 40–49.
- [24] Z. Luo, B.S. Murray, et al., Particle-stabilizing effects of flavonoids at the oil–water interface, *J. Agric. Food Chem.* 59 (6) (2011) 2636–2645.
- [25] B.S. Murray, K. Durga, et al., Stabilization of foams and emulsions by mixtures of surface active food-grade particles and proteins, *Food Hydrocolloids* 25 (4) (2011) 627–638.
- [26] A. Yusoff, B.S. Murray, Modified starch granules as particle-stabilizers of oil-in-water emulsions, *Food Hydrocolloids* 25 (1) (2011) 42–55.
- [27] M.V. Tzoumakis, T. Moschakis, et al., Oil-in-water emulsions stabilized by chitin nanocrystal particles, *Food Hydrocolloids* 25 (6) (2011) 1521–1529.
- [28] B.P. Binks, Particles as surfactants—similarities and differences, *Curr. Opin. Colloid Interface Sci.* 7 (1–2) (2002) 21–41.
- [29] T.N. Hunter, R.J. Pugh, et al., The role of particles in stabilising foams and emulsions, *Adv. Colloid Interface Sci.* 137 (2) (2008) 57–81.
- [30] E. Dickinson, Interfacial particles in food emulsions and foams, in: B.P. Binks, T.S. Horozov (Eds.), *Colloidal Particles at Liquid Interfaces*, Cambridge University Press, Cambridge, 2006.
- [31] S. Frasch-Melnik, F. Spyropoulos, et al., W<sub>1</sub>/O/W<sub>2</sub> double emulsions stabilised by fat crystals – formulation, stability and salt release, *J. Colloid Interface Sci.* 350 (1) (2010) 178–185.
- [32] D.A. Garrec, S. Frasch-Melnik, et al., Designing colloidal structures for micro and macro nutrient content and release in foods, *Faraday Discuss.* (2012).
- [33] M. Rayner, M. Sjoo, et al., Quinoa starch granules as stabilizing particles for production of Pickering emulsions, *Faraday Discuss.* 158 (0) (2012) 139–155.
- [34] M. Rayner, A. Timgren, et al., Quinoa starch granules: a candidate for stabilising food-grade Pickering emulsions, *J. Sci. Food Agric.* 92 (9) (2012) 1841–1847.
- [35] Timgren, A., M. Rayner, et al. (2013). Emulsion stabilizing capacity of intact starch granules modified by heat treatment or octenyl succinic anhydride. *Food Sci. Nutr.*, <http://dx.doi.org/10.1002/fsn3.17>
- [36] D. Marku, M. Wahlgren, et al., Characterization of starch Pickering emulsions for potential applications in topical formulations, *Int. J. Pharm.* 428 (2012) 1–7.
- [37] A. Timgren, M. Rayner, et al., Starch particles for food based Pickering emulsions, *Procedia Food Sci.* 1 (2011) 95–103.
- [38] P. Adela, Food colorants derived from natural sources by processing, in: C. Socaciu (Ed.), *Food Colorants*, CRC Press, Boca Raton, 2007, pp. 303–426.
- [39] J. Su, J. Flanagan, et al., Synergistic effects of polyglycerol ester of polyricinoleic acid and sodium caseinate on the stabilisation of water-oil-water emulsions, *Food Hydrocolloids* 20 (2–SPEC. ISS) (2006) 261–268.
- [40] E.H.C. Bromley, I. Hopkinson, Confocal microscopy of a dense particle system, *J. Colloid Interface Sci.* 245 (1) (2002) 75–80.
- [41] J.O'Regan, D.M. Mulvihill, Sodium caseinate–maltodextrin conjugate stabilized double emulsions: encapsulation and stability, *Food Res. Int.* 43 (1) (2010) 224–231.
- [42] J.Wu, W.Jing, et al., Preparation of W/O emulsions by membrane emulsification with a mullite ceramic membrane, *Desalination* 193 (1–3) (2006) 381–386.

### **III. Preparation of water-in-oil-in-water ( $W_1/O/W_2$ ) double emulsions containing *trans*-resveratrol**

*Trans*-resveratrol is a natural occurring polyphenol found in a wide variety of plants. It has beneficial effects for human health, with anti-oxidant, anti-inflammatory, cardioprotective and anti-tumour properties. However, its applications are limited because it is an easily oxidizable and extremely photosensitive compound, with low water solubility, short biological half-life, and fast metabolism and elimination. Several encapsulation studies have been carried out to protect *trans*-resveratrol from degradation, increasing its solubility in water and targeting it to specific locations via multiparticulate forms and colloidal carriers.

The aim of this work was to prepare water-in-oil-in-water emulsions ( $W_1/O/W_2$ ) containing *trans*-resveratrol, either by mechanical agitation or membrane emulsification (ME). In addition, the encapsulation stability (ES) was determined by RP-HPLC using UV-VIS and fluorescence detectors.

**Article 3. M. Matos, G. Gutiérrez, J. Coca and C. Pazos. "Preparation of water-in-oil-in-water ( $W_1/O/W_2$ ) double emulsions containing resveratrol".**

**Colloids and Surfaces A: Physicochemical and Engineering Aspects**  
<http://dx.doi.org/10.1002/fsn3.17>.

#### **Personal contribution to work**

I was responsible for the performance of the experiments, selecting and applying analytical techniques, such as Reversed-Phase High-Performance Liquid Chromatography (RP-HPLC). Finally, I wrote the first draft of the manuscript and prepared the figures included.

### **III. Preparación de emulsiones dobles agua-aceite-agua ( $W_1/O/W_2$ ) conteniendo *trans*-resveratrol**

El *trans*-resveratrol es un polifenol natural que se encuentra en una amplia variedad de plantas. Presenta efectos beneficiosos para la salud humana, ya que, además de sus propiedades antioxidantes y anti-inflamatorias, es cardioprotector y antitumoral. Sin embargo, sus aplicaciones están limitadas por ser un compuesto fácilmente oxidable, extremadamente fotosensible, con baja solubilidad en agua, corta vida media biológica, rápido metabolismo y eliminación. Se han llevado a cabo diversos estudios de encapsulación con el fin de proteger el *trans*-resveratrol de la degradación, aumentando su solubilidad en agua y facilitando su vehiculización a lugares específicos, a través de formas multiparticuladas y sistemas coloidales.

El objetivo de este trabajo era preparar emulsiones dobles del tipo agua- aceite-agua ( $W_1/O/W_2$ ) conteniendo *trans*-resveratrol, ya fuera por agitación mecánica o emulsificación con membranas. Paralelamente, se determinó la estabilidad de encapsulación, analizando la concentración de *trans*-resveratrol mediante RP-HPLC con detectores UV-VIS y de fluorescencia.

**Artículo 3. M. Matos, G. Gutiérrez, J. Coca y C. Pazos. "Preparation of water-in-oil-in-water ( $W_1/O/W_2$ ) double emulsions containing *trans*-resveratrol".**

**Colloids and Surfaces A: Physicochemical and Engineering Aspects**  
<http://dx.doi.org/10.1002/fsn3.17>.

#### **Aportación personal al trabajo**

En este trabajo llevé a cabo la labor experimental, lo que me permitió adquirir experiencia en el manejo de técnicas poco conocidas para mí hasta entonces, caso de la cromatografía líquida de alta eficacia (HPLC) y fase reversa (RP). Al mismo tiempo, realicé la búsqueda bibliográfica correspondiente. Finalmente, redacté la mayor parte del manuscrito y preparé las figuras incluidas en el mismo.



### Preparation of water-in-oil-in-water ( $W_1/O/W_2$ ) double emulsions containing *trans*-resveratrol

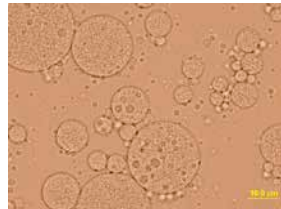
M. Matos, G. Gutiérrez, J. Coca, C. Pazos\*

Department of Chemical and Environmental Engineering, University of Oviedo, Julián Clavería 8, 33006 Oviedo, Spain

#### HIGHLIGHTS

- Resveratrol was encapsulated in water-in-oil-in-water double emulsions.
- These emulsions were prepared by mechanical agitation and membrane emulsification.
- Resveratrol encapsulation efficiency was determined by RP-HPLC method.
- An appropriate selection of emulsion stabilizers increased resveratrol encapsulation.
- Encapsulation and release of resveratrol were influenced by PGPR content.

#### GRAPHICAL ABSTRACT



#### ARTICLE INFO

##### Article history:

Received 30 November 2012

Received in revised form 20 March 2013

Accepted 16 May 2013

Available online xxx

##### Keywords:

*trans*-Resveratrol

Encapsulation

Double emulsions

RP-HPLC

Stability

#### ABSTRACT

*trans*-Resveratrol (3,5,4'-trihydroxystilbene) is a naturally occurring polyphenol phytoalexin easily oxidizable and extremely photosensitive with a short biological half-life. The goal of this work was to prepare  $W_1/O/W_2$  double emulsions of food-grade formulation to encapsulate *trans*-resveratrol. Mechanical agitation and membrane emulsification (ME) were the techniques used for emulsion preparation. A technique based on RP-HPLC to determine *trans*-resveratrol concentration in the external aqueous phase with UV-vis and fluorescence detectors was developed. Several inner emulsifiers were tested to produce stable water-in-oil ( $W_1/O$ ) emulsions containing 20% (v/v) of ethanol. Polyglycerol polyricinoleate (PGPR) was the only emulsifier with good stabilizing properties. Non-ionic surfactants (Tween 20 and Tween 80) were used as outer emulsifiers. Other food bioemulsifiers, such as sodium caseinate (NaCn), sodium carboxymethylcellulose (CMCNa) or gelatin, were also added as stabilizers to improve  $W_1/O/W_2$  double emulsions stability. Initial encapsulation efficiency (EE) and encapsulation stability (ES) were measured. The combination of Tween 20 and CMCNa in the external aqueous phase seemed to have a synergistic effect leading to better initial EE values. More stable emulsions were obtained with mechanical agitation. An increase in PGPR content yielded a slight increase in initial EE values.

© 2013 Elsevier B.V. All rights reserved.

#### 1. Introduction

*trans*-Resveratrol (3,5,4'-trihydroxystilbene) is a natural occurring polyphenol found in a wide variety of plants. It has beneficial effects for human health, such as anti-oxidant, anti-inflammatory, cardioprotective and anti-tumor properties.

However, the applications of *trans*-resveratrol are limited because it is an easily oxidizable and extremely photosensitive compound, with low water solubility, short biological half-life, and rapid metabolism and elimination [1–3]. The level of *trans*-resveratrol in wines depends on the production technology and is usually lower in white wines [4]. The average content in red wines reported by Gürbüz et al. was  $1.089 \pm 0.002$  mg/L [5].

Encapsulation of polyphenols can effectively mitigate these limitations [1,6]. Encapsulation studies have been carried out to protect *trans*-resveratrol from degradation, increasing its solubility

\* Corresponding author. Tel.: +34 985103509; fax: +34 985103434.  
E-mail address: [cpazos@uniovi.es](mailto:cpazos@uniovi.es) (C. Pazos).

in water and targeting it to specific locations via multiparticulate forms and colloidal carriers [1,3,7–14].

Several methods for the encapsulation of polyphenols have been reported, such as spray drying, coacervation, liposome entrapment [11,12,14,15], inclusion complexation [13], cocrystallization, nanoencapsulation [7,10], freeze drying and emulsification [8,9].

Multiple emulsions were first reported in 1925 by Seifriz. The simplest multiple emulsions are called double emulsions and they are ternary systems, having either a water-in-oil-in-water ( $W_1/O/W_2$ ) or an oil-in-water-in-oil ( $O_1/W/O_2$ ) structure, whereby the dispersed droplets contain smaller droplets of a different phase [16]. The structural properties of this kind of multiple emulsions permit controlled release of a component from the inner to the outer phase. This leads to a number of potential applications in the fields of medicine, pharmacy, cosmetics and separation processes [16–23].

$W_1/O/W_2$  double emulsions have potential applications in food, cosmetic and pharmaceutical industries as vehicles for encapsulation and delivery of nutrients during food digestion or for drug release [24–30,22]. This type of emulsions may also be used for the encapsulation of sensitive food materials and flavors and in the formulation of low calorie food products [26]. The main problem in the production of double emulsions is their instability, due to the excess of free energy associated with the surface of the emulsion droplets [16,17].

The suitability of  $W_1/O/W_2$  double emulsions to encapsulate *trans*-resveratrol has been reported by Hemar et al. [31]. Its concentration in the external aqueous phase was measured by a simple UV method. However, other techniques have been developed for determining *trans*-resveratrol content, such as gas chromatography with mass selective detection (GC-MS) and high-performance liquid chromatography (HPLC) with UV or fluorescence detection [4,5,32,33].

The aim of this work was to prepare  $W_1/O/W_2$  double emulsions containing *trans*-resveratrol, either by mechanical agitation or membrane emulsification (ME). Encapsulation stability (ES) was determined by RP-HPLC using UV-vis and fluorescence detectors.

## 2. Materials and methods

### 2.1. Materials

*trans*-Resveratrol, absolute ethanol, Tween 20, Tween 80, Span 80, sodium carboxymethylcellulose (CMCNa), gelatin and sodium caseinate salt from bovine milk (NaCn) were purchased from Sigma-Aldrich (USA). Miglyol 812 (density 945 kg/m<sup>3</sup> at 20°C) was supplied by Sasol GmbH (Germany). Polyglycerol polyricinoleate (PGPR) was supplied by Brenntag AG (Germany). Sodium chloride was obtained from Panreac (Spain). Plurol oleique (polyglyceril-6-dioleate) and Peceoil (glycerylmonoleate, type 40) were purchased from Gattefossé SAS (France). Methanol, acetonitrile, 2-propanol and acetic acid of HPLC-grade were obtained from Sigma-Aldrich (USA).

### 2.2. Methods

#### 2.2.1. Water-in-oil ( $W_1/O$ ) emulsions preparation

Primary  $W_1/O$  single emulsions were prepared using 20% (v/v) of the inner aqueous phase ( $W_1$ ) and 80% (v/v) of the continuous oily phase (O). *trans*-Resveratrol is barely soluble in water and its solubility in alcohols decreases as the carbon number of the alcohol increases [33]. Thus, a 20% ethanol (v/v) solution was used as the dispersed phase containing 50 mg/L of *trans*-resveratrol.

Miglyol 812 was used as the continuous phase containing the corresponding hydrophobic emulsifier previously dissolved

by stirring at 50 °C for 30 min. The hydrophilic-lipophilic balance (HLB) of an emulsifier is an adequate parameter to predict the resulting emulsion type (W/O or O/W) [20,27]. The HLB values of the inner emulsifiers tested in this study are as follows: Span 80 = 4.3, PGPR = 3.0, Peceoil = 3.0, and Plurol oleique = 6.0. PGPR is commonly used in food formulation and it has been demonstrated to be highly effective for stabilizing  $W_1/O$  emulsions [24,34].

It has been reported that the addition of electrolytes to the aqueous phase increases the  $W_1/O$  emulsion stability. It has been suggested that the presence of electrolytes lowers the attractive force between water droplets, decreasing the dielectric constant of the aqueous phase and therefore reducing collision frequency [24,29,30]. Consequently, 0.1 M NaCl was added to the internal aqueous phase to ensure inner droplets stability.

Both continuous and dispersed phases were emulsified in glass vessels by high shear mixing (Micra D-9 mixer, ART, Germany) using a 6 mm dispersing tool at 20,000 rpm for 2 min.

#### 2.2.2. Water-in-oil-in-water ( $W_1/O/W_2$ ) double emulsions preparation

$W_1/O/W_2$  double emulsions were prepared either by mechanical agitation or ME by dispersion of 20% (v/v) of  $W_1/O$  emulsions in an external continuous phase ( $W_2$ ) containing 0.1 M NaCl in order to match the osmotic pressure between the two aqueous phases.

When Tween 20, Tween 80 and NaCn were used as outer stabilizers they were previously dissolved by stirring for 30 min. Nevertheless, when CMCNa and gelatin were used they needed to be agitated overnight.

For mechanical agitation, the continuous and dispersed phases were emulsified using the aforementioned Micra D-9 mixer at 11,000 rpm for 2 min.

A 200 mL Amicon model 8200 stirred batch ultrafiltration cell (Amicon Inc., USA) was fitted to the membrane emulsification experiments. The dispersed phase was injected from the bottom side of the cell by a syringe pump KDS-100-CE (KD Scientific, USA) at a rate of 20 mL/min. The continuous phase was placed on the upper part of the cell being continuously stirred at 600 rpm, to enhance droplet detachment. Operating conditions were selected based on results obtained from previous studies (results not shown).

The membrane used was a hydrophilic metallic membrane with 5 µm pore size, supplied by Micropore Ltd. (UK). When using this membrane emulsification technique, the diameter of the droplets produced is approximately between 2 and 10 times the diameter of the membrane pore [25,35].

After each experiment membranes were cleaned with a dish-washing detergent and rinsed with deionized water and acetone in an ultrasound bath for 15 min. Finally, they were dried using compressed air and pre-soaked in the continuous phase.

#### 2.2.3. Emulsion characterization

Droplet size distributions were obtained by the laser light scattering technique in a Mastersizer S long bench apparatus (Malvern Instruments, Ltd., UK). For double emulsions a refractive index of 1.54 was used.

Samples were first diluted with deionized water to prevent multiple scattering effects. They were then circulated through the measuring zone using a Hydro SM small volume sample dispersion unit, following the manufacturer recommendations for this type of emulsions. For the single  $W_1/O$  emulsion, the water refractive index was used and the samples were dispersed in paraffin oil (VWR Int., USA).

Several measurements were made for each emulsion changing the dilution ratio. No significant differences were observed in the mean droplet diameters, ranging from 1:10 to 1:100 dilution ratios. Three replicates were obtained for each emulsion and

results were reported as the typical droplet size distribution in  $\mu\text{m}$ . The mean diameters,  $D_{[4,3]}$  and  $D_{[3,2]}$ , were calculated by Eqs. (1) and (2):

$$D_{[4,3]} = \frac{\sum n_i d_i^4}{\sum n_i d_i^3} \quad (1)$$

$$D_{[3,2]} = \frac{\sum n_i d_i^3}{\sum n_i d_i^2} \quad (2)$$

where  $d_i$  is the droplet diameter and  $n_i$  the number of droplets with diameter  $d_i$ .  $D_{[4,3]}$  is the volume weighted mean diameter and  $D_{[3,2]}$  is the surface weighted mean diameter or Sauter mean.

A Zetasizer NanoZS (Malvern Instruments Ltd., UK) was utilized for zeta potential ( $\zeta$ ) measurements of the  $W_1/O/W_2$  double emulsions. Three replicates were conducted for each sample at constant temperature of  $25^\circ\text{C}$ .

Micrographs of the emulsions were obtained with a light microscope Olympus BX50 (Olympus, Japan) with  $10\text{--}100\times$  magnification using UV-vis and fluorescence lamps.

Emulsion stability was analyzed by measuring backscattering (BS) and transmission (TS) profiles in a Turbiscan apparatus (Formulaction, France). Emulsions samples were placed without dilution in the test cells and transmitted and backscattered light was monitored as a function of time and cell height for 7 days at  $30^\circ\text{C}$ . The optical reading head scans the sample in the cell, providing TS and BS data every  $40\text{ }\mu\text{m}$  in % relative to standards (suspension of monodisperse spheres and silicone oil) as a function of the sample height (in mm). These profiles build up a macroscopic fingerprint of the emulsion at a given time, providing useful information about changes in droplet size distribution or appearance of a creaming layer or a clarification front with time [36,37].

Emulsions viscosity measurements were performed with a Haake RS50 rheometer (Haake, Germany) using plate-plate configuration at  $25^\circ\text{C}$ . Viscosity was measured at  $20\text{ s}^{-1}$  constant shear rate for 180 s.

The viscosities of external aqueous phases were measured by an Ubbelohde type viscometer PSL-Rheotek (Poulten Selfe & Lee Ltd., UK) at  $25^\circ\text{C}$ .

Interfacial tension ( $\gamma$ ) was determined following the Du Noüy's platinum ring method at  $20^\circ\text{C}$  using a Sigma 700 tensiometer (KSV Instruments Ltd., Finland).

#### 2.2.4. Determination of the initial encapsulation efficiency (EE) and encapsulation stability (ES) by RP-HPLC analysis

*trans*-Resveratrol content in the external aqueous phase was determined by chromatography (HP series 1100 chromatograph, Hewlett Packard, USA). The system was equipped with a UV-vis absorbance detector HP G1315A and a fluorescence detector 1260 Infinity A (Agilent Technologies, USA).

The column used for the separation was a reversed phase column Zorbax Eclipse Plus C<sub>18</sub> of  $5\text{ }\mu\text{m}$  particle size,  $4.6\text{ mm} \times 150\text{ mm}$  (Agilent Technologies, USA). The mobile phase consisted of a mixture of (A) 100% milliQ-water and (B) 100% methanol with gradient elution at a flow rate of  $0.8\text{ mL/min}$ . The step gradient started with 80% mobile phase (A) running 100% of mobile phase (B) in min 5 for 10 min. The mobile phase (B) was run for 2 min after each injection to prepare the column for the next run. The separation was carried out at room temperature.

A wavelength of  $305\text{ nm}$  was used for UV-vis detector while fluorescence detector was used at  $\lambda_{\text{excitation}}/\lambda_{\text{emission}}$  at  $310/410\text{ nm}$ . The column was cleaned after each analysis by running first mobile phase (A) for 20 min and a mobile phase (C) consisting of 50% acetonitrile, 25% milliQ-water, 25% 2-propanol and 0.01% acetic acid for 40 min at a flow rate of  $0.25\text{ mL/min}$ . Finally, the column was

rinsed with 50% of mobile phase (A) and 50% of mobile phase (B) for another 20 min.

The external aqueous phase injected in the HPLC system was previously recovered by centrifugation at low speed ( $1000\text{ rpm}$  for 20 min) and filtration with a  $0.22\text{ }\mu\text{m}$  polyvinylidene difluoride (PVDF) syringe filter, to eliminate all the cream oily phase still present.

Other filters as polyethersulfone (PES) or nylon were also tested although considerably high resveratrol retention values were obtained: 29 and 100%, respectively.

The recovery yield ( $R_y$ ) was determined to measure the amount of *trans*-resveratrol retained during the centrifugation and filtration processes. A standard emulsion, where 100% of the  $W_1$  is present in  $W_2$ , was required. For this purpose, an oil-in-water emulsion ( $O/W_2$ ) was prepared using the same formulation as in the experiments. This  $O/W_2$  emulsion was then diluted at the same ratio with  $W_1$ , which contained the appropriate amount of *trans*-resveratrol. Then, the concentration of *trans*-resveratrol in the recovered aqueous phases ( $C_{\text{recovered}}$ ) was determined by RP-HPLC, using the absorbance and fluorescence calibration curves previously obtained. For this analysis, a blank reference was used. It consisted of an  $O/W_2$  emulsion diluted with  $W_1$ , in which *trans*-resveratrol was not present. Finally, the  $R_y$  was calculated as:

$$R_y (\%) = \frac{C_{\text{recovered}} \times 100}{C_0} \quad (3)$$

where  $C_0$  is the maximum concentration of *trans*-resveratrol expected in the external aqueous phase.

The encapsulation efficiency (EE) of these double emulsions was defined as the percentage of *trans*-resveratrol in  $W_1$  that remained in the primary emulsion ( $W_1/O$ ) after the second emulsification step [26,38]. It was calculated by Eq. (4):

$$\text{EE } (\%) = 100 - \frac{C_{\text{recovered}} \times 100}{C_0 R_y} \quad (4)$$

The encapsulation stability (ES) was defined as the amount of *trans*-resveratrol that remained entrapped in the inner aqueous phase ( $W_1$ ) during storage or after double emulsion exposure to environmental stresses [38]. It was calculated by Eq. (5):

$$\text{ES } (\%) = 100 - \frac{C_{\text{recovered}} \times 100}{C_0 R_y} \quad (5)$$

Several samples were prepared and stored at room temperature to measure the ES weekly along a month. Three replicates of each sample were determined.

## 3. Results and discussion

### 3.1. Water-in-oil ( $W_1/O$ ) emulsions

To obtain a stable double emulsion, the stability of the single  $W_1/O$  emulsion must be ensured. This stability depends on droplet size (normally around  $1\text{ }\mu\text{m}$ ), amounts of dispersed and continuous phase (water is usually in the range 20–30%, v/v), and emulsifier affinity for both phases (HLB) [17–20,27].

Several  $W_1/O$  emulsions were prepared at the same concentration, 5% (w/v), varying the type of inner emulsifier present in the oily phase. The droplet size distributions of the resulting emulsions were measured and their stability was determined and compared by laser light scattering.

The mean diameters obtained with the Malvern Mastersizer S are shown in Table 1. The  $D_{[3,2]}$  values are in the  $0.3\text{--}1.7\text{ }\mu\text{m}$  range, except for Peceol, which leads to sizes considerably higher. The polydispersity of the droplet size distribution was expressed in

# ARTICLE IN PRESS

M. Matos et al. / Colloids and Surfaces A: Physicochem. Eng. Aspects xxx (2013) xxx–xxx

**Table 1**

Mean droplet diameters and span values of W<sub>1</sub>/O emulsions with different inner emulsifiers at 5% (w/v) (SD = standard deviation).

Inner emulsifier	D <sub>[4,3]</sub> (μm)	SD	D <sub>[3,2]</sub> (μm)	SD	Span	SD
PGPR	0.74	0.16	0.27	0.18	1.68	0.47
Span 80	3.73	0.05	0.64	0.04	2.32	0.32
Plurol oleique	2.81	0.08	1.73	0.01	3.81	0.21
Peceol	10.34	1.31	4.39	5.11	2.05	0.70

terms of span, which is a measure of the width of the droplet size distribution. It is defined as:

$$\text{span} = \frac{D(v, 0.9) - D(v, 0.1)}{D(v, 0.5)} \quad (6)$$

where D(v,0.5), D(v,0.1) and D(v,0.9) are standard percentile readings from the analysis. D(v,0.5) is the size in microns at which 50% of the sample is smaller and 50% is larger. D(v,0.1) and D(v,0.9) are the size of the droplets below 10% and 90% respectively of the sample lies. It can be observed in Fig. 1 that droplet size distributions are highly polydisperse. When PGPR was used lower span values were obtained.

Fig. 2A shows the kinetic BS profiles obtained in the middle zone of the cell (from 10 to 30 mm). The corresponding TS profiles obtained at the bottom of the cell (from 0 to 10 mm) are also shown for a better understanding of emulsions behavior. Samples were monitored for a week. A photograph of the glass cells, containing the W<sub>1</sub>/O emulsions after being measured, is shown in Fig. 2B.

The stability of W<sub>1</sub>/O emulsions prepared with PGPR and Spans as emulsifiers had been studied by Márquez et al. using a similar

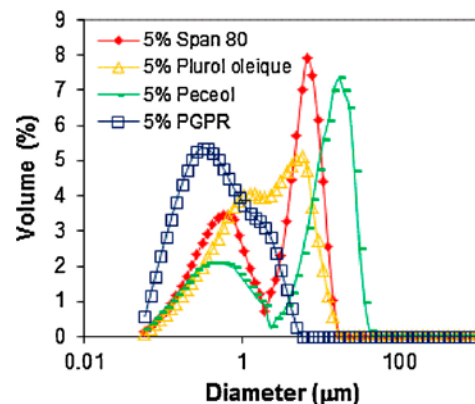


**Fig. 1.** Droplet size distributions of W<sub>1</sub>/O emulsions with different inner emulsifiers at 5% (w/v).

vertical scan analyzer [24,39]. It was reported that a decrease of the BS values, along the height of the cell, implies an increase of the water droplets size due to a coalescence process. It was also confirmed that an increase of BS at the bottom corresponds to sedimentation of the water droplets [24,39]. This trend was observed for Peceol and Span 80 (Fig. 2A).

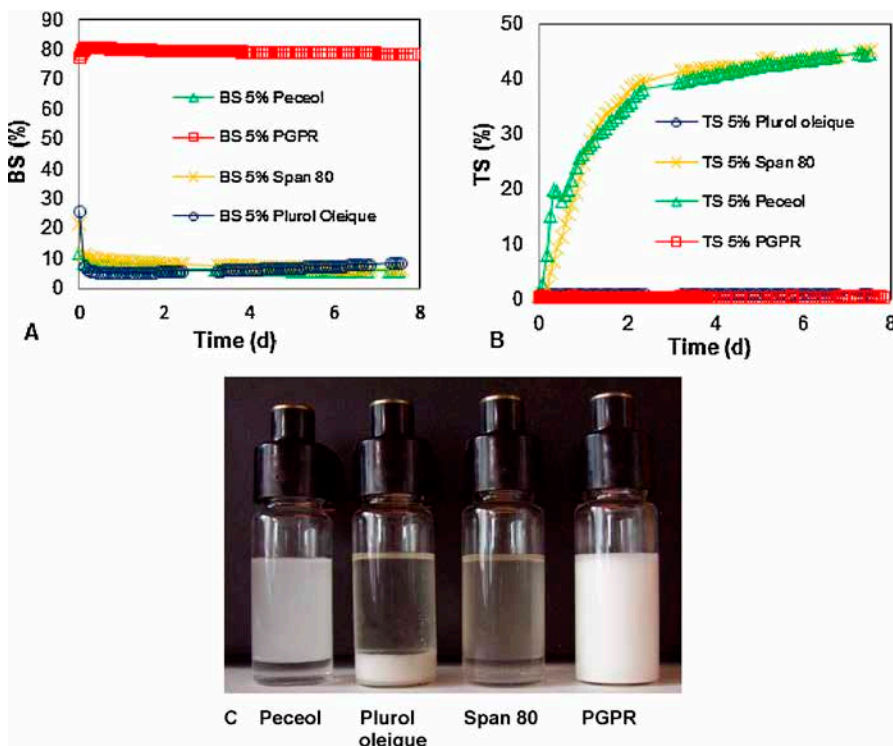


**Fig. 2.** Kinetic backscattering and transmission profiles of W<sub>1</sub>/O emulsions prepared with different inner emulsifiers at 5% (w/v) (A and B). Turbiscan glass cells showing these emulsions after being measured (C).

Please cite this article in press as: M. Matos, et al., Preparation of water-in-oil-in-water (W<sub>1</sub>/O/W<sub>2</sub>) double emulsions containing *trans*-resveratrol, Colloids Surf. A: Physicochem. Eng. Aspects (2013), <http://dx.doi.org/10.1016/j.colsurfa.2013.05.065>

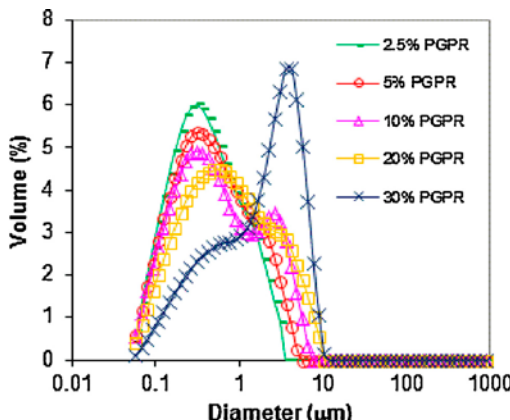


**Fig. 3.** Influence of PGPR concentration on droplet size distributions of  $W_1/O$  emulsions.

In addition, a simultaneous increase in TS values was also observed at the bottom what indicates the formation of the water layer. This behavior was confirmed regarding Fig. 2B where the water layer appears in the cells containing these emulsions.

However, the opposite behavior in the TS profiles was observed when Plurhol oleique and PGPR were used. This indicates the presence of an emulsion in this area, as shown in Fig. 2B. In the case of Plurhol oleique, an oil-in-water ( $O/W_1$ ) emulsion was formed and settled at the bottom. This may be explained because this emulsifier has the largest HLB value (6.0) and shows higher affinity for the aqueous phase. The emulsion prepared with PGPR offers higher stability, giving the lowest variation of BS with time (2.5%). This indicates that there are no changes in droplet size, remaining the emulsion stable.

Therefore, all the emulsifiers studied offered poor stabilizing properties, except PGPR, as was previously reported by de los Reyes and Charcosset [19]. They determined that more stable ethanol-in-water ( $E/O$ ) emulsions were obtained using polyglycerol esters of oleic acid.

Several  $W_1/O$  emulsions were prepared at different concentrations of PGPR: 2.5, 5, 10, 20 and 30% (w/v) to determine the optimum value. The resulting droplet size distributions are shown in Fig. 3.

All the emulsions prepared with PGPR had a mean diameter  $D_{[3,2]}$  lower than 1  $\mu\text{m}$  (Table 2). Comparing emulsions prepared with 2.5–10% (w/v) of PGPR, it was observed that the mean droplet size decreased as the amount of PGPR increased, as it might be expected.

Otherwise, for emulsions prepared with 20 and 30% (w/v) of PGPR an increase in  $D_{[4,3]}$  was observed, with values up to 2  $\mu\text{m}$ . This effect of PGPR on the stability of  $W_1/O$  emulsions had been previously reported [24]. A lower droplet size at higher surfactant content reduces coalescence, as a result of lower collision efficiency due to the higher emulsion viscosity.

Márquez et al. determined that the presence of salts may also interfere on the adsorption density of PGPR at the interfacial film and concluded that the increase of stability produced by increasing salt or PGPR concentration (0.2–0.5 and 1.0% (w/w)) could be attributed to the reduction of the interfacial tension, rather than to the viscoelastic properties of the film [24].

In Table 2 are shown the interfacial tension ( $\gamma$ ) and viscosity ( $\mu$ ) values of the emulsions as a function of PGPR content. There were no considerable differences between the interfacial

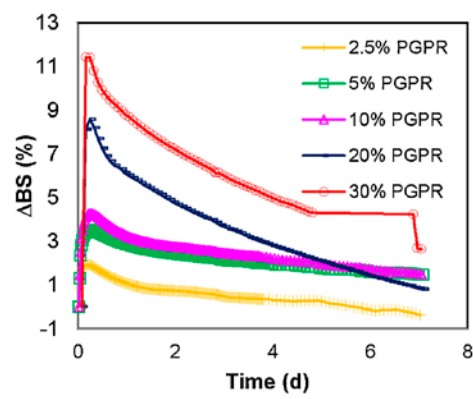


**Fig. 4.** Kinetic  $\Delta\text{BS}$  profiles of  $W_1/O$  emulsions with different PGPR concentrations.

tensions obtained, probably due to the presence of NaCl and the large amount of PGPR added. Furthermore, an increase in viscosity values as PGPR content rises was observed, as predicted.

For better comparison of these emulsions stability, the kinetic BS profiles were obtained plotting incremental values of BS ( $\Delta\text{BS}$ ) versus time for a week. Table 2 also shows maximum  $\Delta\text{BS}$  ( $\Delta\text{BS}_{\max}$ ) values obtained applying Eq. (7):

$$\Delta\text{BS}_{\max} = \Delta\text{BS}_{\max\ 10-30} - \Delta\text{BS}_{\min\ 10-30} \quad (7)$$

No significant backscattering variation with time was observed for emulsions prepared with 2.5, 5 and 10% (w/v), as shown in Fig. 4. The values of  $\Delta\text{BS}_{\max}$  obtained with these emulsions were quite low (<2.5%) indicating high stability, probably due to 0.1 M NaCl addition. Emulsions prepared with 20 and 30% (w/v) of PGPR showed BS variations slightly higher with values of 8–9%.

Márquez et al. also compared the stability of  $W_1/O$  emulsions prepared with PGPR and studied the influence of  $\text{CaCl}_2$  addition at several concentrations [24]. Using 1% of PGPR they obtained BS variations from 15%, with no addition of  $\text{CaCl}_2$ , to 1% when 1000 mg/100 g of  $\text{CaCl}_2$  was added. The low  $\Delta\text{BS}$  values obtained indicate that there was no considerable change in droplet size, remaining the emulsions stable after one week.

### 3.2. Water-in-oil-in-water ( $W_1/O/W_2$ ) double emulsions

$W_1/O/W_2$  double emulsions were prepared with several outer emulsifiers to choose the best formulation, i.e. which provides the higher initial EE. The addition of stabilizing agents, such as CMCNa or gelatin, was also studied.

In  $W_1/O/W_2$  double emulsions preparation, Tween 20, Tween 80 and NaCn at the same concentration, 2% (w/v), were selected as outer emulsifiers. The resulting droplet size distributions and their stability in terms of initial EE were compared. The oily phase used in this set of experiments was Miglyol 812 containing 5% (w/v) of PGPR.

The bimodal droplet size distributions shown in Fig. 5 were highly polydisperse. Droplet sizes were in the 1–30  $\mu\text{m}$  range with two well-defined peaks at 4 and 10  $\mu\text{m}$  when Tween 20 and Tween 80 were used. With NaCn small droplets (0.1–0.6  $\mu\text{m}$  range) and large droplets from 1.5 to 56  $\mu\text{m}$  were obtained.

Hemar et al. prepared double emulsions containing *trans*-resveratrol using NaCn 0.5% (w/w) and also obtained a bimodal droplet size distribution, with small particles in the 0.1–1  $\mu\text{m}$  range and large particles in the 1–100  $\mu\text{m}$  range [31].

**Table 2**

Mean droplet diameters, span, maximum backscattering variation ( $\Delta BS_{max}$ ), interfacial tensions ( $\gamma$ ) and viscosity ( $\mu$ ) values of  $W_1/O$  emulsions with different PGPR concentrations (SD = standard deviation).

PGPR (% w/v)	$D_{[4,3]}$ ( $\mu\text{m}$ )	SD	$D_{[3,2]}$ ( $\mu\text{m}$ )	SD	$\Delta BS_{max}$	$\gamma$ (mN/m)	SD	$\mu$ (mPa s)	SD
2.5	0.57	0.06	0.25	0.02	2.33	0.56	0.09	3788	44
5	0.74	0.16	0.27	0.18	2.20	0.41	0.11	4075	74
10	1.02	0.18	0.29	0.17	2.03	0.39	0.10	4801	659
20	1.29	0.28	0.35	0.16	7.78	0.28	0.09	8660	495
30	2.33	0.20	0.65	0.23	8.87	0.20	0.08	14,832	974

When Tween 20 was used as outer emulsifier, the  $R_y$  value for *trans*-resveratrol was  $97.84 \pm 2.96\%$  using the UV-vis detector, and  $97.78 \pm 2.74\%$  with the fluorescence detector. For Tween 80 similar values were obtained, being  $95.14 \pm 3.37\%$  and  $97.42 \pm 1.01\%$ , respectively.

Otherwise, for NaCn neither signal was obtained being 0% the corresponding  $R_y$  value. In conclusion, it was not possible to determine the EE by this method for double emulsions prepared with this emulsifier. However, if *trans*-resveratrol concentration was measured in aqueous samples prepared only in presence of NaCn, the expected signals appeared. Taking into account that *trans*-resveratrol binds to diary proteins [40,41], it may be located at the interface between the oil and the external aqueous phase containing the NaCn layer.

A slightly higher *trans*-resveratrol concentration (2% w/v) was obtained in  $W_2$  for emulsions prepared with Tween 20. Consequently, it was selected as the most appropriate emulsifier for the subsequent experiments.

Several  $W_1/O/W_2$  emulsions with three different concentration values, 2, 5, and 10% (w/v) were prepared to determine the optimal concentration of Tween 20. Two sets of experiments were performed containing 5 and 10% (w/v) of PGPR in the oily phase. In both cases it was observed that increasing Tween 20 concentration led to a decrease in the mean droplet diameter  $D_{[4,3]}$  (Fig. 6). No significant variations in zeta potential were appreciated by increasing emulsifier content, being negative values in all cases in the range of (-1.29 mV)–(-2.98 mV).

An increase in Tween 20 concentration led to a systematic decrease in the initial EE values (Fig. 7), presumably because of the mean droplet size reduction.

Kawashima et al. [42] also found that high concentrations of hydrophilic surfactant gave emulsions with lower entrapment capacity. It had been previously reported that a high concentration

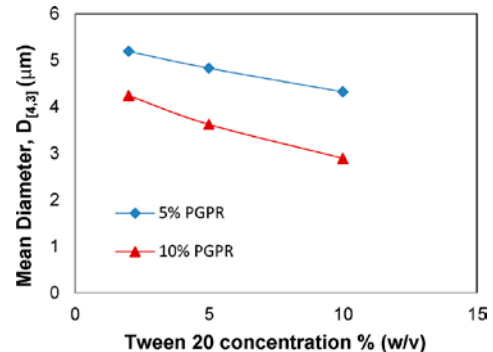


Fig. 6. Mean droplet diameter  $D_{[4,3]}$  of  $W_1/O/W_2$  emulsions with 5% and 10% (w/v) of PGPR in Miglyol 812 as oily phase and different Tween 20 concentrations in  $W_2$  phase.

of hydrophilic surfactant led to the oil film rupture and facilitated the release of inner water droplets [19]. Therefore, a 2% (w/v) value was the concentration selected for the rest of the experiments.

The use of soluble polysaccharides acting as thickening/gelling agents, to stabilize the outer droplets of double emulsions preventing creaming and coalescence phenomena, has been previously reported [26,43]. One of the advantages of polysaccharides solutions is their low plastic viscosity at low concentrations, which prevents the breakdown of multiple droplets during double emulsion manufacturing [43].

Several  $W_1/O/W_2$  emulsions were prepared adding CMCNa, in the range 0–0.5% (w/v), to the  $W_2$  phase, which consisted of 2% (w/v) of Tween 20 and 0.1 M NaCl. Two sets of experiments were performed using 5% and 10% (w/v) of PGPR, respectively, in the oily phase. Table 3 presents the external aqueous phase viscosity values measured at 25 °C.

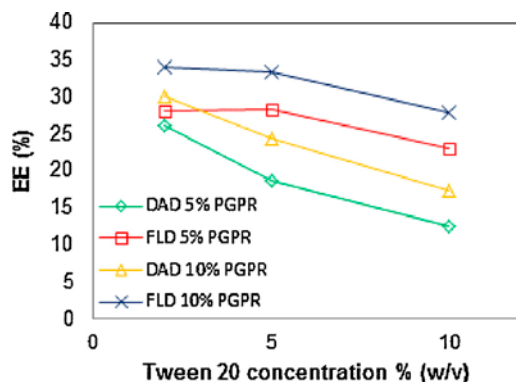


Fig. 7. Influence of Tween 20 concentration on encapsulation efficiency of  $W_1/O/W_2$  emulsions.

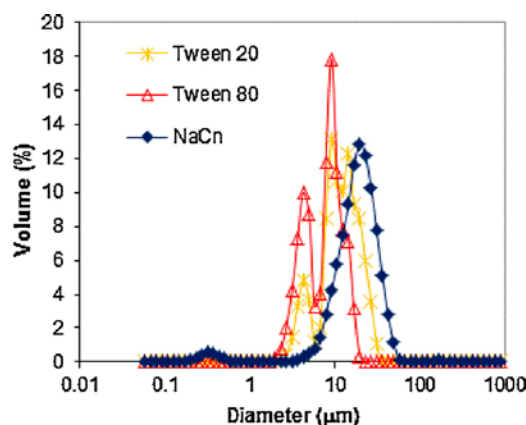


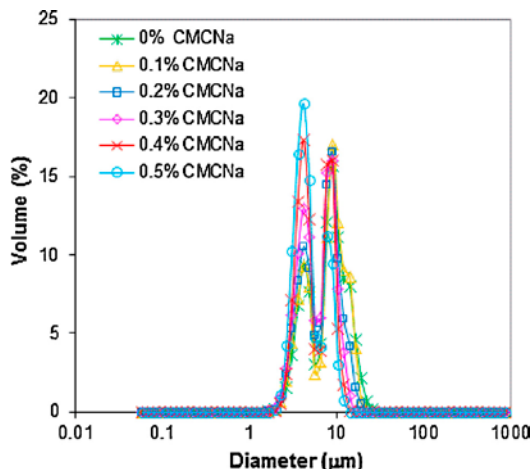
Fig. 5. Droplet size distributions of  $W_1/O/W_2$  emulsions with 5% (w/v) of PGPR in Miglyol 812 as oily phase and different outer emulsifiers.

Please cite this article in press as: M. Matos, et al., Preparation of water-in-oil-in-water ( $W_1/O/W_2$ ) double emulsions containing *trans*-resveratrol, *Colloids Surf. A: Physicochem. Eng. Aspects* (2013), <http://dx.doi.org/10.1016/j.colsurfa.2013.05.065>

**Table 3**

Viscosity values of external aqueous phases at different CMCNa concentrations.

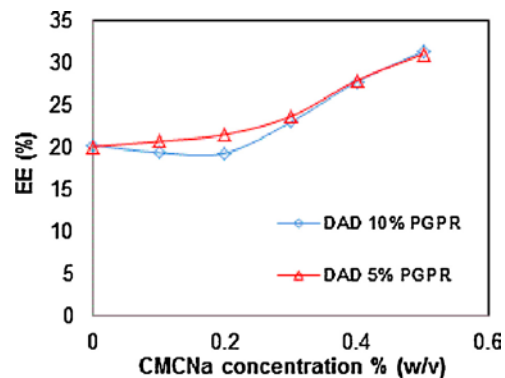
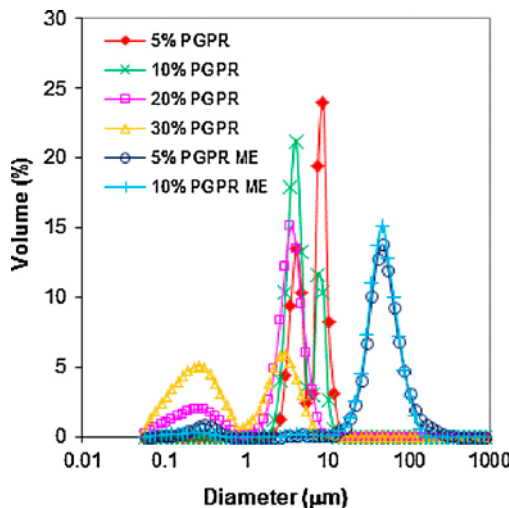
CMCNa (% w/v)	Viscosity (mPa s)
0	1.14
0.1	1.75
0.2	2.37
0.3	3.64
0.4	5.34
0.5	6.85

**Fig. 8.** Droplet size distributions of  $W_1/O/W_2$  emulsions with 5% (w/v) of PGPR in Miglyol 812 as oily phase, 2% (w/v) of Tween 20 as outer emulsifier and different CMCNa concentrations added to  $W_2$  phase.

The bimodal droplet size distributions obtained with 5% PGPR (w/v) are shown in Fig. 8, although the same trend was observed in both cases. As CMCNa concentration increased, a gradual and slight increase in the number of droplets of 4 μm was detected, while the number of droplets of 10 μm size decreased. As a result, the mean diameter decreased as CMCNa concentration rose (Table 4).

It was also observed a decrease in the interfacial tension ( $\gamma$ ) of the outer interface when CMCNa was added. Values of  $3.43 \pm 0.03$  and  $2.57 \pm 0.16$  mN/m were obtained without CMCNa, when 5 and 10% (w/v) of PGPR were respectively used. Values of  $2.84 \pm 0.03$  and  $2.34 \pm 0.24$  mN/m were obtained with 0.5% (w/v) CMCNa addition. This reduction of interfacial tension would also explain the decrease of the mean diameters values when CMCNa was added to  $W_2$ .

Apart from reducing the interfacial tension and increase the viscosity of  $W_2$ , CMCNa could also affect the interactions between Tween 20 molecules adsorbed at the interface. As Fig. 9 shows, the increase of CMCNa concentration resulted in a systematic enhancement of initial encapsulation efficiency value. These results

**Fig. 9.** Encapsulation efficiency of  $W_1/O/W_2$  emulsions prepared with 5% and 10% (w/v) of PGPR in Miglyol 812 as oily phase and different CMCNa concentrations in  $W_2$  phase.**Fig. 10.** Droplet size distributions of  $W_1/O/W_2$  emulsions with 2% (w/v) of Tween 20 as outer emulsifier and different PGPR concentrations.

suggested that CMCNa played a significant role in the stabilization of the outer interface. The combination of Tween 20 and CMCNa seemed to have a synergistic effect. Thus, a cumulative adsorption at the interface, instead of competitive, was suggested. Similar behavior was observed when  $W_1/O/W_2$  double emulsions were prepared in presence of bovine serum albumin (BSA) and Tween 20 in the external aqueous phase [28].

**Table 4**Mean droplet diameters of  $W_1/O/W_2$  emulsions with 5% and 10% (w/v) of PGPR in Miglyol 812 as oily phase and different CMCNa concentrations in  $W_2$  phase (SD = standard deviation).

CMCNa (% w/v)	PGPR 5% (w/v)				PGPR 10% (w/v)			
	$D_{[4,3]}$ (μm)	SD	$D_{[3,2]}$ (μm)	SD	$D_{[4,3]}$ (μm)	SD	$D_{[3,2]}$ (μm)	SD
0.5	5.05	0.16	4.31	0.12	4.24	0.38	3.68	0.37
0.4	5.61	0.19	4.71	0.15	4.56	0.30	3.91	0.15
0.3	6.42	0.38	5.21	0.22	4.76	0.18	4.03	0.05
0.2	6.77	0.04	5.39	0.04	5.16	0.03	4.30	0.01
0.1	7.65	0.12	5.90	0.09	6.01	0.37	4.81	0.42
0	8.28	0.33	6.27	0.13	6.63	0.31	5.20	0.30

Please cite this article in press as: M. Matos, et al., Preparation of water-in-oil-in-water ( $W_1/O/W_2$ ) double emulsions containing *trans*-resveratrol, *Colloids Surf. A: Physicochem. Eng. Aspects* (2013), <http://dx.doi.org/10.1016/j.colsurfa.2013.05.065>

# ARTICLE IN PRESS

M. Matos et al. / Colloids and Surfaces A: Physicochem. Eng. Aspects xxx (2013) xxx–xxx

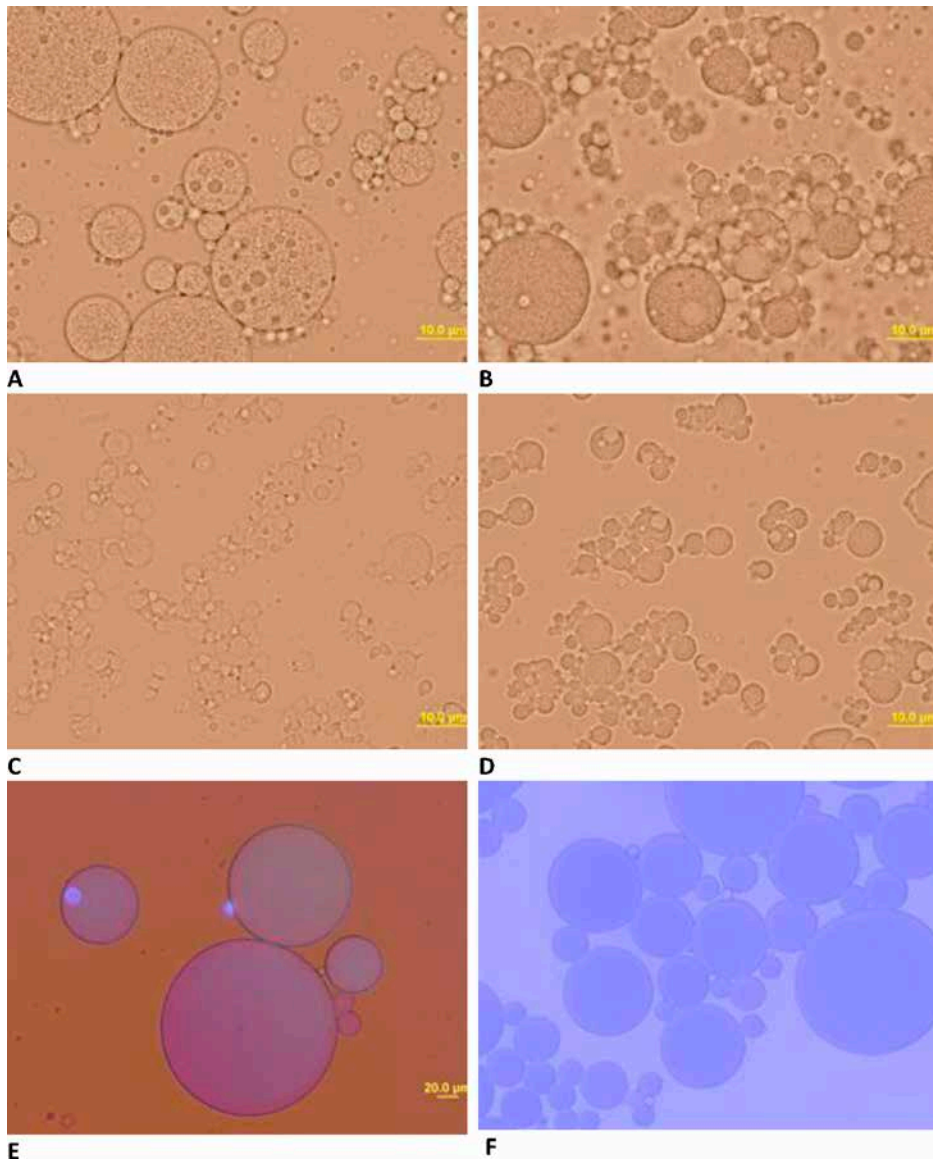


**Fig. 11.** Confocal image obtained using UV-vis lamp of the  $W_1/O/W_2$  emulsions prepared by mechanical agitation with 5% (A) 10% (B) 20% (C) and 30% (D) of PGPR. Fluorescence confocal image of  $W_1/O/W_2$  emulsions prepared by ME using 5% (E) and 10% (F) of PGPR.

Hence, the subsequent experiments were carried out by adding 0.5% (w/v) of CMCNa to the external aqueous phase.

A strategy to improve the initial EE value consists of incorporating various food biopolymers in the internal aqueous phase, to provide long-term stability to the first  $W_1/O$  emulsion by converting it into soft solid-like particles [44].

The use of compounds such as gelatin or NaCn has been reported showing that 1 wt% gelatin content produced a considerable encapsulation increase, improving the stability against coalescence occurred during the emulsification process [26].

It was also found that  $W_1/O/W_2$  emulsions prepared with 0.5% (w/v) of NaCn resulted in stable emulsions, requiring lower PGPR concentration [45].

Therefore,  $W_1/O$  emulsions were prepared by dispersing 0.5% (w/v) of gelatin in  $W_1$  in an oily phase containing 5% (w/v) of PGPR. The resulting emulsion was immediately cooled at 4 °C to allow the sol-gel transition of the gelatin. On the contrary, the second stage of homogenization was developed at room temperature as previous studies showed that emulsification at low temperatures could be inefficient [44].

Please cite this article in press as: M. Matos, et al., Preparation of water-in-oil-in-water ( $W_1/O/W_2$ ) double emulsions containing *trans*-resveratrol, *Colloids Surf. A: Physicochem. Eng. Aspects* (2013), <http://dx.doi.org/10.1016/j.colsurfa.2013.05.065>

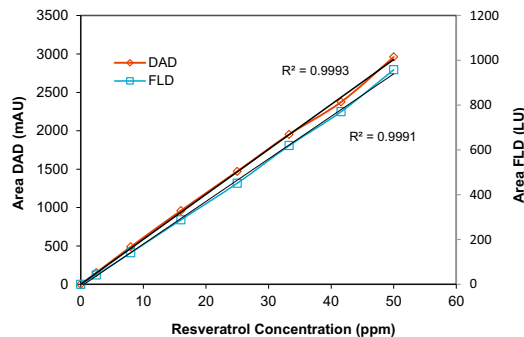


**Fig. 12.** RP-HPLC calibration curves using UV-vis absorbance and fluorescence detectors.

The same procedure was also applied adding CMCNa 0.5% (w/v) to the internal aqueous phase. The corresponding W<sub>1</sub>/O/W<sub>2</sub> double emulsions were prepared and *trans*-resveratrol content was determined. No improvement was observed obtaining similar initial encapsulation values, around 33% in both cases.

### 3.3. Encapsulation stability

Several W<sub>1</sub>/O/W<sub>2</sub> emulsions were prepared by the aforementioned methods, varying the PGPR content, to study the encapsulation capacity of these emulsions. The resulting droplet size distributions were measured and their structures were also analyzed by confocal laser microscopy (Figs. 10 and 11).

Emulsions prepared by mechanical agitation contained 5%, 10%, 20% and 30% (w/v) of PGPR. W<sub>1</sub>/O/W<sub>2</sub> double emulsions with 5% and 10% (w/v) PGPR were also prepared by ME yielding  $D_{4,3}$  values of 56.1 and 49.2  $\mu\text{m}$ , respectively. These values correspond to 10 times the pore size used, as expected.

Two peaks were clearly appreciated at 4  $\mu\text{m}$  and 10  $\mu\text{m}$  comparing the emulsions prepared with 5% and 10% (w/v) of PGPR by mechanical agitation. Furthermore, emulsions prepared with 5% (w/v) of PGPR yielded more droplets with 10  $\mu\text{m}$  size. However, more droplets of 4  $\mu\text{m}$  size appeared for 10% (w/v) of PGPR.

In addition, emulsions prepared with 20% and 30% (w/v) of PGPR showed small droplets in the range of 0.1–0.9  $\mu\text{m}$  and large droplets in the range 2–4  $\mu\text{m}$ . Consequently, the mean droplet sizes of these double emulsions decreased as PGPR concentration increased.

Zeta potentials for these emulsions were also measured, obtaining negative values very close to zero, range ( $-0.15 \text{ mV}$ )–( $-2.02 \text{ mV}$ ), in all cases.

In Fig. 11A and B, oil fat globules containing small droplets inside (inner phase) can be clearly identified. Smaller droplets (around 4  $\mu\text{m}$ ) were observed for 10% (w/v) of PGPR, according to the droplet size distributions for this emulsion. Smaller oil fat globules were detected in the case of emulsions with 20% and 30% (w/v) of PGPR.

Fig. 11E and F shows the bigger droplet size (50–60  $\mu\text{m}$  range) for emulsions prepared by ME. In Fig. 11E the oil fat globules have a blue color, due to the fluorescence of entrapped *trans*-resveratrol, while in Fig. 11F the blue color is also observed in the external aqueous phase.

These emulsions were stored at room temperature in darkness and ES was monitored weekly for one month. The calibration curves obtained by RP-HPLC using UV-vis absorbance (signal DAD) and fluorescence (signal FLD) detectors are shown in Fig. 12. A linear trend was obtained with high correlation coefficients.

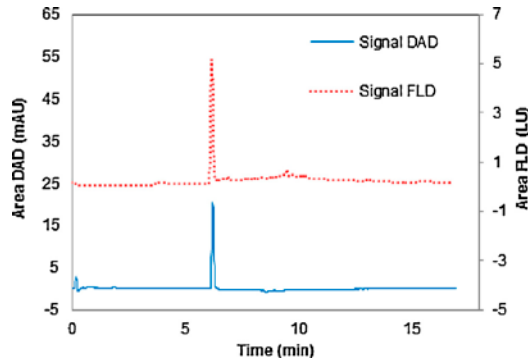


**Fig. 13.** Typical chromatographic peaks using UV-vis and fluorescence detectors for the recovered external aqueous phase from a W<sub>1</sub>/O/W<sub>2</sub> emulsion containing *trans*-resveratrol.

Fig. 13 shows a typical chromatographic profile where DAD and FLD signals are plotted versus time. It was observed that *trans*-resveratrol peaks were eluted in both cases at a retention time of 6 min, when 100% methanol was run as mobile phase.

It has been reported that release of encapsulated compounds in W<sub>1</sub>/O/W<sub>2</sub> double emulsions can mainly occur by two permeation mechanisms through the oil phase: (a) reverse micellar transport and (b) diffusion across a very thin lamellae of surfactant formed in areas where the oil layer is very thin [28]. Hemar et al. confirmed the difficulty demonstrating unequivocally the *trans*-resveratrol release mechanism [31].

Fig. 14 shows encapsulation stability (ES) versus time for all the emulsions studied. As it can be appreciate, ES values obtained with FLD were slightly higher than those obtained with DAD, although both signals showed the same trend. Comparing emulsions formulated with the same PGPR content, higher values were obtained for emulsions prepared by mechanical agitation. It has been previously reported that relatively high concentrations of hydrophilic surfactant in the outer aqueous phase are required for the production of stable emulsions by ME [19–21].

Emulsions prepared both by mechanical agitation or ME processes yielded slightly higher initial EE values with higher PGPR content, up to 40% when 30% (w/v) of PGPR was added. The same influence with PGPR concentration in the oil phase had been obtained by Su et al. [45].

Hemar et al. reported that the amount of *trans*-resveratrol released after two weeks under storage was lower than 10% of the total *trans*-resveratrol initially encapsulated. Initial EE values were not mentioned.

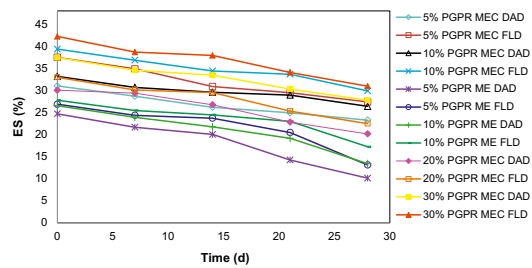


**Fig. 14.** Encapsulation stability versus time for W<sub>1</sub>/O/W<sub>2</sub> emulsions with different PGPR content (w/v) prepared by mechanical agitation (MEC) or by membrane emulsification (ME).

For double emulsions prepared by mechanical agitation with 10, 20 and 30% (w/v) of PGPR, *trans*-resveratrol release after two weeks was 10%, while for emulsions prepared with 5% the release was 15%. Thereby, the stability of double emulsions was also influenced by PGPR concentration. Similar results were reported by Su et al. [45].

Emulsions prepared by ME showed higher release probably due to the bigger size of the oil fat globules obtained by this technique.

#### 4. Conclusions

A procedure to determine the encapsulation efficiency (EE) of W<sub>1</sub>/O/W<sub>2</sub> double emulsions containing *trans*-resveratrol using RP-HPLC with UV-vis absorbance and fluorescence detectors was described.

For the formulation of water-in-oil-in-water (W<sub>1</sub>/O/W<sub>2</sub>) double emulsions to encapsulate *trans*-resveratrol, polyglycerol polyricinoleate (PGPR) was the best inner emulsifier. The combination of Tween 20 and CMCNa in the external aqueous phase seemed to have a synergistic effect leading to better initial EE values.

More stable emulsions were obtained when they were prepared by mechanical agitation. An increase in PGPR content yielded a slight increase in initial EE values.

W<sub>1</sub>/O/W<sub>2</sub> double emulsions formulated to encapsulate *trans*-resveratrol are complex systems due to ethanol present in W<sub>1</sub>, which was required to dissolve *trans*-resveratrol in water. Further formulations tests should be undertaken to improve the encapsulation ability of these emulsions.

#### Acknowledgments

M. Matos is recipient of a FPI pre-doctoral fellowship (MEC, Spain). Financial support by the Ministerio de Ciencia e Innovación (MICINN, Spain) and the European Commission (projects Ref.: CTQ2007-65348 and MICINN-10-CTQ2010-20009-C02-01 European Regional Development Fund) are gratefully acknowledged.

This study was co-financed by the Consejería de Educación y Ciencia del Principado de Asturias (PCTI Asturias 2006–2009, Ref.: EQP06-024).

#### References

- [1] A. Amri, J.C. Chaumeil, S. Sfar, C. Charreau, Administration of resveratrol: what formulation solutions to bioavailability limitations? *J. Control. Release* 158 (2012) 182–193.
- [2] P. Saiko, A. Szakmary, W. Jaeger, T. Szekeres, Resveratrol and its analogs: defense against cancer, coronary disease and neurodegenerative maladies or just a fad? *Mutat. Res.: Rev. Mutat. Res.* 658 (2008) 68–94.
- [3] H. Peng, H. Xiong, J. Li, M. Xie, Y. Liu, C. Bai, L. Chen, Vanillin cross-linked chitosan microspheres for controlled release of resveratrol, *Food Chem.* 121 (2010) 23–28.
- [4] I. Kolouchová-Hanzlíková, K. Melzoch, V. Filip, J. Šamídrk, Rapid method for resveratrol determination by HPLC with electrochemical and UV detections in wines, *Food Chem.* 87 (2004) 151–158.
- [5] O. Gürbüz, D. Göçmen, F. Dağdelen, M. Gürsoy, S. Aydin, İ. Şahin, L. Büyükuysal, M. Usta, Determination of *flavan-3-ols* and *trans*-resveratrol in grapes and wines using HPLC fluorescence detection, *Food Chem.* 100 (2007) 518–525.
- [6] Z.X. Fang, B. Bhandari, Encapsulation of polyphenols—a review, *Trends Food Sci. Technol.* 21 (2010) 510–523.
- [7] K. Teskac, J. Kristl, The evidence for solid lipid nanoparticles mediated cell uptake of resveratrol, *Int. J. Pharm.* 390 (2010) 61–69.
- [8] J.Y. Fang, C.F. Hung, M.H. Liao, C.C. Chien, A study of the formulation design of acoustically active liposomes as carriers for drug delivery, *Eur. J. Pharm. Biopharm.* 67 (2007) 67–75.
- [9] F. Donsi, M. Sessa, H. Mediouni, A. Mgaidi, G. Ferrari, Encapsulation of bioactive compounds in nanomulsion-based delivery systems, *Procedia Food Sci.* 1 (2011) 1666–1671.
- [10] J. Shao, X. Li, X. Lu, C. Jiang, Y. Hu, Q. Li, Y. You, Z. Fu, Enhanced growth inhibition effect of resveratrol incorporated into biodegradable nanoparticles against glioma cells is mediated by the induction of intracellular reactive oxygen species levels, *Colloids Surf. B: Biointerfaces* 72 (2009) 40–47.
- [11] B. Caddeo, K. Teskac, C. Sinicco, J. Kristl, Effect of resveratrol incorporated in liposomes on proliferation and UV-B protection of cells, *Int. J. Pharm.* 363 (2008) 183–191.
- [12] X.-X. Wang, Y.-B. Li, H.-J. Yao, R.-J. Ju, Y. Zhang, R.-J. Li, Y. Yu, L. Zhang, W.-L. Lu, The use of mitochondrial targeting resveratrol liposomes modified with a dequalinium polyethylene glycol-distearoylphosphatidyl ethanolamine conjugate to induce apoptosis in resistant lung cancer cells, *Biomaterials* 32 (2011) 5673–5687.
- [13] C. Lucas-Abellán, I. Fortea, J.M. López-Nicolás, E. Núñez-Delicado, Cyclodextrins as resveratrol carrier system, *Food Chem.* 104 (2007) 39–44.
- [14] J. Kristl, K. Teskac, C. Caddeo, Z. Abramovic, M. Sentjurc, Improvements of cellular stress response on resveratrol in liposomes, *Eur. J. Pharm. Biopharm.* 773 (2009) 253–259.
- [15] S. Fabris, F. Momo, G. Ravagnan, R. Stevanato, Antioxidant properties of resveratrol and piceid on lipid peroxidation in micelles and monolamellar liposomes, *Biophys. Chem.* 135 (2008) 76–83.
- [16] A. Aserin, Multiple Emulsions: Technology and Applications, Wiley Interscience, Hoboken, USA, 2008.
- [17] N. Garti, Double emulsions—scope, limitations and new achievements, *Colloids Surf. A: Physicochem. Eng. Aspects* 123/124 (1997) 233–246.
- [18] H. Okochi, M. Nakano, Comparative study of two preparation methods of W/O/W emulsions: stirring and membrane emulsification, *Chem. Pharm. Bull.* 45 (1997) 1323–1326.
- [19] J.S. de los Reyes, C. Charcosset, Preparation of water-in-oil and ethanol-in-oil emulsions by membrane emulsification, *Fuel* 89 (2010) 3482–3488.
- [20] T. Schmidts, D. Dobler, A.-C. Guldau, N. Paulus, F. Runkel, Multiple W/O/W emulsions—using the required HLB for emulsifier evaluation, *Colloids Surf. A: Physicochem. Eng. Aspects* 372 (2010) 48–54.
- [21] S. van der Graaf, C.G.P.H. Schröen, R.M. Boom, Preparation of double emulsions by membrane emulsification—a review, *J. Membr. Sci.* 251 (2005) 7–15.
- [22] T. Nakashima, M. Shimizu, M. Kukizaki, Particle control of emulsion by membrane emulsification and its applications, *Adv. Drug Deliv. Rev.* 45 (2000) 47–56.
- [23] Y. Mine, M. Shimizu, T. Nakashima, Preparation and stabilization of simple and multiple emulsions using a microporous glass membrane, *Colloids Surf. B: Biointerfaces* 16 (1996) 261–268.
- [24] A.L. Márquez, A. Medrano, L.A. Panizzolo, J.R. Wagner, Effect of calcium salts and surfactant concentration on the stability of water-in-oil emulsions prepared with polyglycerol polyricinoleate, *J. Colloid Interface Sci.* 341 (2010) 101–108.
- [25] C. Charcosset, Preparation of emulsions and particles by membrane emulsification for the food processing industry, *J. Food Eng.* 92 (2009) 241–249.
- [26] E. Dickinson, Double emulsions stabilized by food biopolymers, *Food Biophys.* 6 (2011) 1–11.
- [27] N. Krog, Functions of emulsifiers in food systems, *J. Am. Oil Chem. Soc.* 54 (1977) 124–131.
- [28] N. Garti, Progress in stabilization and transport phenomena of double emulsions in food applications, *LWT – Food Sci. Technol.* 30 (1997) 222–235.
- [29] S. Frasch-Melnik, F. Spyropoulos, I.T. Norton, W<sub>1</sub>/O/W<sub>2</sub> double emulsions stabilised by fat crystals—formulation, stability and salt release, *J. Colloid Interface Sci.* 350 (2010) 178–185.
- [30] S. Frasch-Melnik, I.T. Norton, F. Spyropoulos, Fat-crystal stabilised w/o emulsions for controlled salt release, *J. Food Eng.* 98 (2010) 437–442.
- [31] Y. Hemar, L.J. Cheng, C.M. Oliver, L. Sangansri, M. Augustin, Encapsulation of resveratrol using water-in-oil-in-water double emulsions, *Food Biophys.* 5 (2010) 120–127.
- [32] P. Viñas, C. López-Erro, J.J. Marín-Hernández, M. Marín-Hernández, Determination of phenols in wines by liquid chromatography with photodiode array and fluorescence detection, *J. Chromatogr. A* 871 (2000) 85–93.
- [33] Xilan Sun, Bin Peng, Weidong Yan, Measurement and correlation of solubility of trans-resveratrol in 11 solvents at T=278.2, 288.2, 298.2, 308.2 and 318.2 K, *J. Chem. Thermodyn.* 40 (2008) 735–738.
- [34] R. Wilson, B.J. Van Schie, D. Howes, Overview of the preparation, use and biological studies on polyglycerol polyricinoleate (PGPR), *Food Chem. Toxicol.* 36 (1998) 711–718.
- [35] G. Gutierrez, M. Rayner, P. Dejmek, Production of vegetable oil in milk emulsions using membrane emulsification, *Desalination* 245 (2009) 631–638.
- [36] Y.P. Zhao, R. Turay, L. Hundley, Monitoring and predicting emulsion stability of metalworking fluids by salt titration and laser light scattering method, *Tribol. Trans.* 49 (2006) 117–123.
- [37] M. Matos, A. Lobo, J.M. Benito, A. Cambiella, J. Coca, C. Pazos, Extending the useful life of metalworking fluids in a copper wire drawing industry by monitoring their functional properties, *Tribol. Trans.* 55 (2012) 685–692.
- [38] J. O'Regan, D.M. Mulivhill, Water soluble inner aqueous phase markers as indicators of the encapsulation properties of water-in-oil-in-water emulsions stabilized with sodium caseinate, *Food Hydrocolloids* 23 (2009) 2339–2345.
- [39] A.L. Márquez, G.G. Palazolo, J.R. Wagner, Water in oil (w/o) and double (w/o/w) emulsions prepared with spans: microstructure, stability, and rheology, *Colloid Polym. Sci.* 285 (2007) 1119–1128.
- [40] L. Liang, H.A. Tajmir-Riahi, M. Subirade, Interaction of beta-lactoglobulin with resveratrol and its biological implications, *Biomacromolecules* 9 (2008) 50–56.
- [41] Y. Hemar, M. Gerbeaud, C.M. Oliver, M.A. Augustin, Investigation into the interaction between resveratrol and whey proteins using fluorescence spectroscopy, *Int. J. Food Sci. Technol.* 46 (2011) 2137–2144.

## ARTICLE IN PRESS

M. Matos et al. / Colloids and Surfaces A: Physicochem. Eng. Aspects xxx (2013) xxx–xxx

11

- [42] Y. Kawashima, T. Hino, H. Takeuchi, T. Niwa, K. Horibe, Shear-induced phase inversion and size control of water/oil/water emulsion droplets with porous membrane, *J. Colloid Interface Sci.* 145 (1991) 512–523.
- [43] M. Benha-Zayani, N. Kbir-Ariguib, N. Trabelsi-Ayadi, J.-L. Grossiard, Stabilisation of W/O/W double emulsion by polysaccharides as weak gels, *Colloids Surf. A: Physicochem. Eng. Aspects* 316 (2008) 46–54.
- [44] L. Sapei, M.A. Naqvi, D. Rousseau, Stability and release properties of double emulsions for food applications, *Food Hydrocolloids* 27 (2012) 316–323.
- [45] J. Su, J. Flanagan, Y. Hemar, H. Singha, Synergistic effects of polyglycerol ester of polyricinoleic acid and sodium caseinate on the stabilisation of water–oil–water emulsions, *Food Hydrocolloids* 20 (2006) 261–268.

Please cite this article in press as: M. Matos, et al., Preparation of water-in-oil-in-water ( $W_1/O/W_2$ ) double emulsions containing *trans*-resveratrol, *Colloids Surf. A: Physicochem. Eng. Aspects* (2013), <http://dx.doi.org/10.1016/j.colsurfa.2013.05.065>

#### IV. Preparation of HIPEs with controlled droplet size containing lutein

Lutein is a natural carotenoid of lipophilic character which possesses exceptional physiological functions since it enhances body immunity against atherosclerosis and cataracts. It is also found naturally in human skin, where it acts as a potential antioxidant maintaining skin health by reducing UV-induced erythema and inflammation. Because of the link between UV radiation exposure and skin cancer, lutein may play a protective role against skin cancer. Nevertheless, lutein applications in food and cosmetic formulations are limited due to its instability towards oxygen, light and heat. So, the use of oil droplets as lutein carriers is a way to avoid those limitations.

The aim of this study was to prepare highly concentrated O/W emulsions containing lutein, with controlled droplet size by a two-step technique, using a non-ionic surfactant as stabilizer. For this purpose, a 50% (v/v) emulsion was prepared by either mechanical agitation or membrane emulsification, and it was subsequently concentrated by vacuum evaporation to obtain a gel emulsion.

**Article 3.** G. Gutiérrez, **M. Matos**, J.M. Benito, J. Coca and C. Pazos. "Preparation of HIPEs with controlled droplet size containing lutein".

**Colloids and Surfaces A: Physicochemical and Engineering Aspects**  
<http://dx.doi.org/10.1016/j.colsurfa.2013.05.077>

#### Personal contribution to work

I developed experiments to optimize the emulsions preparation technique by membrane emulsification and vacuum evaporation. I prepared lutein-containing emulsions and established the procedure for measuring encapsulation efficiency by spectroscopy. Finally, I shared with my thesis co-supervisor, Dr. Gemma Gutiérrez, the task of writing the manuscript and preparing the figures included.

#### IV. Preparación de HIPES con tamaño de gota controlado contenido luteína

La luteína es un carotenoide natural con carácter lipófilo que posee funciones fisiológicas excepcionales, ya que mejora la inmunidad del cuerpo contra la aterosclerosis y las cataratas. También se encuentra de manera natural en la piel humana, donde actúa como antioxidante potencial manteniendo la salud de este órgano, al reducir el eritema inducido por radiación UV y la inflamación. Debido a la relación entre la exposición a la radiación UV y el cáncer de piel, la luteína podría jugar un papel protector contra el mismo. Sin embargo, su aplicación en alimentos y formulaciones de tipo cosmético se encuentra limitada por su inestabilidad frente al oxígeno, la luz y la temperatura. En este sentido, el uso de gotas de aceite portadoras de luteína se ofrece como una alternativa para paliar estas limitaciones.

El objetivo de este trabajo fue preparar emulsiones aceite-agua (O/W) con elevada proporción de fase interna conteniendo luteína y tamaño de gota controlado mediante una técnica en dos etapas, usando un tensioactivo no iónico como estabilizante. Para ello, se preparó inicialmente una emulsión del 50% (v/v), mediante agitación mecánica o emulsificación con membranas, que posteriormente se concentró por evaporación a vacío hasta obtener una emulsión tipo gel.

**Artículo 3.** G. Gutiérrez, **M. Matos**, J.M. Benito, J. Coca y C. Pazos. "Preparation of HIPEs with controlled droplet size containing lutein".

**Colloids and Surfaces A: Physicochemical and Engineering Aspects**  
<http://dx.doi.org/10.1016/j.colsurfa.2013.05.077>

#### Aportación personal al trabajo

Desarrollé los experimentos para optimizar el proceso de preparación de emulsiones concentradas mediante emulsificación con membranas y evaporación a vacío. Preparé las emulsiones conteniendo luteína y establecí el procedimiento para medir la eficacia de encapsulación mediante espectroscopía. Finalmente, compartí con mi co-directora de Tesis, Dr. Gemma Gutiérrez, la tarea de redactar el manuscrito y preparar las figuras en él incluidas.



Contents lists available at SciVerse ScienceDirect

## Colloids and Surfaces A: Physicochemical and Engineering Aspects

journal homepage: [www.elsevier.com/locate/colsurfa](http://www.elsevier.com/locate/colsurfa)

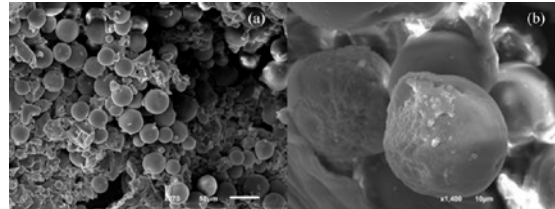
## Preparation of HIPEs with controlled droplet size containing lutein

Gemma Gutiérrez<sup>a</sup>, María Matos<sup>a</sup>, José M. Benito<sup>b</sup>, José Coca<sup>a</sup>, Carmen Pazos<sup>a,\*</sup><sup>a</sup> Department of Chemical and Environmental Engineering, University of Oviedo, Julián Clavería 8, 33006 Oviedo, Spain<sup>b</sup> Department of Chemical Engineering, University of Burgos, Plaza Misael Bañuelos s/n, 09001 Burgos, Spain

## HIGHLIGHTS

- HIPEs with controlled droplet size were prepared by a two-step process.
- Vacuum evaporation allowed to obtain HIPEs with no variation of mean droplet size.
- HIPEs are suitable systems for lutein encapsulation showing efficiencies up to 97%.
- HIPEs show high creaming resistance and retard lutein delivery.

## GRAPHICAL ABSTRACT



## ARTICLE INFO

## Article history:

Received 30 November 2012

Received in revised form 23 April 2013

Accepted 27 May 2013

Available online xxx

## Keywords:

High internal phase emulsions

Gel emulsions

Membrane emulsification

Vacuum evaporation

Lutein

## ABSTRACT

A two-step technique for preparing highly concentrated oil-in-water (O/W) emulsions, also called high internal phase emulsions (HIPEs) is proposed. Four different oils were selected as the internal phase: castor oil, heavy mineral oil, soybean oil and light mineral oil, and a non-ionic surfactant Tween 20 (polyoxyethylene sorbitan monolaurate) was chosen as stabilizer. Deionized water with 1% (w/v) NaCl was the external phase. First, a dilute O/W emulsion was prepared either by mechanical agitation or membrane emulsification and then concentrated by evaporation at high vacuum and temperatures not exceeding 40 °C to avoid emulsion phase inversion. Oil droplet size distribution and viscosity were measured to assess the vacuum evaporation performance. Visual inspection of the emulsion using soluble dyes and conductivity measurements showed the nature and characteristics of the final emulsion. Creaming stability of the formulated emulsions was also studied. O/W emulsions with an internal phase concentration up to 90% (v/v) could be prepared by mechanical agitation and evaporation. Emulsions obtained by membrane emulsification showed high monodispersity and could be concentrated up to 75% (v/v) of internal phase. High internal phase emulsions were used as lutein carriers. An appropriate selection of oily internal phase and the addition of sodium carboxymethylcellulose (CMCNa) as stabilizer in the external phase increased lutein encapsulation efficiency (EE) up to 97%.

© 2013 Elsevier B.V. All rights reserved.

## 1. Introduction

Highly concentrated oil-in-water (O/W) emulsions play an important role in pharmaceutical, food, cosmetic, paints and other applications, including their utilization as a primary step in the preparation of microcapsules for drug delivery systems [1–4]. These

highly concentrated emulsions are also called high internal phase emulsions (HIPEs) or gels, the latter being high viscosity emulsions.

HIPEs contain typically more than 74% (v/v) of oil (internal phase), which corresponds to the Ostwald critical volume (volume filled by completely packed droplets), and 26% (v/v) of external phase filling the free space between them [3,5–11].

The same size for each droplet is assumed to determine the Ostwald critical volume. It is possible to reach high packing values by concentration of a polydisperse emulsion, since small droplets may fill the voids between the large ones [8]. Moreover, droplets can lose their spherical shape becoming hexagonal [12].

\* Corresponding author. Tel.: +34 985103509; fax: +34 985103434.  
E-mail address: [c.pazos@uniovi.es](mailto:c.pazos@uniovi.es) (C. Pazos).

0927-7757/\$ – see front matter © 2013 Elsevier B.V. All rights reserved.  
<http://dx.doi.org/10.1016/j.colsurfa.2013.05.077>

Please cite this article in press as: G. Gutiérrez, et al., Preparation of HIPEs with controlled droplet size containing lutein, *Colloids Surf. A: Physicochem. Eng. Aspects* (2013), <http://dx.doi.org/10.1016/j.colsurfa.2013.05.077>

Although these types of emulsions were formulated long ago, their preparation arouses great interest, as some recent studies point out [6,13–19]. The most common method for preparing a gel emulsion consists of the slow addition of an internal phase into an external phase, followed by homogenization [8,20,21]. An alternative method is the *Phase Inversion Temperature* (PIT) method [14,22], in which an initial dilute emulsion is prepared using a non-ionic surfactant. The temperature is then increased to reach the phase transition of the emulsion. A concentrated HIPE is the result where the external phase is the internal phase of the initial dilute emulsion and *vice versa*. This technique has some advantages with respect to conventional ones, since lower energy and less surfactant concentration are required and the final emulsion is more stable and less prone to creaming.

Membrane emulsification is a technique widely studied for the last 20 years [23–25], which consists of the injection of an internal phase through the membrane pores while the external phase moves over the membrane surface enhancing droplet detachment. Two techniques are mainly used: (i) tubular membranes in which internal phase is injected from the outer part of the membrane while the external phase flows through the membrane lumen [26,27], and (ii) flat membranes where the internal phase is injected from the bottom side of the membrane and the external phase is placed in the upper part [28].

Membrane emulsification gives high control on droplet size, since the droplet diameter is in the range of 2–10 times the membrane pore diameter [23–25].

Emulsions are often used as carriers of biocompounds either for food or cosmetic applications. The use of HIPEs as carriers offers clear advantages from the transport point of view. Moreover, the addition of small amounts of a concentrated system can increase the added value of previously formed product.

Lutein is a natural carotenoid with lipophilic character, found in several vegetables and egg yolk [29–31]. Lutein possesses exceptional physiological functions since it enhances body immunity against atherosclerosis and cataracts. Lutein is also found naturally in human skin, where acts as a potential antioxidant maintaining skin health by reducing UV-induced erythema and inflammation. Because of the link between UV radiation (particularly its UVB component) exposure and skin cancer, lutein may play a protective role against skin cancer [29].

Lutein concentration was based on studies where it was demonstrated that topical treatment with 50 mg/L lutein twice per day induces immediate increase in superficial skin lipids and significant reduction in skin lipid peroxidation, improving the photoprotective activity and also the skin elasticity and hydration [29].

Lutein application in food and cosmetic formulations is limited by its instability towards oxygen, light and temperature, and hence the use of oil droplets as lutein carriers is considered a suitable technique [29,30].

The aim of this study was to prepare highly concentrated O/W emulsions containing lutein, a lipophilic biocompound, with controlled droplet size by a two-step technique, using a non-ionic surfactant as stabilizer. A 50% (v/v) emulsion was prepared by either mechanical agitation or membrane emulsification and it was concentrated by vacuum evaporation to obtain a gel emulsion. Several oils were selected as internal phase and the effect of viscosity and emulsion stability was studied.

## 2. Materials and methods

### 2.1. Materials

Four types of oil supplied by Sigma-Aldrich (USA) were tested as internal phase: castor oil ( $\eta_d = 541 \text{ mPa s}$ ,  $\rho_d = 836 \text{ kg/m}^3$  at 25 °C),

heavy mineral oil ( $\eta_d = 99.3 \text{ mPa s}$ ,  $\rho_d = 832 \text{ kg/m}^3$  at 25 °C), soybean oil ( $\eta_d = 64.8 \text{ mPa s}$ ,  $\rho_d = 850 \text{ kg/m}^3$  at 25 °C) and light mineral oil ( $\eta_d = 15.9 \text{ mPa s}$ ,  $\rho_d = 838 \text{ kg/m}^3$  at 25 °C).

A non-ionic surfactant Tween® 20 (polyoxyethylenesorbitan monolaurate) from Sigma-Aldrich (USA), which has hydrophilic-lipophilic balance (HLB) of 16.7, was selected as stabilizer for all emulsions.

Two dyes were used to visualize the external phase of the formulated emulsions, *i.e.* water-soluble copper II phthalocyanine-tetrasulfonic acid tetrasodium salt (blue), and oil-soluble fat red bluish (red) (Sigma-Aldrich, USA). Traces of both dyes were added to the emulsion after mechanical agitation to identify the nature of the external phase (water or oil). Deionized water with 1% (w/v) NaCl to increase conductivity (17.2 mS/cm at 25 °C) was used as the aqueous phase.

For the encapsulation experiments pure lutein supplied by Applichem GmbH (Germany) was dissolved in soybean oil and used as internal phase. To improve lutein encapsulation, 0.5% (w/v) medium viscosity sodium carboxymethylcellulose (CMCNa) with polymerization degree 1100 (molar mass = 982 g/mol) supplied by Sigma-Aldrich (USA) was used as viscosity modifier.

The following chemicals were used to prepare samples for scanning electron microscopy (SEM): agar bacteriological European type (Cultimed, Spain), glutaraldehyde solution 50% (v/v) (Panreac, Spain), imidazole and osmium tetroxide (Sigma-Aldrich, USA).

### 2.2. Equipments and methods

#### 2.2.1. Emulsions prepared by mechanical agitation

Emulsions were prepared in a first step by mechanical agitation being their surfactant concentration the same as for the emulsions prepared by vacuum evaporation. During the evaporation step the surfactant remained in the concentrate and its concentration (and also the oil concentration) increased. Thus, for emulsions prepared by mechanical agitation with volumetric water fraction ( $f_w$ ) of 0.5, 0.3 and 0.1, surfactant concentrations were 5, 6 and 8% (w/w), respectively. The amounts of aqueous and oil phases were weighed, mixed and left for 24 h before emulsion preparation. Emulsion samples (150 g) were prepared by mechanical agitation using a DIAx 900 homogenizer (Heidolph, Germany) with a shaft of 3 mm, at 15,000 rpm for 15 min.

#### 2.2.2. Emulsions prepared by membrane emulsification

A 200 mL stirred batch ultrafiltration cell Amicon model 8200 (Millipore, USA) was used for membrane emulsification experiments. The internal phase was injected from the bottom part of the cell, with the external phase in the upper part.

A tailor-made hydrophilic metallic membrane supplied by Micropore Ltd. (Hatton, Derbyshire, UK) was used in the experiments. The membrane had an active diameter of 62.5 mm and 200 μm of thickness, with a regular array of circular uniform pores of 5 μm diameter, being 200 μm the distance between pores.

The internal phase was gently fed into the cell by a syringe pump KDS-100-CE (KD Scientific, USA) at a rate of 20 mL/min. The emulsion was continuously stirred at 600 rpm, to favour droplet detachment.

In previous works with lutein, the oil concentration was in the range of 20–40 mg/L [29,32]. In this work, emulsions containing 40 mg/L of lutein in the oil phase were prepared. Lutein was previously dissolved in the oil, and the resulting solution was injected into the membrane emulsification device. A schematic diagram of the equipment is shown in Fig. 1.

Membranes were cleaned after each experiment with a dish-washing detergent, and rinsed with deionised water (for 15 min)

Please cite this article in press as: G. Gutiérrez, et al., Preparation of HIPEs with controlled droplet size containing lutein, *Colloids Surf. A: Physicochem. Eng. Aspects* (2013), <http://dx.doi.org/10.1016/j.colsurfa.2013.05.077>

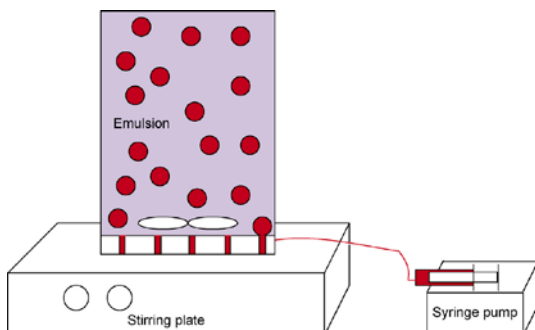


**Fig. 1.** Schematic diagram of the membrane emulsification equipment.

and acetone (for 15 min) in an ultrasound bath. Finally, they were dried using compressed air and pre-soaked in the external phase.

#### 2.2.3. Emulsions concentrated by vacuum evaporation

Emulsions with  $f_w = 0.5$ , prepared either by mechanical agitation or membrane emulsification, were used to produce the emulsions with  $f_w = 0.3$  and  $f_w = 0.1$  by vacuum evaporation. Evaporation experiments were performed with 150 g of emulsion using a R205 evaporator (Büchi, Switzerland), which consisted of a rotating flask immersed in a heating bath, a water-cooled condenser and a receiving flask as described in previous works [33,34]. The evaporator working pressure was 3.5 kPa with a vapour temperature of 27 °C. The heating bath temperature was kept at 40 °C to avoid emulsion inversion because of the decrease of non-ionic surfactant solubility in water at higher temperatures. Highly hydrophilic surfactants usually decrease their water affinity as the temperature increases, which lead to emulsion inversion from oil-in-water (O/W) to water-in-oil (W/O) [35].

#### 2.2.4. Emulsion characterization

Conductivity measurements were made at room temperature using a Seven Go conductimeter (Mettler Toledo, USA), to identify the internal phase nature (oil or water) for all prepared emulsions.

Droplet size distributions were determined by laser light scattering technique using a Mastersizer S long bench equipment (Malvern Instruments Ltd., UK).

Viscosity measurements were carried out in a RS50 rheometer (Haake, Germany) using plate-plate configuration at 25 °C. Two types of plots were obtained: (i) viscosity vs. time, at 20 s<sup>-1</sup> constant shear rate for 180 s, and (ii) viscosity vs. shear rate, at shear rate increasing from 0 to 100 s<sup>-1</sup> for 100 s. Samples were deposited on the rheometer plate for 15 min before making measurements to minimize any internal stress. Viscosities were calculated using the Rheowin 3 Data Manager software supplied with the rheometer.

Emulsion stability was determined with a Turbiscan Lab Expert (Formulaction Co., France) by static multiple light scattering (MLS), which consists of sending a light beam through a cylindrical glass cell containing the sample. Emulsions were placed without dilution in the test cells and the transmitted and backscattered lights were monitored as a function of time and cell height for 7 days at 30 °C. The Turbiscan software allowed calculation of the height of the clarification front and the migration velocity of the creaming oil droplets along time.

Interfacial tensions were measured at 25 °C, following the Du Noüy's platinum ring method [36] using a KSV Sigma 700 tensiometer (KSV Instruments Ltd., Finland).

The morphology of the formulated emulsions was determined with an Olympus BX61 optical microscope and a JEOL-6610 scanning electron microscope (Japan).

#### 2.2.5. Emulsion preparation for SEM microscopy

One day after emulsion preparation, samples were dehydrated and placed under the SEM microscope. The dehydration procedure was the same as described in the literature to dehydrate mayonnaise and cosmetic emulsions [37–39].

Samples were carefully encapsulated in 2.5% (w/v) agar and fixed overnight in 2% (v/v) glutaraldehyde in 0.1 M phosphate buffer (pH = 7). The samples were rinsed using several changes of buffer and post-fixed overnight in 2% (w/v) OsO<sub>4</sub> solution with 0.1 M imidazole. Samples were dehydrated in graded water–ethanol and ethanol–acetone series finishing in 100% acetone. Then, they were dried with CO<sub>2</sub> in a Balzers CPD 030-Critical Point Dryer, Polaron (Quorum Technologies, UK). Dry fractions were fractured and torn with a blade, and fragments were mounted on aluminium SEM stubs and coated with gold in a Balzers SCD 004 sputter coater (Bal-Tec AG, Liechtenstein).

#### 2.2.6. Encapsulation efficiency

Encapsulation efficiency (EE) was calculated as:

$$EE = \frac{C_m}{C_e} \times 100 \quad (1)$$

where  $C_m$  is the concentration of lutein in the recovered aqueous phase and  $C_e$  is the concentration of lutein expected in this phase if all the lutein had been released. To collect the lutein-containing aqueous phase, samples were placed inside a separator funnel, where the aqueous phase could be easily removed from the bottom. Lutein concentration in the aqueous phase,  $C_m$ , was determined at 443 nm wavelength in a T80 UV/vis spectrophotometer (PG Instruments Ltd., UK).

Several samples were stored at room temperature and EE was weekly measured for a month to determine the release of lutein along time.

### 3. Results and discussion

#### 3.1. Emulsions prepared by mechanical agitation

In a first series of experiments, emulsions with 5, 6 and 8% (w/w) of non-ionic surfactant and volumetric water fractions ( $f_w$ ) of 0.5, 0.3 and 0.1, respectively, were prepared by mechanical agitation using the four aforementioned types of oil. Once the emulsions were made, traces of both dyes were added. All emulsions turned into blue, indicating the presence of water as external phase.

Conductivity measurements also showed the external phase nature (water or oil). Moreover, the conductivity values could identify double emulsions [40–42], using the following equation:

$$f_{wef} = \left( \frac{\kappa_e}{\kappa_w} \right)^{2/3} \quad (2)$$

where  $f_{wef}$  is the effective volumetric water fraction, and  $\kappa_e$  and  $\kappa_w$  are the conductivities of the emulsion and the aqueous phase, respectively. Double emulsions are formed when  $f_{wef} > f_w$ , since some water droplets remain inside the oil droplets.

Experimental and calculated  $f_{wef}$  values using Eq. (2) are shown in Supporting Information Table S1. Conductivity measurements indicated that all emulsions were O/W type. Similar values for  $f_{wef}$  and  $f_w$  verified the absence of double emulsions. Furthermore, conductivity decreased as  $f_w$  did, which indicated the proximity to the emulsion inversion point [40].

Fig. 2 shows the emulsions droplet size distribution, reported as volume-weighted size distribution. As an example optical images

# ARTICLE IN PRESS

G. Gutiérrez et al. / Colloids and Surfaces A: Physicochem. Eng. Aspects xxx (2013) xxx-xxx

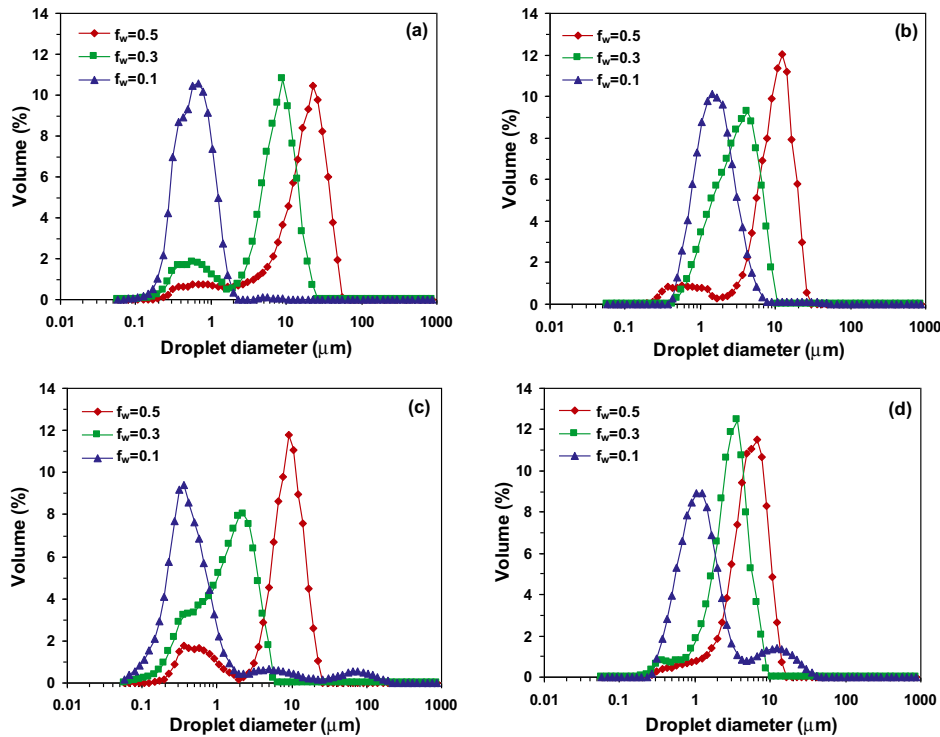


**Fig. 2.** Droplet size distribution of emulsions prepared by mechanical agitation with different volumetric water fractions ( $f_w$ ) using castor oil (a), heavy mineral oil (b), soybean oil (c), or light mineral oil (d) as internal phase.

of the emulsions prepared with castor oil are given in Fig. 3 (optical microscopy could not be used for emulsions with  $f_w = 0.1$  because of their very small droplet size). A decrease in droplet size was observed for lower  $f_w$  values, indicating the proximity to the emulsion inversion point. Similar behaviour had been reported by other authors [19].

Droplet mean diameters,  $d(0.5)$ , for all formulated emulsions are listed in Table 1. It could be observed that emulsions with  $f_w = 0.5$  and  $f_w = 0.3$  had larger oil droplet sizes, as the viscosity of the oil used as internal phase was higher [19]. However, the opposite trend was detected for emulsions with  $f_w = 0.1$  (smaller droplet size at

higher oil viscosity), which indicated that the emulsion inversion point would be reached earlier if the internal phase viscosity was higher. These results confirmed that viscosity of the internal phase was a key factor in monitoring the emulsion inversion point, while the viscosity of the external phase seemed to be less important, as it had been previously reported [9,19].

Supporting Information Fig. S1 shows the viscosity of the emulsions at a constant shear rate of  $20\text{ s}^{-1}$  and for shear rates increasing from 0 to  $100\text{ s}^{-1}$ . A rise in emulsion viscosity was observed as  $f_w$  decreased, due to the increase in internal phase content. No significant differences in emulsion viscosity were found for the

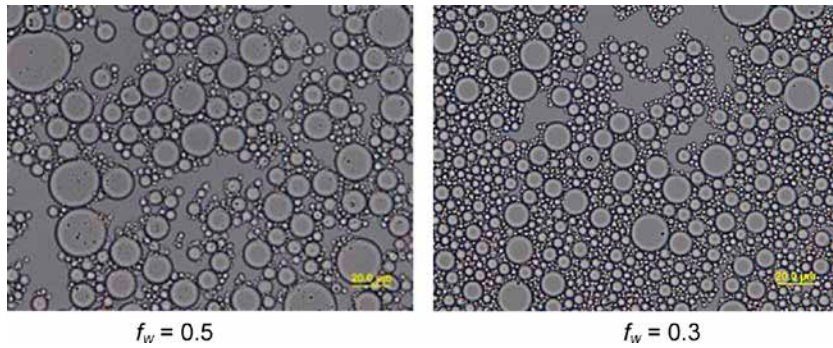


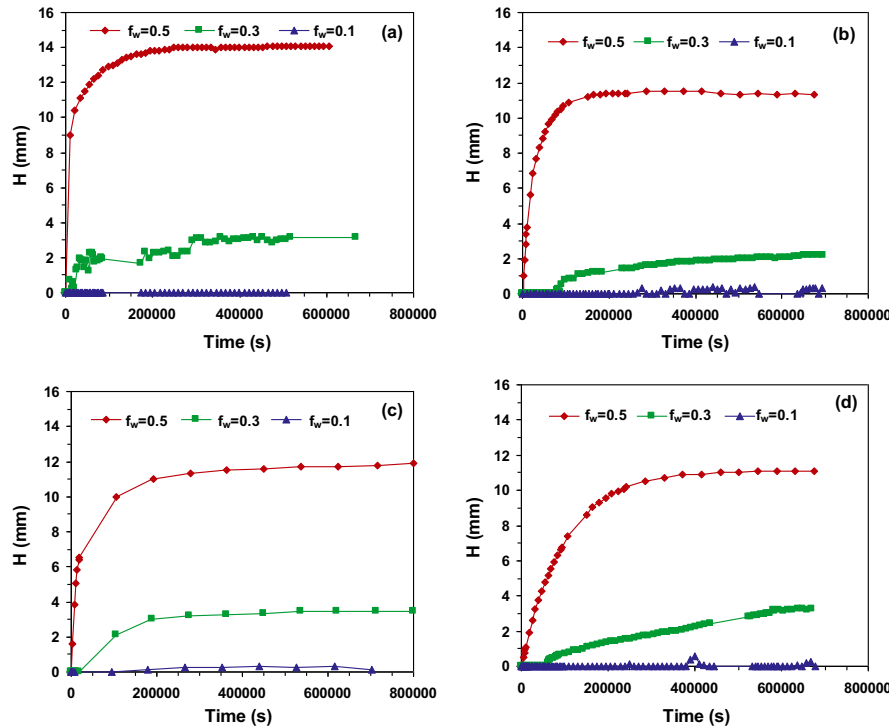
**Fig. 3.** Optical microscopy images of emulsions prepared by mechanical agitation using castor oil as internal phase.

**Table 1**Droplet mean diameter,  $d(0.5)$ , for emulsions prepared by mechanical agitation using castor oil, heavy mineral oil, soybean oil or light mineral oil as internal phase.

$f_w$	Castor oil ( $\mu\text{m}$ )	Heavy mineral oil ( $\mu\text{m}$ )	Soybean oil ( $\mu\text{m}$ )	Light mineral oil ( $\mu\text{m}$ )
0.5	22.5	12.2	8.89	6.63
0.3	9.00	4.19	3.92	3.60
0.1	0.78	1.44	0.71	1.24

**Table 2**Calculated ( $\eta_{emC}$ ) and experimental ( $\eta_{emE}$ ) viscosities for emulsions prepared by mechanical agitation using castor oil, heavy mineral oil, soybean oil or light mineral oil as internal phase.

$f_w$	Castor oil		Heavy mineral oil		Soybean oil		Light mineral oil	
	$\eta_{emC}$ (mPa s)	$\eta_{emE}$ (mPa s)						
0.5	18.2	31.1	21.9	30.7	21.5	28.0	18.9	29.0
0.3	117.2	143.3	140.6	194.1	120.1	170	114.7	163.4
0.1	1134 <sup>a</sup>	5043	1441 <sup>a</sup>	3129	1464 <sup>a</sup>	4335	1983 <sup>a</sup>	2917
0.1	1599 <sup>b</sup>	5043	1998 <sup>b</sup>	3129	2014 <sup>b</sup>	4335	2030 <sup>b</sup>	2917
0.1	3554 <sup>c</sup>	5043	3960 <sup>c</sup>	3129	3669 <sup>c</sup>	4335	1918 <sup>c</sup>	2917

<sup>a</sup> Calculated using Eq. (5).<sup>b</sup> Calculated using Eq. (7).<sup>c</sup> Calculated using Eq. (3).**Fig. 4.** Heights ( $H$ ) of the clarification front vs. time for emulsions prepared by mechanical agitation using castor oil (a), heavy mineral oil (b), soybean oil (c) or light mineral oil (d) as internal phase.**Table 3**Calculated ( $V_C$ ) and experimental ( $V_E$ ) oil droplet migration velocities for emulsions prepared by mechanical agitation using castor oil, heavy mineral oil, soybean oil or light mineral oil as internal phase.

$f_w$	Castor oil		Heavy mineral oil		Soybean oil		Light mineral oil	
	$V_C$ ( $\mu\text{m}/\text{s}$ )	$V_E$ ( $\mu\text{m}/\text{s}$ )	$V_C$ ( $\mu\text{m}/\text{s}$ )	$V_E$ ( $\mu\text{m}/\text{s}$ )	$V_C$ ( $\mu\text{m}/\text{s}$ )	$V_E$ ( $\mu\text{m}/\text{s}$ )	$V_C$ ( $\mu\text{m}/\text{s}$ )	$V_E$ ( $\mu\text{m}/\text{s}$ )
0.5	5.10	4.80	5.47	4.60	3.57	3.26	1.89	1.90
0.3	0.49	0.70	0.39	0.60	0.37	0.45	0.34	0.30
0.1	0.001	0.04	0.015	0.30	0.004	0.21	0.013	0.10

Please cite this article in press as: G. Gutiérrez, et al., Preparation of HIPEs with controlled droplet size containing lutein, *Colloids Surf. A: Physicochem. Eng. Aspects* (2013), <http://dx.doi.org/10.1016/j.colsurfa.2013.05.077>

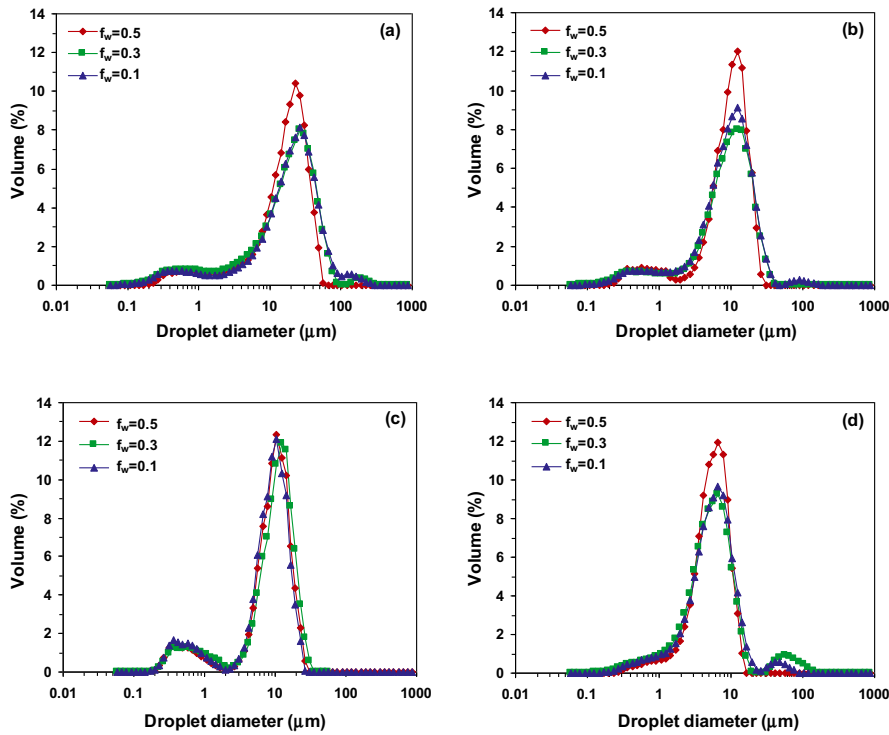


**Fig. 5.** Droplet size distributions of emulsions prepared by mechanical agitation with  $f_w = 0.5$  using castor oil (a), heavy mineral oil (b), soybean oil (c) or light mineral oil (d) as internal phase, and further concentrated by vacuum evaporation till  $f_w = 0.3$  and  $f_w = 0.1$ .

four oils. Higher viscosity was obtained for castor oil emulsion at  $f_w = 0.1$ , because of the smaller droplet size [7]. Moreover, a viscosity decrease was appreciated as shear rate increased, indicating that these emulsions behaved as plastic fluids [43,44].

From these experimental results, it could be concluded that the internal phase (oil) had minor influence on the emulsion viscosity, while oil droplet size had a major influence. Emulsions with smaller droplet size showed a higher viscosity, as it had been reported by several authors [7,12,45].

For semi-concentrated emulsions ( $f_w = 0.4\text{--}0.7$ ), Yaron and Gal-Or [46] suggested that emulsion viscosity ( $\eta_{em}$ ) can be calculated as:

$$\eta_{em} = \eta_c \left( 1 + I(f_0^{1/3}, p) f_o \right) \quad (3)$$

where  $\eta_c$  is the external phase viscosity,  $f_o$  the internal phase fraction, and  $I(f_0^{1/3}, p)$  is expressed by:

$$I(f_0^{1/3}, p) = \frac{5.5[4f_0^{7/3} + 10 - (84f_0^{2/3}/11) + (4(1-f_0^{7/3})/p)]}{10(1-f_0^{10/3}) - 25f_0(1-f_0^{4/3}) + 10((1-f_0)(1-f_0^{7/3})/p)} \quad (4)$$

where  $p$  is defined as the ratio between viscosities of internal and external phases.

Vankova et al. [47] and Tcholakova et al. [19,48] reported a model to estimate the viscosity of concentrated emulsions,  $f_w < 0.3$ . This model, Eq. (5), is able to describe the rheological behaviour of emulsions and foams with  $0.8 \leq f_o \leq 0.98$  at high shear rates when the effect of the yield stress can be neglected [19].

$$\eta_{em} = \eta_c \left( 1.16 Ca^{-0.53} f_o^{5/6} (f_o - 0.74)^{0.1} / (1-f_o)^{0.5} \right) \quad (5)$$

$Ca$  is the capillary number, given by:

$$Ca = \frac{\eta_c \gamma d}{2\sigma} \quad (6)$$

where  $\gamma$  is the shear rate,  $d$  the droplet diameter and  $\sigma$  the interfacial tension.

This model takes into account the effect of the interfacial tension and droplet diameter, which are not included in Eq. (3).

Princen and Kiss [49] reported another model to calculate HYPEs viscosity. This model, Eq. (7), includes yield stress ( $\tau_0$ ) which is very important in emulsions with small droplet size.

$$\eta_{em} = \frac{\tau_0}{\gamma} + 32(f_o - 0.73)\eta_c Ca^{-1/2} \quad (7)$$

Yield stress,  $\tau_0$ , is given by Eq. (8):

$$\tau_0 = \frac{2\sigma}{d} f_o^{1/3} Y(f_o) \quad (8)$$

$Y(f_o)$  can be calculated using Eq. (9):

$$Y(f_o) = -0.080 - 0.114 \log(1-f_o) \quad (9)$$

Eq. (3) was selected to calculate  $\eta_{em}$  of emulsions with  $f_w = 0.5$  and  $0.3$ , while Eqs. (5) and (7) were used for emulsions with  $f_w = 0.1$ .

The interfacial tension measurements gave the following results: 2.3, 5.9, 2.5 and 5.3 mN/m for systems containing castor, heavy mineral, soybean and light mineral oil, respectively.

Experimental emulsion viscosities, measured at a shear rate of  $100\text{s}^{-1}$ , were larger than calculated for all cases, as shown in Table 2, especially for emulsions with  $f_w = 0.1$ . Even larger differences were obtained for lower shear rates (data not shown), so

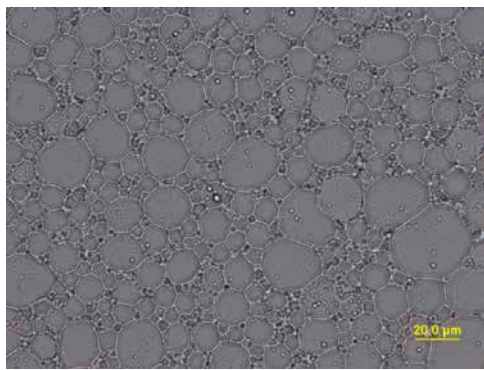


**Fig. 6.** Optical microscopy image of emulsion prepared by mechanical agitation and further concentrated by vacuum evaporation till  $f_w = 0.1$  using castor oil as internal phase.

experimental viscosity values will probably be in good agreement with calculated ones for shear rates higher than those used in this study.

Viscosities for concentrated emulsions ( $f_w = 0.1$ ) were also determined using Eq. (3), and in most of cases the differences between calculated and experimental values were surprisingly lower than obtained when using Eqs. (5) and (7).

The smallest differences between experimental and calculated viscosity values, from Eqs. (5) and (7), corresponded to the last one.

This proved the important effect of yield stress at low shear rates, especially for emulsions with small droplet size [19].

Furthermore, the viscosity discrepancies found using Eq. (7) could be attributed to the very small droplet size, as in this size range the thickness of the aqueous films between droplets was not negligible regarding to droplet size. This really implied that effective volume fraction of emulsion was larger than the nominal one [49].

Backscattering profiles obtained with the Turbiscan equipment were analyzed to evaluate emulsion stability. Supporting Information Fig. S2 shows the backscattering profiles of castor oil emulsion with  $f_w = 0.5$ . Similar profiles were obtained for all emulsions.

Experimental results indicated that creaming phenomena were very important for emulsions with  $f_w = 0.5$ . Migration of oil droplets towards the emulsion surface (air–liquid interface) led to a clarification front at the bottom of the measuring cell for all samples. Nevertheless, emulsion stability was higher for emulsions with  $f_w = 0.1$ , showing no creaming in the range studied. Fig. 4 shows the height of clarification front ( $H$ ) vs. time for all the emulsions. This height was higher as  $f_w$  increased for all the emulsions, whereas it was close to zero for all the emulsions with  $f_w = 0.1$ . Moreover, it could be observed that the clarification seemed to be higher for the emulsions with larger oil droplet size (e.g. for emulsions formulated with castor oil and  $f_w = 0.5$ ).

The migration velocity of oil droplets towards the emulsion surface depends directly on droplet size, density difference between both phases and aqueous phase viscosity, as indicated by Stokes' law:

$$V_S = \frac{gd^2(\rho_w - \rho_o)}{18\mu} \quad (10)$$

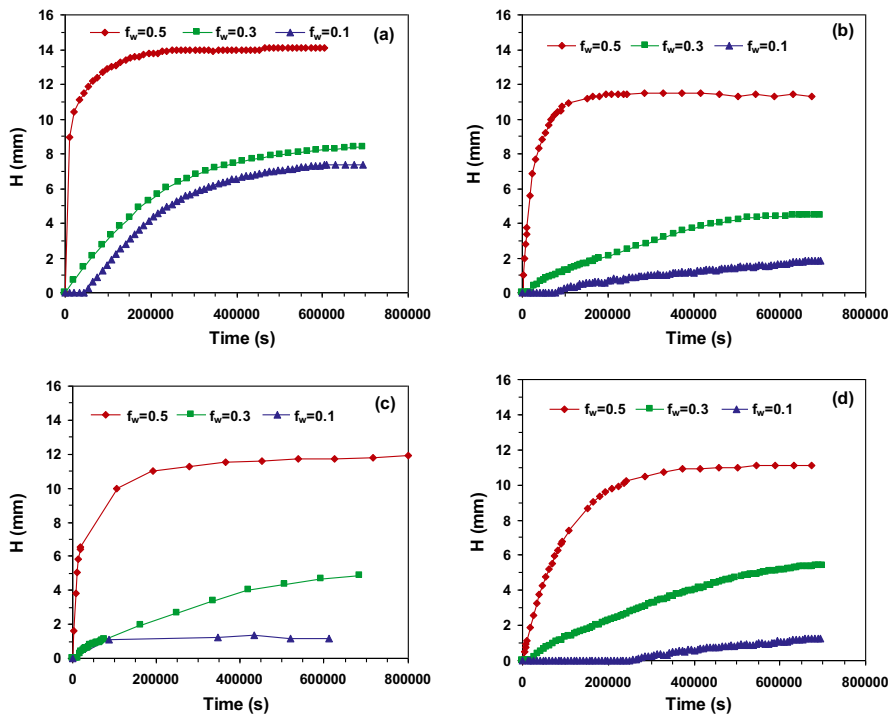


**Fig. 7.** Heights ( $H$ ) of the clarification front vs. time for emulsions prepared by mechanical agitation with  $f_w = 0.5$  using castor oil (a), heavy mineral oil (b), soybean oil (c) or light mineral oil (d) as internal phase, and further concentrated by vacuum evaporation till  $f_w = 0.3$  and  $f_w = 0.1$ .

**Table 4**

Calculated ( $\eta_{emC}$ ) and experimental ( $\eta_{emE}$ ) viscosities for emulsions prepared by mechanical agitation and vacuum evaporation using castor oil, heavy mineral oil, soybean oil or light mineral oil as internal phase.

$f_w$	Castor oil		Heavy mineral oil		Soybean oil		Light mineral oil	
	$\eta_{emC}$ (mPa s)	$\eta_{emE}$ (mPa s)						
0.3	98.7	76.7	222.8	250.6	102.3	183.2	102.6	134.1
0.1	286.1 <sup>a</sup>	309.1	611.5 <sup>a</sup>	667.7	361.7 <sup>a</sup>	326.9	608.5 <sup>a</sup>	600.9
0.1	416.2 <sup>b</sup>	309.1	742.5 <sup>b</sup>	667.7	494.0 <sup>b</sup>	326.9	879.4 <sup>b</sup>	600.9

<sup>a</sup> Calculated using Eq. (5).

<sup>b</sup> Calculated using Eq. (7).

where  $V_S$  is the droplet migration velocity,  $d$  the droplet diameter,  $g$  the gravitational acceleration,  $\rho_w$  and  $\rho_o$  the densities of the aqueous phase and oil phase, respectively, and  $\mu$  the viscosity of the external (aqueous) phase.

$V_S$  should be corrected taking into account the percentage of the aqueous phase present in the emulsion:

$$V_C = V_S f_w \quad (11)$$

where  $V_C$  is the corrected droplet migration velocity.

Experimental droplet migration velocities obtained from Turbiscan measurements were compared with corrected values calculated with Eq. (11), as shown in Table 3. Experimental data for emulsions with  $f_w = 0.3$ , and especially for  $f_w = 0.5$ , were in close agreement with the calculated values.

For emulsions with  $f_w = 0.1$ , migration velocity values were close to zero in all cases, according to the clarification profiles obtained from Turbiscan measurements where the height of the front was negligible (see Fig. 4).

It is important to point out that Eq. (10) assumes monodispersity, what is not true for emulsions prepared by mechanical agitation. This fact could explain the discrepancies found between experimental and calculated values.

According to Eq. (10), migration velocity will be higher for larger oil droplets, reaching the emulsion surface faster and causing creaming. Nevertheless, emulsion viscosity plays also a key role. Emulsions with  $f_w = 0.1$  showed a higher viscosity than the other emulsions, so the migration velocity of an oil droplet was very low, no creaming was observed and the emulsion remained more stable.

Experimental migration velocities for emulsions with  $f_w = 0.1$  seemed to be larger than the calculated values. It might be explained by diverse destabilization processes, such as droplet coalescence or Ostwald ripening [50,51]. Either processes would lead to an increase in droplet size and consequently to higher droplet migration velocities.

### 3.2. Emulsions prepared by mechanical agitation and vacuum evaporation

In a second series of experiments, emulsions with  $f_w = 0.5$  were prepared by mechanical agitation using the four oils at the same operating conditions previously described. They were subsequently evaporated to obtain emulsions with  $f_w = 0.3$  and  $f_w = 0.1$ .

Low pressures and therefore low temperatures were used for the vacuum evaporation experiments in order to avoid emulsion inversion. Preliminary analysis of the condensate showed a very low chemical oxygen demand (COD), an indication that only water was evaporated.

Traces of both dyes were added to the emulsions with  $f_w = 0.5$  before vacuum evaporation. All emulsions turned into blue, and this colour remained during the whole evaporation process. This indicated the presence of water as external phase and no emulsion inversion.

To confirm the absence of double emulsions and water-in-oil (W/O) emulsions, the conductivity was measured and  $f_{wef}$  was

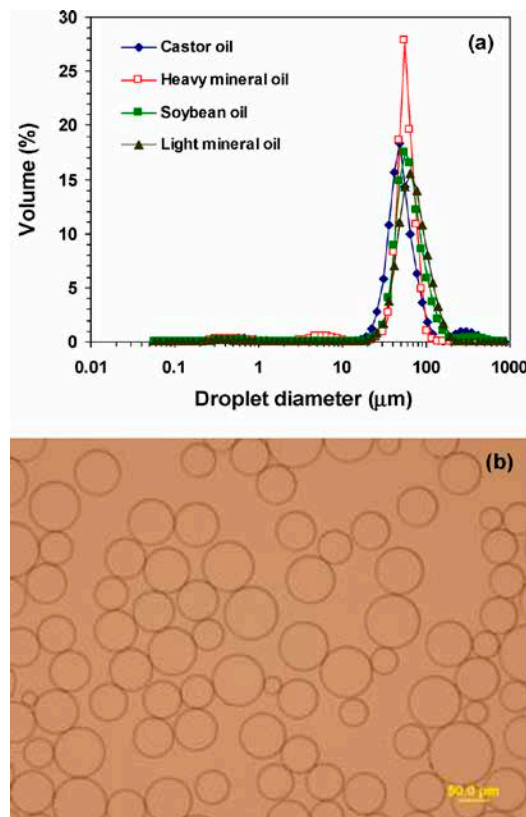


**Fig. 8.** Droplet size distributions of emulsions prepared by membrane emulsification with  $f_w = 0.5$  using castor oil, heavy mineral oil, soybean oil or light mineral oil as internal phase (a); optical microscopy image of the emulsion prepared with heavy mineral oil as internal phase (b).

calculated and compared with the actual  $f_w$  values (Supporting Information Table S2). Conductivity values followed the same trend as the visual observation of the dye colour, confirming the O/W nature of the emulsion and the absence of double emulsions in all of the experiments.

A constant oil droplet size was observed in all cases (Fig. 5), which indicated that this parameter was not affected by vacuum evaporation and was independent of the internal phase concentration and the type of oil used as internal phase.

As an example Fig. 6 shows a photograph, obtained by optical microscopy, of an emulsion prepared by vacuum evaporation till  $f_w = 0.1$  using castor oil as internal phase. It must be pointed out that the oil droplets in this emulsion were well packed. It was observed

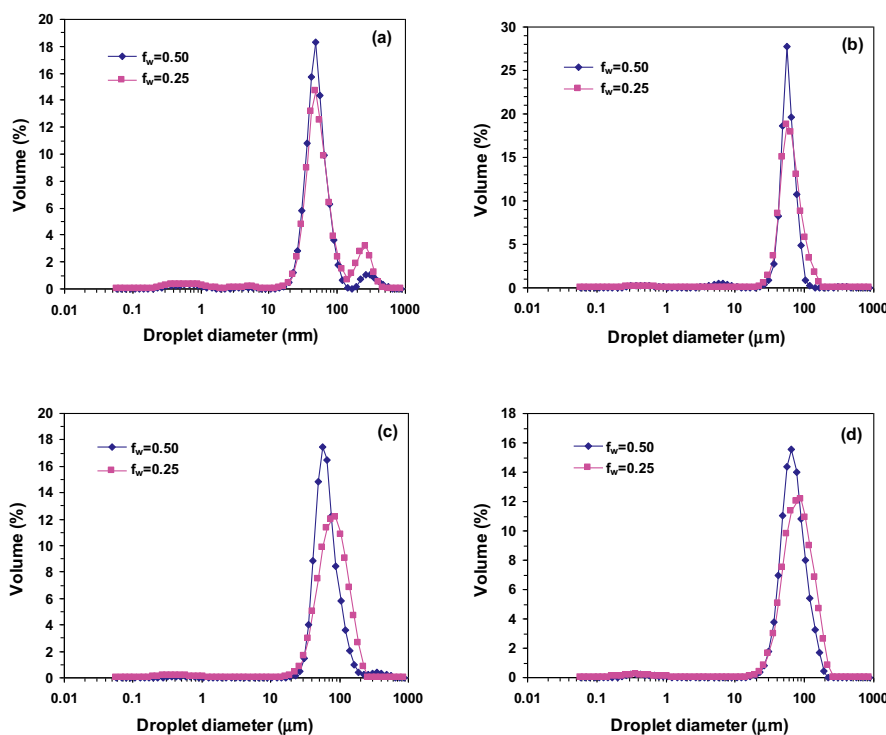


**Fig. 9.** Droplet size distributions of emulsions prepared by membrane emulsification with  $f_w = 0.5$  using castor oil (a), heavy mineral oil (b), soybean oil (c) or light mineral oil (d) as internal phase, and further concentrated by vacuum evaporation till  $f_w = 0.25$ .

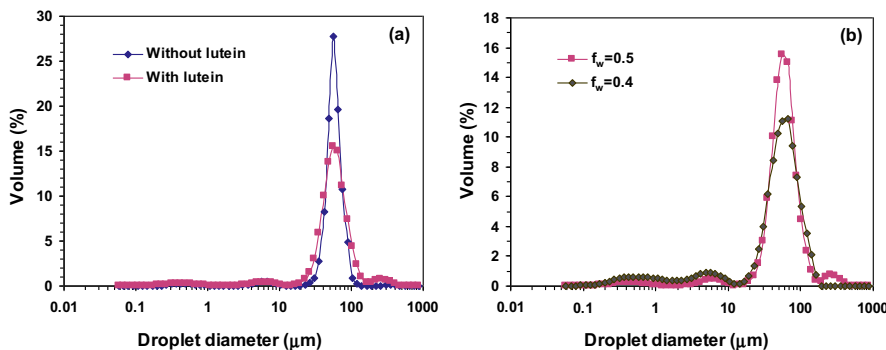


**Fig. 10.** Droplet size distribution of emulsion prepared by membrane emulsification with  $f_w = 0.5$  using heavy mineral oil as internal phase with and without lutein (a); droplet size distribution of emulsion prepared by membrane emulsification with  $f_w = 0.5$  using heavy mineral oil containing lutein, and further concentrated by vacuum evaporation till  $f_w = 0.40$  (b).

that these droplets had lost their original spherical shape due to the high internal phase concentration, which brought the oil droplets in closer contact.

Emulsion viscosities are given in Table 4. Supporting Information Fig. S3 shows the viscosity of the emulsions at a constant shear rate of  $20\text{ s}^{-1}$  and for shear rates increasing from 0 to  $100\text{ s}^{-1}$ .

In spite of the fact that all emulsions prepared with the same oil as internal phase had the same droplet size, their viscosity differences were remarkable. These differences were likely due to the different internal phase concentration. However, it is important to

point out that the increase in viscosity as  $f_w$  decreased was not as noticeable as in the case of emulsions prepared by mechanical agitation, indicating that the influence of the oil droplet size was more important than the internal phase concentration.

Eqs. (5) and (7) were also used to calculate the emulsion viscosity. Experimental and calculated results are also listed in Table 4. No large differences were found in any case: calculated values using Eq. (5) and experimental values were more similar than those presented in Table 3 for emulsions prepared by mechanical agitation. This indicated the importance of droplet size parameter, which

was not considered in the semi-concentrated emulsions model. Larger differences between calculated and experimental values were found when Eq. (7) was used.

Consequently, Eq. (5) could be used to calculate the viscosity of emulsions with droplet diameter in the range 6–25  $\mu\text{m}$  for any shear rate tested. However, emulsion viscosity seemed not be appropriately predicted with this equation for emulsions containing droplets with diameters smaller than 1  $\mu\text{m}$ . Moreover, yield stress had an important effect on emulsions with small droplet size.

Emulsion stability and migration velocity of oil droplets were also studied using the software provided with the Turbiscan equipment. Fig. 7 shows the height of the clarification front ( $H$ ) vs. time for all the emulsions prepared by vacuum evaporation and for the original emulsions prepared by mechanical agitation. Higher  $H$  values were obtained for emulsions prepared by mechanical agitation with  $f_w = 0.3$  and  $f_w = 0.1$ , mainly because of their larger oil droplet sizes. Moreover, for castor oil high  $H$  values appeared at all  $f_w$  studied.

Table 5 shows the experimental and calculated droplet migration velocities for these emulsions, whose values were similar in all cases. Migration velocities were higher than for the emulsions only prepared by mechanical agitation, due again to the larger oil droplet size.

### 3.3. Emulsions prepared by membrane emulsification and vacuum evaporation

Emulsions with the same composition as those previously described were prepared by membrane emulsification. Membrane emulsification allowed to control the emulsion droplet size. Emulsions with  $f_w = 0.5$  and narrow droplet size distribution were prepared. More concentrate emulsions could be performed by this technique. However, wider droplet size distributions would be obtained as the internal phase concentration increased.

From Fig. 8a it can be observed that no much difference was noticed on the mean droplet size for all the emulsions prepared. However, the emulsion prepared with heavy mineral oil as internal phase had a size distribution narrower than emulsions prepared with castor oil, soybean oil and light mineral oil. Mean droplet size was quite similar for the four emulsions prepared by membrane emulsification, and its value was close to 10 times the membrane pore diameter. Fig. 8b shows an optical image of the emulsion prepared with heavy mineral oil as internal phase.

Each emulsion was evaporated up to  $f_w = 0.25$  (Fig. 9). More concentrated emulsions without varying the mean droplet size could not be reached, because the narrower size distribution did not probably allow higher packing [10,11]. The mean droplet size remained constant for all the emulsions prepared, even when a slight wider size distribution was obtained.

### 3.4. Lutein-containing emulsions

As the narrowest droplet size distribution, for emulsions prepared by membrane emulsification, was obtained using heavy mineral oil as internal phase, lutein was dissolved in this oil. Although lutein is a lipophilic compound, its solubility in heavy mineral oil seemed to be quite low, and several hours were needed for its complete dissolution at 40°C.

Droplet size distributions of emulsion with lutein and heavy mineral oil as internal phase showed a wider distribution than emulsion prepared without lutein in the oily phase (Fig. 10a). Moreover, when the emulsion was evaporated up to  $f_w = 0.25$ , the emulsion was completely destabilized. The minimum  $f_w$  value that was possible to obtain when a stable lutein-containing emulsion was prepared was 0.4 (Fig. 10b). Encapsulation efficiency for this emulsion was 80.1%.

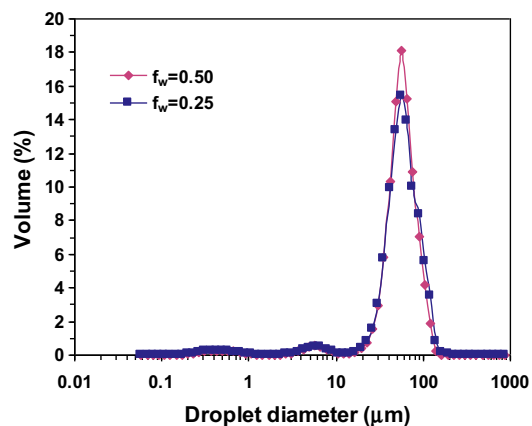


**Fig. 11.** Droplet size distribution of emulsion prepared by membrane emulsification with  $f_w = 0.5$  using soybean oil as internal phase with lutein, and further concentrated by vacuum evaporation till  $f_w = 0.25$ .

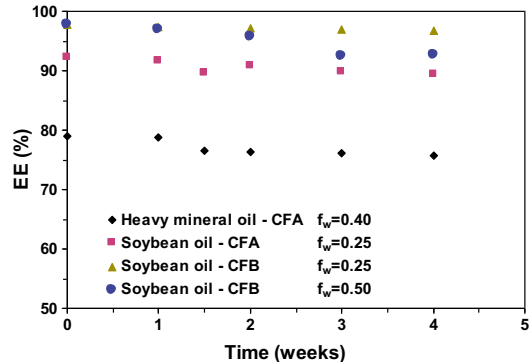


**Fig. 12.** Encapsulation efficiency vs. time for lutein-containing emulsions. CFA: continuous phase with 5% (w/v) Tween 20 and 1% (w/v) NaCl; CFB: continuous phase with 2% (w/v) Tween 20, 0.5% (w/v) CMCNa and 1% (w/v) NaCl.

In order to increase lutein encapsulation other alternative formulations were tested. The use of light mineral oil as internal phase offered similar problems to those found when heavy mineral oil was used. Lutein solubility in light mineral oil was also poor.

Soybean and castor are vegetable oils, very different from mineral oils previously tested. Castor oil has a high viscosity that made also difficult lutein solubilization. By contrast, lutein exhibits good solubility in soybean oil, so this oil was selected for encapsulation experiments.

The experiments carried out with soybean oil and lutein as internal phase allowed to obtain emulsions with  $f_w = 0.25$  and controlled droplet size using vacuum evaporation (Fig. 11). Moreover, encapsulation efficiency was increased up to 93.3%.

In order to improve encapsulation efficiency, 0.5% (w/v) CMCNa was added to the external phase as viscosity modifier, and the surfactant concentration was reduced up to 2% (w/v). The presence of CMCNa increased the external phase viscosity from 1.14 to 6.04 mPa s, making impossible to obtain an emulsion with  $f_w$  lower than 0.6 by membrane emulsification.

However, the emulsion with  $f_w = 0.6$  could be evaporated up to  $f_w = 0.25$  without changing droplet size distribution. The presence of CMCNa increased the encapsulation efficiency up to 97%. The

**Table 5**

Calculated ( $V_C$ ) and experimental ( $V_E$ ) oil droplet migration velocities for emulsions prepared by mechanical agitation with  $f_w = 0.5$  using castor oil, heavy mineral oil, soybean oil or light mineral oil as internal phase, and further concentrated by vacuum evaporation till  $f_w = 0.3$  and  $f_w = 0.1$ .

$f_w$	Castor oil		Heavy mineral oil		Soybean oil		Light mineral oil	
	$V_C$ ( $\mu\text{m}/\text{s}$ )	$V_E$ ( $\mu\text{m}/\text{s}$ )	$V_C$ ( $\mu\text{m}/\text{s}$ )	$V_E$ ( $\mu\text{m}/\text{s}$ )	$V_C$ ( $\mu\text{m}/\text{s}$ )	$V_E$ ( $\mu\text{m}/\text{s}$ )	$V_C$ ( $\mu\text{m}/\text{s}$ )	$V_E$ ( $\mu\text{m}/\text{s}$ )
0.5	5.10	4.80	5.47	4.60	3.57	3.26	1.89	1.90
0.3	3.10	2.70	3.30	2.50	3.40	2.21	1.13	0.87
0.1	1.00	1.30	1.10	0.90	0.88	0.74	0.38	0.25

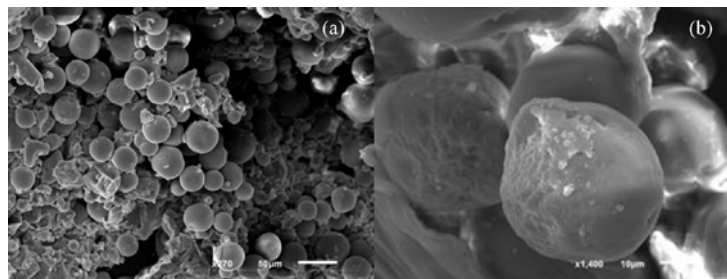


**Fig. 13.** SEM images of the dried emulsion with soybean oil and lutein as internal phase: micrograph of several droplets (a) and micrograph of a single droplet at higher magnification (b).

further evaporation step did not affect the emulsion encapsulation efficiency.

Encapsulation efficiency of the three concentrated emulsions was measured for four weeks, and the results are shown in Fig. 12. The presence of CMCNa not only increased the encapsulation efficiency, but also diminished lutein release along time. Even though the initial encapsulation efficiency was the same, the lutein release was retarded as  $f_w$  decreased for emulsions prepared with soybean oil as internal phase, if CMCNa was present in the external phase.

SEM images of the lutein-containing emulsion are shown in Fig. 13. The oil droplets of the dried emulsion had spherical and regular shapes. The microstructures showed a close packing structure for oil droplets, as expected, due to the high internal phase concentration of the emulsion studied.

#### 4. Conclusions

O/W emulsions with high internal phase concentration, up to 90% (v/v), and controlled droplet size were prepared by a two-step process, consisting of mechanical agitation followed by vacuum evaporation.

A lower droplet size was observed as volumetric water fraction ( $f_w$ ) decreased for emulsions prepared by mechanical agitation, indicating the proximity to emulsion inversion point. Viscosity of the internal phase was a key factor to monitor the emulsion inversion point.

Emulsion viscosity depended greatly on oil droplet size, whereas the viscosity of the oil used as internal phase had small influence. As a general trend, an emulsion with smaller droplet size had a higher viscosity.

Stability of formulated O/W emulsions was highly affected by oil droplet size and internal phase concentration. Creaming appeared earlier for O/W emulsions with large oil droplet size and low internal phase concentration. Moreover, O/W emulsions with high internal phase concentration showed more creaming resistance. In this case, emulsion viscosity was more important than oil droplet size regarding emulsion stability.

Vacuum evaporation allowed to obtain high internal phase emulsions with no variation of the original oil droplet size. This

parameter was not affected by the internal phase concentration and the type of oil used as internal phase.

The use of membrane emulsification, instead of mechanical agitation, to prepare the primary emulsion before vacuum evaporation improved droplet size control.

Oil viscosity slightly affected the mean droplet size for emulsions prepared by membrane emulsification. However, the type of oil used had a major influence on the final emulsion monodispersity.

HIEPs prepared by membrane emulsification and vacuum evaporation can be used to encapsulate lipophilic biocompounds, such as lutein. The selection of a proper oil as internal phase and the addition of CMCNa as stabilizer increased the lutein encapsulation efficiency up to 97%. An appropriate emulsion formulation would help not only to obtain monodisperse HIEPs but also to improve encapsulation efficiency and to retard biocompound release.

#### Acknowledgments

M. Matos is recipient of a FPI pre-doctoral fellowship (MEC, Spain). Financial support by the Ministerio de Ciencia e Innovación (MICINN, Spain) and the European Commission (Projects CTQ2007-65348 and CTQ2010-20009-C02-01, European Regional Development Fund) is also gratefully acknowledged.

This study was also co-financed by the Consejería de Educación y Ciencia del Principado de Asturias (PCTI Asturias 2006–2009, Ref.: EQP06-024).

#### Appendix A. Supplementary data

Supplementary data associated with this article can be found, in the online version, at <http://dx.doi.org/10.1016/j.colsurfa.2013.05.077>.

#### References

- [1] T.W. Dubensky, S.G. Reed, Adjuvants for cancer vaccines, *Semin. Immunol.* 22 (2010) 155–161.
- [2] K.P. Galvin, S.J. Pratten, N.G. Shankar, G.M. Evans, S.R. Biggs, D. Tunaley, Production of high internal phase emulsions using rising air bubbles, *Chem. Eng. Sci.* 56 (2001) 6285–6293.

# ARTICLE IN PRESS

G. Gutiérrez et al. / Colloids and Surfaces A: Physicochem. Eng. Aspects xxx (2013) xxx–xxx

- [3] K.J. Lissant, The geometry of high-internal-phase-ratio emulsions, *J. Colloid Interface Sci.* 22 (1966) 462–468.
- [4] G. Pilcer, K. Amighi, Formulation strategy and use of excipients in pulmonary drug delivery, *Int. J. Pharm.* 392 (2010) 1–19.
- [5] K.J. Lissant, Geometry of emulsions, *J. Soc. Cosmet. Chem.* 21 (1970) 141–154.
- [6] Y. Liu, S.E. Friberg, Role of liquid crystal in the emulsification of a gel emulsion with high internal phase ratio, *J. Colloid Interface Sci.* 340 (2009) 261–268.
- [7] M. Rondón-González, V. Sadtler, L. Choplin, J.L. Salager, Emulsion catastrophic inversion from abnormal to normal morphology. 5. Effect of the water-to-oil ratio and surfactant concentration on the inversion produced by continuous stirring, *Ind. Eng. Chem. Res.* 45 (2006) 3074–3080.
- [8] M. Rondón-González, V. Sadtler, P. Marchal, L. Choplin, J.L. Salager, Emulsion catastrophic inversion from abnormal to normal morphology. 7. Emulsion evolution produced by continuous stirring to generate a very high internal phase ratio emulsion, *Ind. Eng. Chem. Res.* 47 (2008) 2314–2319.
- [9] E. Tyrode, J. Allouche, L. Choplin, J.L. Salager, Emulsion catastrophic inversion from abnormal to normal morphology 4. Following the emulsion viscosity during three inversion protocols and extending the critical dispersed-phase concept, *Ind. Eng. Chem. Res.* 44 (2005) 67–74.
- [10] H.M. Princen, Highly concentrated emulsions: I. Cylindrical systems, *J. Colloid Interface Sci.* 71 (1979) 55–66.
- [11] H.M. Princen, M.P. Aronson, J.C. Moser, Highly concentrated emulsions: II. Real systems. The effect of thin film thickness and contact angle on the volume fraction in creamed emulsions, *J. Colloid Interface Sci.* 75 (1980) 246–270.
- [12] H. Rivas, X. Gutiérrez, F. Silva, M. Chirinos, Sobre emulsiones de bitumen en agua, *Cient. Venez.* 54 (2003) 216–234.
- [13] O.A. Alvarez, L. Choplin, V. Sadtler, P. Marchal, M.-J. Stébé, J. Mougel, C. Baravian, Influence of semibatch emulsification process conditions on the physical characteristics of highly concentrated water-in-oil emulsions, *Ind. Eng. Chem. Res.* 49 (2010) 6042–6064.
- [14] J. Esquena, G.S.R. Ravi-Sankar, C. Solans, Highly concentrated W/O emulsions prepared by the PIT method as templates for solid foams, *Langmuir* 19 (2003) 2983–2988.
- [15] Y. Matsumoto, M.M. Alam, K. Aramaki, Phase behaviour, formation, and rheology of cubic and hexagonal phase based gel emulsion in water/tetraglyceryl lauryl ether/oil systems, *Colloid Surf. A: Physicochem. Eng. Asp.* 341 (2009) 27–32.
- [16] N.A. Mishchuk, A. Sanfeld, A. Steinchen, Interparticle interaction in concentrate water-oil emulsions, *Adv. Colloid Interface Sci.* 112 (2004) 129–157.
- [17] P.A. Reynolds, E.P. Gilbert, M.J. Henderson, J.W. White, Structure of high aqueous-in-oil emulsions and related inverse micelle solutions. 4. Surfactant mixtures, *J. Phys. Chem. B* 113 (2009) 12243–12256.
- [18] S.B. Campbell, T. Larson, N.M.B. Smeets, U. El-Jaby, T.F.L. McKenna, Miniemulsification by catastrophic phase inversion, *Chem. Eng. J.* 183 (2012) 534–541.
- [19] S. Tcholakova, I. Lesov, K. Golemanov, N.D. Denkov, S. Judat, R. Engel, T. Danner, Efficient emulsification of viscous oils at high drop volume fraction, *Langmuir* 27 (2011) 14783–14796.
- [20] E. Paruta-Tuarez, P. Marchal, V. Sadtler, L. Choplin, Equation to model the storage modulus of highly concentrated emulsions, *Ind. Eng. Chem. Res.* 50 (2011) 10359–10365.
- [21] S. Sajadi, Formulation of fine emulsions at high viscosity or low interfacial tension: a comparative study, *Colloid Surf. A: Physicochem. Eng. Asp.* 299 (2007) 73–78.
- [22] K. Ozawa, C. Solans, H. Kunieda, Spontaneous formation of highly concentrated oil-in-water emulsions, *J. Colloid Interface Sci.* 188 (1997) 275–281.
- [23] S.M. Joscelyne, G. Trágardh, Membrane emulsification—a literature review, *J. Membr. Sci.* 169 (2000) 107–117.
- [24] A. Nazir, K. Schröen, R. Boom, Premix emulsification: a review, *J. Membr. Sci.* 362 (2010) 1–11.
- [25] S. van der Graaf, C.G.P.H. Schröen, R.M. Boom, Preparation of double emulsion by membrane emulsification—a review, *J. Membr. Sci.* 251 (2005) 7–15.
- [26] Q. Yuan, R.A. Williams, N. Aryanti, Innovations in high throughput manufacturing of uniform emulsions and capsules, *Adv. Powder Technol.* 21 (2010) 599–608.
- [27] T. Darvishzadeh, N.V. Priezjev, Effects of crossflow velocity and transmembrane pressure on microfiltration of oil-in-water emulsions, *J. Membr. Sci.* 423–424 (2012) 466–470.
- [28] E. Egidi, G. Gasparini, R.G. Holdich, G.T. Vladislavljević, S.R. Kosintsev, Membrane emulsification using membranes of regular pore spacing: droplet size and uniformity in the presence of surface shear, *J. Membr. Sci.* 323 (2008) 414–420.
- [29] K. Mitri, R. Shegokar, S. Ghosh, C. Anselmi, R.H. Müller, Lipid nanocarriers for dermal delivery of lutein: preparation, characterization, stability and performance, *Int. J. Pharm.* 414 (2011) 267–275.
- [30] X.-Y. Qv, Z.-P. Zeng, J.-G. Jiang, Preparation of lutein microencapsulation by complex coacervation method and its physicochemical properties and stability, *Food Hydrocolloids* 25 (2011) 1596–1603.
- [31] M.W. Davey, I. Van den Berg, R. Markham, R. Swennen, J. Keulemans, Genetic variability in Musa fruit provitamin A carotenoids, lutein and mineral micronutrient contents, *Food Chem.* 115 (2009) 806–813.
- [32] S. Shanmugam, J.-H. Park, K.S. Kim, Z.Z. Piao, C.S. Yong, H.-G. Choi, J.S. Woo, Enhanced bioavailability and retinal accumulation of lutein from self-emulsifying phospholipid suspensions (SEPS), *Int. J. Pharm.* 412 (2011) 99–105.
- [33] G. Gutiérrez, A. Cambiella, J.M. Benito, C. Pazos, J. Coca, The effect of additives on the treatment of oil-in-water emulsions by vacuum evaporation, *J. Hazard. Mater.* 144 (2007) 649–654.
- [34] G. Gutiérrez, J.M. Benito, J. Coca, C. Pazos, Vacuum evaporation of waste oil-in-water emulsions from a copper metalworking industry, *Ind. Eng. Chem. Res.* 48 (2009) 2100–2106.
- [35] V.G. Babak, M.-J. Stébé, Highly concentrated emulsions: physicochemical principles of formulation, *J. Disp. Sci. Technol.* 23 (2002) 1–22.
- [36] T.F. Tadros, B. Vincent, Liquid/liquid interfaces, in: P. Becher (Ed.), *Encyclopedia of Emulsion Technology*, 1, Marcel Dekker Inc., New York, 1983, pp. 1–56.
- [37] B. Egelandal, Ø. Langsrød, T. Nyvold, P.K. Søntum, C. Sørensen, G. Enersen, S. Hølland, R. Ofstad, Estimating significant causes of variation in emulsions' droplet size distribution obtained by the electrical sensing zone and laser low angle light scattering techniques, *Food Hydrocolloids* 15 (2001) 521–532.
- [38] A. Laca, B. Paredes, M. Díaz, Lipid-enriched egg yolk fraction as ingredient in cosmetic emulsions, *J. Texture Stud.* 43 (2012) 12–28.
- [39] A. Laca, M.C. Sáenz, B. Paredes, M. Díaz, Rheological properties, stability and sensory evaluation of low-cholesterol mayonnaises prepared using egg yolk granules as emulsifying agent, *J. Food Eng.* 97 (2010) 243–252.
- [40] I. Mira, N. Zambrano, E. Tyrode, L. Márquez, A.A. Peña, A. Pizzino, J.L. Salager, Emulsion catastrophic inversion from abnormal to normal morphology. 2. Effect of the stirring intensity on the dynamic inversion frontier, *Ind. Eng. Chem. Res.* 42 (2003) 57–61.
- [41] E. Tyrode, I. Mira, N. Zambrano, L. Márquez, M. Rondón-González, J.L. Salager, Emulsion catastrophic inversion from abnormal to normal morphology. 3. Conditions for triggering the dynamic inversion and application to industrial processes, *Ind. Eng. Chem. Res.* 42 (2003) 4311–4318.
- [42] N. Zambrano, E. Tyrode, I. Mira, L. Márquez, M.P. Rodríguez, J.L. Salager, Emulsion catastrophic inversion from abnormal to normal morphology. 1. Effect of the water-to-oil ratio rate of change on the dynamic inversion frontier, *Ind. Eng. Chem. Res.* 42 (2003) 50–56.
- [43] G. Schramm, *A Practical Approach to Rheology and Rheometry*, Thermo Electron, Karlsruhe, 2004.
- [44] J.F. Steffe, *Rheological Methods in Food Process Engineering*, 2nd ed., Freeman Press, East Lansing, 1996.
- [45] M. Rondón-González, L.F. Madariaga, V. Sadtler, L. Choplin, L. Márquez, J.L. Salager, Emulsion catastrophic inversion from abnormal to normal morphology. 6. Effect of the phase viscosity on the inversion produced by continuous stirring, *Ind. Eng. Chem. Res.* 46 (2007) 3595–3601.
- [46] I. Yaron, B. Gal-Or, On viscous flow and effective viscosity of concentrated suspensions and emulsions, *Rheol. Acta* 11 (1972) 241–252.
- [47] N. Vankova, S. Tcholakova, N.D. Denkov, I.B. Ivanov, V.D. Ulchev, T. Danner, Emulsification in turbulent flow. 1. Mean and maximum drop diameters in inertial and viscous regimes, *J. Colloid Interface Sci.* 312 (2007) 363–380.
- [48] S. Tcholakova, N.D. Denkov, K. Golemanov, K.P. Ananthapadmanabhan, A. Lips, Theoretical model of viscous friction inside steadily sheared foams and concentrated emulsions, *Phys. Rev. E* 78 (2008) 011405.
- [49] H.M. Princen, A.D. Kiss, Rheology of foams and highly concentrated emulsions. IV. An experimental study of the shear viscosity and yield stress of concentrated emulsions, *J. Colloid Interface Sci.* 128 (1989) 176–187.
- [50] S.S. Lim, M.Y. Baik, E.A. Decker, L. Henson, L.M. Popplewell, D.J. McClements, S.J. Choi, Stabilization of orange oil-in-water emulsions: a new role for ester gum as an Ostwald ripening inhibitor, *Food Chem.* 128 (2011) 1023–1028.
- [51] K. Ziani, Y. Chang, L. McLandborough, D.J. McClements, Influence of surfactant charge on antimicrobial efficacy of surfactant-stabilized thyme oil nanoemulsions, *J. Agric. Food Chem.* 59 (2011) 6247–6255.

Please cite this article in press as: G. Gutiérrez, et al., Preparation of HIPEs with controlled droplet size containing lutein, *Colloids Surf. A: Physicochem. Eng. Aspects* (2013), <http://dx.doi.org/10.1016/j.colsurfa.2013.05.077>

## **Supporting information**

### **Preparation of HIPEs with controlled droplet size containing lutein**

Gemma Gutiérrez<sup>a</sup>, María Matos<sup>a</sup>, José M. Benito<sup>b</sup>, José Coca<sup>a</sup>, Carmen Pazos<sup>a,\*</sup>

<sup>a</sup>Department of Chemical and Environmental Engineering, University of Oviedo, Julián Clavería 8, 33006 Oviedo, Spain

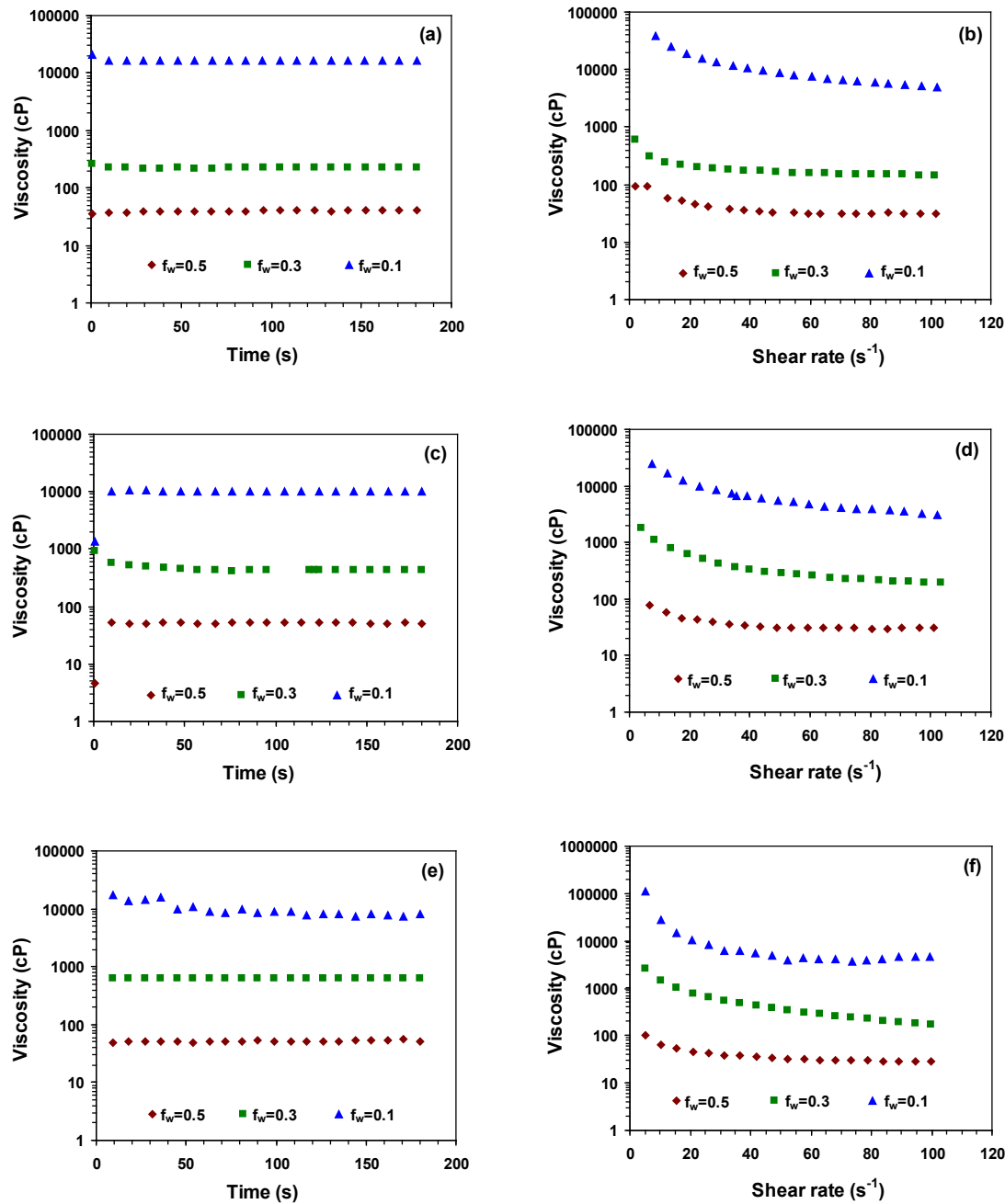
<sup>b</sup>Department of Chemical Engineering, University of Burgos, Plaza Misael Bañuelos s/n, 09001 Burgos, Spain

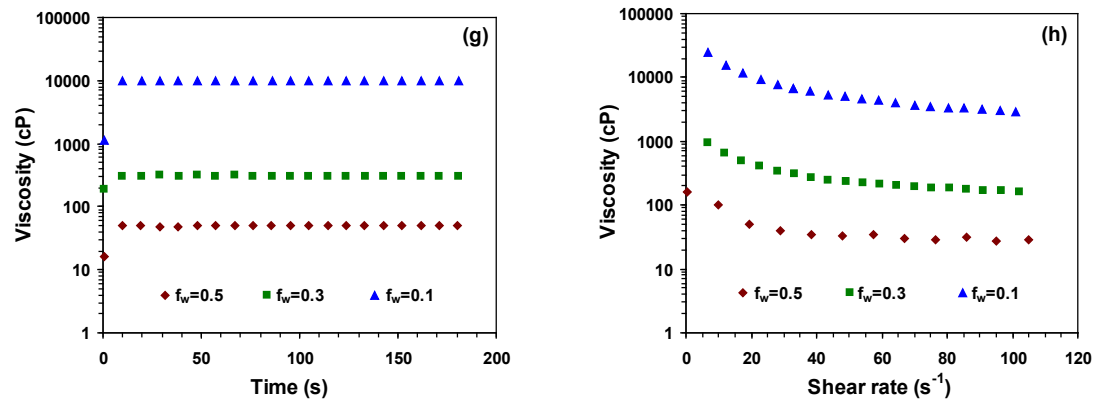
\*Corresponding author: Prof. C. Pazos

Tel: +34 985103509;

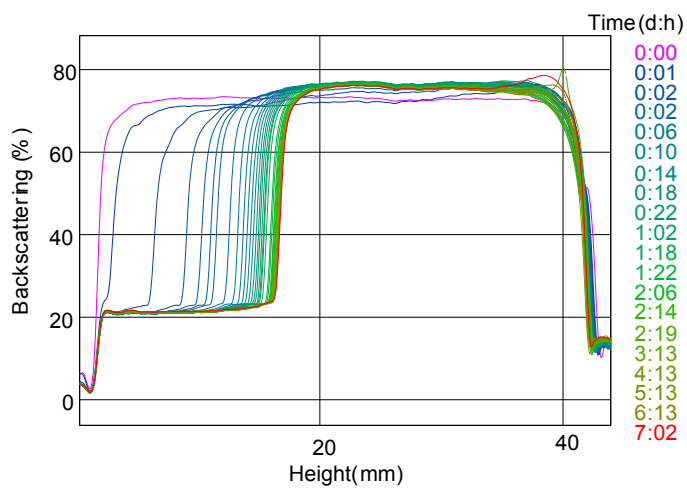
Fax: +34 985103434

E-mail address: [cpazos@uniovi.es](mailto:cpazos@uniovi.es)

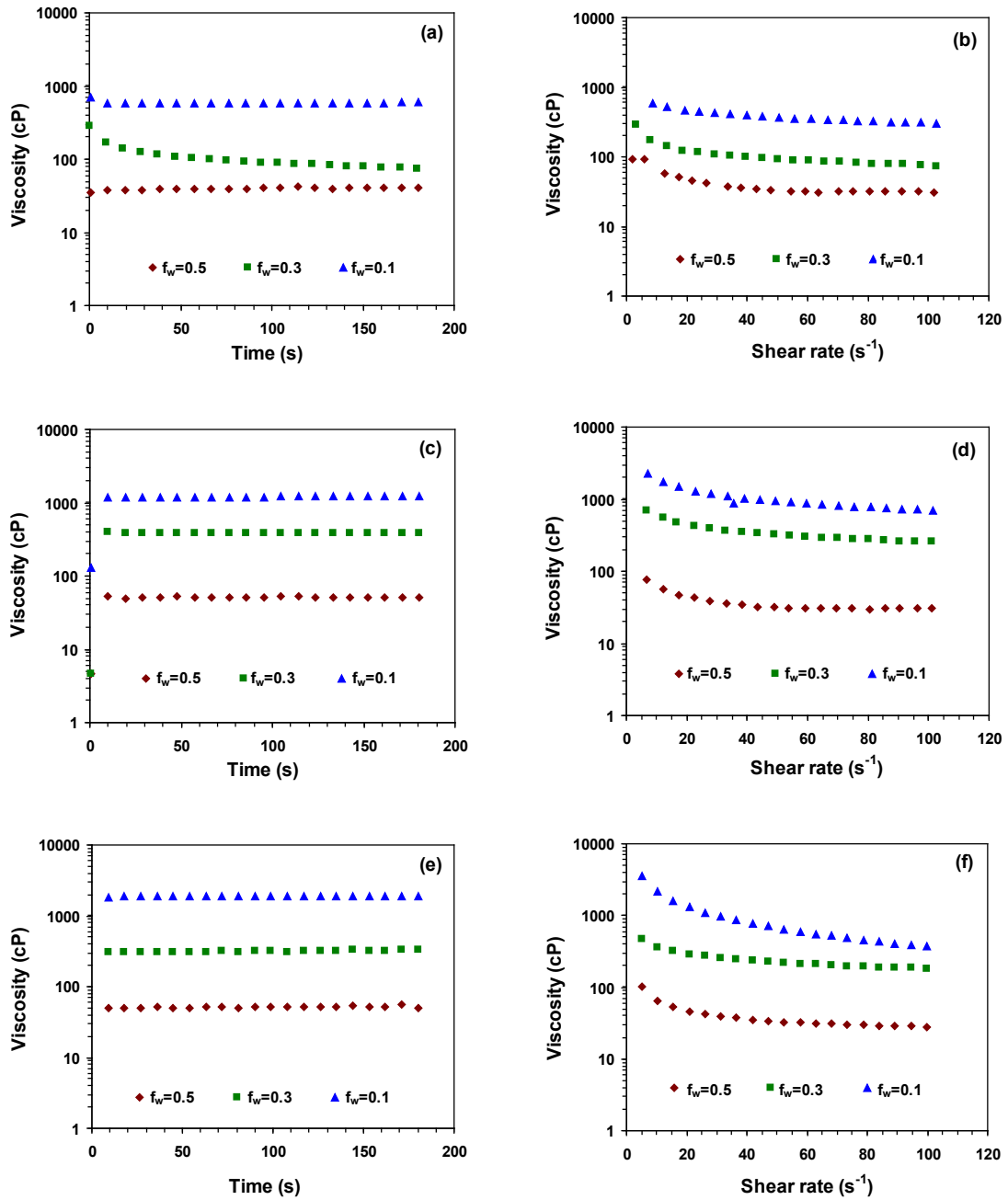




**Figure S1.** Viscosity vs. time and viscosity vs. shear rate curves for emulsions prepared by mechanical agitation using castor oil (a, b), heavy mineral oil (c, d), soybean oil (e, f) or light mineral oil (g, h) as internal phase.



**Figure S2.** Backscattering profiles for the emulsion with  $f_w = 0.5$  prepared by mechanical agitation using castor oil as internal phase.



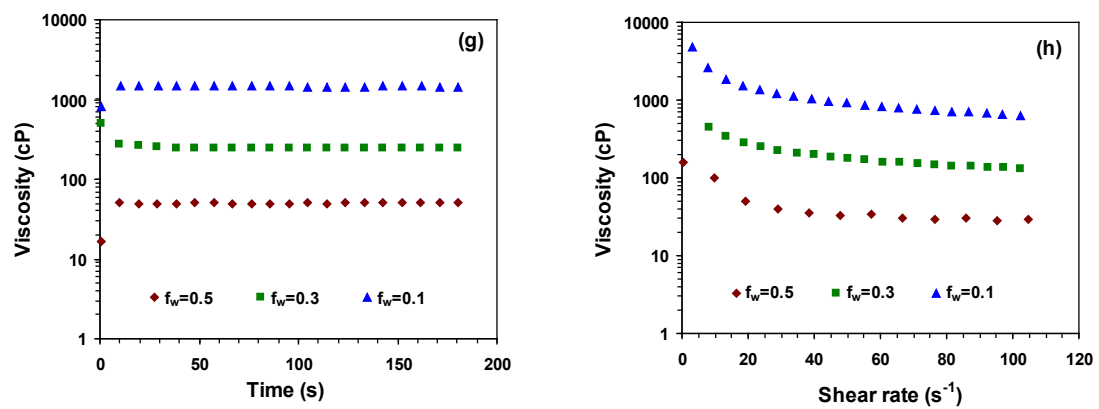


**Figure S3.** Viscosity vs. time and viscosity vs. shear rate curves for emulsions prepared by mechanical agitation and further vacuum evaporation using castor oil (a, b), heavy mineral oil (c, d), soybean oil (e, f) or light mineral oil (g, h) as internal phase.

**Table S1**

Conductivities ( $\kappa_e$ ) and effective volumetric water fractions ( $f_{wef}$ ) for emulsions prepared by mechanical agitation using castor oil, heavy mineral oil, soybean oil or light mineral oil as internal phase.

Castor oil		Heavy mineral oil		Soybean oil		Light mineral oil		
$f_w$	$\kappa_e$ (mS/cm)	$f_{wef}$	$\kappa_e$ (mS/cm)	$f_{wef}$	$\kappa_e$ (mS/cm)	$f_{wef}$	$\kappa_e$ (mS/cm)	$f_{wef}$
0.5	7.3	0.5	7.2	0.5	7.3	0.5	7.3	0.5
0.3	3.4	0.3	2.9	0.3	3.3	0.3	3.1	0.3
0.1	0.61	0.1	0.66	0.1	0.62	0.1	0.64	0.1

**Table S2**

Conductivities ( $\kappa_e$ ) and effective volumetric water fractions ( $f_{wef}$ ) for emulsions prepared by mechanical agitation and further concentrated by vacuum evaporation using castor oil, heavy mineral oil, soybean oil or light mineral oil as internal phase.

Castor oil		Heavy mineral oil		Soybean oil		Light mineral oil		
$f_w$	$\kappa_e$ (mS/cm)	$f_{wef}$	$\kappa_e$ (mS/cm)	$f_{wef}$	$\kappa_e$ (mS/cm)	$f_{wef}$	$\kappa_e$ (mS/cm)	$f_{wef}$
0.3	3.7	0.3	3.7	0.3	3.7	0.3	3.6	0.3
0.1	0.75	0.1	0.80	0.1	0.77	0.1	0.68	0.1





## **GENERAL CONCLUSIONS**

From the results presented in this thesis and in the attached publications the following conclusions can be reached:

1. Stable monodisperse O/W emulsions were obtained using commercial available microfiltration flat and tubular ceramic membranes. Typical operation parameters seemed to have a small influence on mean droplet diameter and size distribution, suggesting that the droplet formation mechanism was not shear stress-based. A spontaneous emulsification mechanism was proposed for both types of membranes.
2. Double Pickering emulsions stabilized with starch granules, isolated from Quinoa and hydrophobically modified, were prepared showing high encapsulation stability after one month of storage at room temperature. These results suggest that this type of starch double Pickering emulsions could be suitable for several applications in food and pharmaceutical products.
3. For water-in-oil-in-water ( $W_1/O/W_2$ ) double emulsions formulated to encapsulate *trans*-resveratrol, polyglycerol polyricinoleate (PGPR) was the best inner emulsifier. The combination of Tween 20 and CMCNa in the external aqueous phase seemed to have a synergetic effect leading to better initial encapsulation efficiencies. An increase in PGPR content yielded a slight increase in initial encapsulation efficiency values.
4. Since vacuum evaporation did not modify emulsion droplet size, a combination of membrane emulsification and vacuum evaporation allowed to obtain O/W emulsions with high internal phase content (HIPEs) and controlled droplet size containing lipophilic bioactive compounds, as lutein.

## **CONCLUSIONES GENERALES**

A partir de todos los resultados obtenidos en este trabajo, se ha llegado a las conclusiones generales que a continuación se exponen:

1. Se obtuvieron emulsiones aceite-agua, monodispersas y estables, usando membranas cerámicas comerciales de microfiltración planas y tubulares. Los parámetros típicos de operación presentaron poca influencia en el tamaño medio de gota y en la distribución de tamaños, lo que sugirió que el mecanismo de formación de gota no estaba basado en el esfuerzo cortante. Se propuso un mecanismo de formación espontánea de gota para ambos tipos de membranas.
2. Las emulsiones dobles tipo Pickering, estabilizadas con partículas de almidón, procedente de la Quinoa y modificadas hidrofóbicamente, presentaron una elevada estabilidad después de un mes de almacenamiento a temperatura ambiente. Por tanto, estas emulsiones podrían resultar apropiadas para su aplicación en diversos alimentos y productos cosméticos.
3. El polirricinoleato de poliglicerol (PGPR) resultó ser el estabilizante más adecuado en la formulación de emulsiones dobles agua-aceite-agua (W/O/W) para encapsular trans-resveratrol. La combinación en la fase externa del tensioactivo Tween 20 y la carboximetilcelulosa sódica (CMCNa) dio lugar a un efecto sinérgico con valores más elevados de eficacia de encapsulación. Se obtuvieron emulsiones más estables, cuando se prepararon mediante agitación mecánica, que cuando se prepararon mediante técnicas con membranas. Un mayor contenido de PGPR condujo a un aumento de la eficacia de encapsulación inicial.
4. La evaporación a vacío no modifica el tamaño de gota de la emulsión de partida. Por ello, la combinación de dos técnicas, emulsificación con membranas y evaporación a vacío, permitió preparar emulsiones O/W con elevado contenido en fase interna (HIEPs) y tamaño de gota totalmente controlado, conteniendo biocompuestos lipófilos como la luteína.

## **REFERENCES**

- Abrahamse A.J., A. van der Padt, R.M. Boom, W.B.C. de Heij (2001) Process fundamentals of membrane emulsification: simulation with CFD, *AIChE J.* 47, 1285–1291.
- Abrahamse A.J., R. van Lierop, R.G.M. van der Sman, A. van der Padt, R.M. Boom (2002) Analysis of droplet formation and interactions during cross-flow membrane emulsification, *J. Membr. Sci.* 204, 125–137.
- Alvarez O.A., L. Choplin, V. Sadtler, P. Marchal, M.-J. Stébé, J. Mougel, C. Baravian (2010) Influence of semibatch emulsification process conditions on the physical characteristics of highly concentrated water-in-oil emulsions, *Ind. Eng. Chem. Res.* 49, 6042–6064.
- Amri A., J.C. Chaumeil, S. Sfar, C. Charreau (2012) Administration of resveratrol: what formulation solutions to bioavailability limitations?, *J. Control. Release* 158, 182–193.
- Aryanti N., R. Hou, R.A. Williams (2009) Performance of a rotating membrane emulsifier for production of coarse droplets, *J. Membr. Sci.* 326, 9–18.
- Aserin A. (2008) *Multiple Emulsions: Technology and Applications*, Wiley Interscience, Hoboken, USA.
- Augustin M.A., Y. Hemar (2009) Nano- and micro-structured assemblies for encapsulation of food ingredients, *Chem. Soc. Rev.* 38, 902–912.
- Aveyard R., B.P. Binks, J.H. Clint (2003) Emulsions stabilised solely by colloidal particles, *Adv. Colloid Interface Sci.* 100–102, 503–546.
- Bancroft W.D. (1913) The theory of emulsification, V, *J. Phys. Chem.* 17, 501–519.
- Bancroft W.D. (1915) The theory of emulsification, VI, *J. Phys. Chem.* 19, 275–309.
- Biesalski H.-K., L.O. Dragsted, I. Elmadafa, R. Grossklaus, M. Müller, D. Schrenk, P. Walter, P. Weber (2009) Bioactive compounds: definition and assessment of activity, *Nutrition* 25, 1202–1205.
- Binks B.P. (2002) Particles as surfactants – similarities and differences, *Curr. Opin. Colloid Interface Sci.* 7, 21–41.
- Caddeo B., K. Teskac, C. Sinico, J. Kristl (2008) Effect of resveratrol incorporated in liposomes on proliferation and UV-B protection of cells, *Int. J. Pharm.* 363, 183–191.
- Campbell S.B., T. Larson, N.M.B. Smeets, U. El-Jaby, T.F.L. McKenna (2012) Miniemulsification by catastrophic phase inversion, *Chem. Eng. J.* 183, 534–541.
- Charcosset C., I. Limayem, H. Fessi (2004) The membrane emulsification process—a review, *J. Chem. Technol. Biotechnol.* 79, 209–218.

- Charcosset C. (2009) Preparation of emulsions and particles by membrane emulsification for the food processing industry, *J. Food. Eng.* 92, 241–249.
- Christov N.C., D.N. Ganchev, N.D. Vassileva, N.D. Denkov, K.D. Danov, P.A. Kralchevsky (2002) Capillary mechanisms in membrane emulsification: oil-in-water emulsions stabilized by Tween 20 and milk proteins, *Colloid Surf. A-Physicochem. Eng. Asp.* 209, 83–104.
- Christov N.C., K.D. Danov, D.K. Danova, P.A. Kralchevsky (2008) The drop size in membrane emulsification determined from the balance of capillary and hydrodynamic forces, *Langmuir* 24, 1397–1410.
- Constantinides P.P. (1995) Lipid microemulsions for improving drug dissolution and oral absorption: physical and biopharmaceutical aspects, *Pharm. Res.* 12, 1561–1572.
- Constantinides P.P., G. Welzel, H. Ellens, P.L. Smith, S. Sturgis, S.H. Yiv, A.B. Owen (1996) Water-in-oil microemulsions containing medium-chain fatty acids/salts: formulation and intestinal absorption enhancement evaluation, *Pharm. Res.* 13, 210–215.
- Danov K.D., D.K. Danova, P.A. Kralchevsky (2007) Hydrodynamic forces acting on a microscopic emulsion drop growing at a capillary tip in relation to the process of membrane emulsification, *J. Colloid Interface Sci.* 316, 844–857.
- De los Reyes J.S., C. Charcosset (2010) Preparation of water-in-oil and ethanol-in-oil emulsions by membrane emulsification, *Fuel* 89, 3482–3488.
- De Luca G., E. Drioli (2006) Force balance conditions for droplet formation in cross-flow membrane emulsifications, *J. Colloid Interface Sci.* 294, 436–448.
- De Luca G., F.P. Di Maio, A. Di Renzo, E. Drioli (2008) Droplet detachment in cross-flow membrane emulsification: comparison among torque- and force-based models, *Chem. Eng. Process.* 47, 1150–1158.
- Dickinson E. (2010) Food emulsions and foams: stabilization by particles, *Curr. Opin. Colloid Interface Sci.* 15, 40–49.
- Dickinson E. (2011) Double emulsions stabilized by food biopolymers, *Food Biophys.* 6, 1–11.
- Donsi F., M. Sessa, H. Mediouni, A. Mgaidi, G. Ferrari (2011) Encapsulation of bioactive compounds in nanoemulsion-based delivery systems, *Procedia Food Sci.* 1, 1666–1671.
- Dubensky T.W., S.G. Reed (2010) Adjuvants for cancer vaccines, *Semin. Immunol.* 22, 155–161.
- Eisner V. (2007) *Emulsion Processing with a Rotating Membrane (ROME)*, PhD Thesis, Laboratory of Food Process Engineering, ETH Zürich, Switzerland.

- Esquena J., G.S.R. Ravi-Sankar, C. Solans (2003) Highly concentrated W/O emulsions prepared by the PIT method as templates for solid foams, *Langmuir* 19, 2983–2988.
- Fabris S., F. Momo, G. Ravagnan, R. Stevanato (2008) Antioxidant properties of resveratrol and piceid on lipid peroxidation in micelles and monolamellar liposomes, *Biophys. Chem.* 135, 76–83.
- Fang J.Y., C.F. Hung, M.H. Liao, C.C. Chien (2007) A study of the formulation design of acoustically active lipospheres as carriers for drug delivery, *Eur. J. Pharm. Biopharm.* 67, 67–75.
- Fang Z.X., B. Bhandari (2010) Encapsulation of polyphenols—a review, *Trends Food Sci. Technol.* 21, 510–523.
- Fanun M. (2009) *Microemulsions: Properties and Applications*. Surfactant Science Series 144, CRC Press, Boca Raton, USA.
- Frasch-Melnik S., I.T. Norton, F. Spyropoulos (2010a) Fat-crystal stabilised w/o emulsions for controlled salt release, *J. Food. Eng.* 98, 437–442.
- Frasch-Melnik S., F. Spyropoulos, I.T. Norton (2010b) W1/O/W2 double emulsions stabilised by fat crystals—Formulation, stability and salt release, *J. Colloid Interface Sci.* 350, 178–185.
- Galvin K.P., S.J. Pratten, N.G. Shankar, G.M. Evans, S.R. Biggs, D. Tunaley (2001) Production of high internal phase emulsions using rising air bubbles, *Chem. Eng. Sci.* 56, 6285–6293.
- Garti N., A. Aserin, Y. Cohen (1994) Mechanistic considerations on the release of electrolytes from multiple emulsions stabilized by BSA and nonionic surfactants, *J. Control. Release* 29, 41–51.
- Garti N. (1997a) Double emulsions—scope, limitations and new achievements. *Colloid Surf. A-Physicochem. Eng. Asp.* 123–124, 233–246.
- Garti N. (1997b) Progress in stabilization and transport phenomena of double emulsions in food applications, *LWT Food Sci. Technol.* 30, 222–235.
- Gijsbertsen-Abrahamse A.J., A. van der Padt, R.M. Boom (2004) Status of cross-flow membrane emulsification and outlook for industrial application, *J. Membr. Sci.* 230, 149–159.
- Groeneweg F., W.G.M. Agterof, P. Jaeger, J.J.M. Janssen, J.A. Wieringa, J.K. Klahn (1998) On the mechanism of the inversion of emulsions, *Chem. Eng. Res. Des.* 76, 55–63.
- Hao D.X., F.L. Gong, G.H. Hu, Y.J. Zhao, G.P. Lian, G.H. Ma, Z. Su (2008) Controlling factors on droplets uniformity in membrane emulsification: experiment and modeling analysis, *Ind. Eng. Chem. Res.* 47, 6418–6425.

- Ho H.O., C.C. Hsiao, M.T. Sheu (1996) Preparation of microemulsions using polyglycerol fatty acids as surfactant for the delivery of protein drugs, *J. Pharm. Sci.* 85, 138–143.
- Holdich R.G., M.M. Dragosavac, G.T. Vladisavljevic, S.T. Kosvintsev (2010) Membrane emulsification with oscillating and stationary membranes, *Ind. Eng. Chem. Res.* 49, 3810–3817.
- Joscelyne S.M., G. Trägårdh (2000) Membrane emulsification—a literature review, *J. Membr. Sci.* 169, 107–117.
- Joubran R., N. Parris, D. Lu, S. Trevino (1994) Synergetic effect of sucrose and ethanol on formation of triglyceride microemulsions, *J. Dispersion Sci. Technol.* 15, 687–704.
- Kahlweit M., G. Busse, B. Faulhaber, H. Eibl (1995) Preparing nontoxic microemulsions, *Langmuir* 11, 4185–4187.
- Kahlweit M., G. Busse, B. Faulhaber (1996) Preparing microemulsions with alkyl monoglycosides and the role of alkanediols as cosolvents, *Langmuir* 12, 861–862.
- Kawakatsu T., Y. Kikuchi, M. Nakajima (1997) Regular-sized cell creation in microchannel emulsification by visual microprocessing method, *J. Am. Oil Chem. Soc.* 74, 317–321.
- Kobayashi I., M. Nakajima, S. Mukataka (2003) Preparation characteristics of oil-in-water emulsions using differently charged surfactants in straight-through microchannel emulsification, *Colloid Surf. A-Physicochem. Eng. Asp.* 229, 33–41.
- Kobayashi I., S. Mukataka, M. Nakajima (2004) Effect of slot aspect ratio on droplet formation from silicon straight-through microchannels, *J. Colloid Interface Sci.* 279, 277–280.
- Kosvintsev S.R., G. Gasparini, R.G. Holdich, I.W. Cumming, M.T. Stillwell (2005) Liquid-liquid membrane dispersion in a stirred cell with and without controlled shear, *Ind. Eng. Chem. Res.* 44, 9323–9330.
- Kristl J., K. Teskac, C. Caddeo, Z. Abramovic, M. Sentjurc (2009) Improvements of cellular stress response on resveratrol in liposomes, *Eur. J. Pharm. Biopharm.* 773, 253–259.
- Krog N. (1977) Functions of emulsifiers in food systems, *J. Am. Oil Chem. Soc.* 54, 124–131.
- Kunieda H., Y. Hasegawa, A.C. John, M. Naito, M. Muto (1996) Phase behavior of polyoxyethylene hydrogenated castor oil in oil/water system, *Colloid Surf. A-Physicochem. Eng. Asp.* 109, 209–216.
- Kukizaki M. (2009) Shirasu porous glass (SPG) membrane emulsification in the absence of shear flow at the membrane surface: influence of surfactant type and

concentration, viscosities of dispersed and continuous phases, and transmembrane pressure, *J. Membr. Sci.* 327, 234–243.

Kukizaki M., M. Goto (2009) A comparative study of SPG membrane emulsification in the presence and absence of continuous-phase flow, *J. Chem. Eng. Jpn.* 42, 520–530.

Lambrich U., H. Schubert (2005) Emulsification using microporous systems, *J. Membr. Sci.* 257, 76–84.

Lim H., A. Kassim, N. Huang, M.A. Yarmo (2009) Palm-based nonionic surfactants as emulsifiers for high internal phase emulsions, *J. Surfactants Deterg.* 12, 355–362.

Lissant K.J. (1970) Geometry of emulsions, *J. Soc. Cosmet. Chem.* 21, 141–154.

Lissant K.J. (1996) The geometry of high-internal-phase-ratio emulsions, *J. Colloid Interface Sci.* 22, 462–468.

Liu Y., S.E. Friberg (2009) Role of liquid crystal in the emulsification of a gel emulsion with high internal phase ratio, *J. Colloid Interface Sci.* 340, 261–268.

Lucas-Abellán C., I. Fortea, J.M. López-Nicolás, E. Núñez-Delicado (2007) Cyclodextrins as resveratrol carrier system, *Food Chem.* 104, 39–44.

Luo Z., B.S. Murray, A. Yusoff, M.R.A. Morgan, M.J.W. Povey, A.J. Day (2011) Particle-stabilizing effects of flavonoids at the oil-water interface, *J. Agric. Food Chem.* 59, 2636–2645.

Maan A.A., K. Schroën, R. Boom (2011) Spontaneous droplet formation techniques for monodisperse emulsions preparation—Perspectives for food applications, *J. Food Eng.* 107, 334–346.

Márquez A.L., G.G. Palazolo, J.R. Wagner (2007) Water in oil (w/o) and double (w/o/w) emulsions prepared with spans: microstructure, stability, and rheology, *Colloid Polym. Sci.* 285, 1119–1128.

Márquez A.L., A. Medrano, L.A. Panizzolo, J.R. Wagner (2010) Effect of calcium salts and surfactant concentration on the stability of water-in-oil emulsions prepared with polyglycerol polyricinoleate, *J. Colloid Interface Sci.* 341, 101–108.

Mason T.G., J.N. Wilking, K. Meleson, C.B. Chang, S.M. Graves (2006) Nanoemulsions: formation, structure, and physical properties, *J. Phys.: Condens. Matter* 18, R635–R666.

Matsumoto Y., M.M. Alam, K. Aramaki (2009) Phase behaviour, formation, and rheology of cubic and hexagonal phase based gel emulsion in water/tetraglyceryl lauryl ether/oil systems, *Colloid Surf. A-Physicochem. Eng. Asp.* 341, 27–32.

Meyer R.F., J.C. Crocker (2009) Universal dripping and jetting in a transverse shear flow, *Phys. Rev. Lett.* 102, 194501.

- Mishchuk N.A., A. Sanfeld, A. Steinchen (2004) Interparticle interaction in concentrate water-oil emulsions, *Adv. Colloid Interface Sci.* 112, 129–157.
- Mitri K., R. Shegokar, S. Gohla, C. Anselmi, R.H. Müller (2011) Lipid nanocarriers for dermal delivery of lutein: preparation, characterization, stability and performance, *Int. J. Pharm.* 414, 267–275.
- Murray B.S., K. Durga, A. Yusoff, S.D. Stoyanov (2011) Stabilization of foams and emulsions by mixtures of surface active food-grade particles and proteins, *Food Hydrocolloids* 25, 627–638.
- Muschiolik G. (2007) Multiple emulsions for food use, *Curr. Opin. Colloid Interface Sci.* 12, 213–220.
- Myers D. (2006) *Surfactant Science and Technology*, 3<sup>rd</sup> Ed. Wiley, Hoboken, USA.
- Nazir A., K. Schroën, R. Boom (2010) Premix emulsification: a review, *J. Membr. Sci.* 362, 1–11.
- Nazir A., K. Schroën, R. Boom (2011) High-throughput premix membrane emulsification using nickel sieves having straight-through pores, *J. Membr. Sci.* 383, 116–123.
- Okochi H., M. Nakano (1997) Comparative study of two preparation methods of W/O/W emulsions: stirring and membrane emulsification, *Chem. Pharm. Bull.* 45, 1323–1326.
- Pando D., C. Caddeo, M. Manconi, A.M. Fadda, C. Pazos (2013a) Nanodesign of olein vesicles for the topical delivery of antioxidant resveratrol, *J. Pharm. Pharmacol.* 65, 1158–1167.
- Pando D., G. Gutiérrez, J. Coca, C. Pazos (2013b) Preparation and characterization of niosomes containing resveratrol, *J. Food Eng.* 117, 227–234.
- Park K.M., M.K. Lee, K.J. Hwang, C.K. Kim (1999) Phospholipid-based microemulsions of flurbiprofen by the spontaneous emulsification process, *Int. J. Pharm.* 183, 145–154.
- Pathak M. (2011) Numerical simulation of membrane emulsification: effect of flow properties in the transition from dripping to jetting, *J. Membr. Sci.* 382, 166–176.
- Pawlak A.K., I.T. Norton (2012) Encapsulation stability of duplex emulsions prepared with SPG cross-flow membrane, SPG rotating membrane and rotor-stator techniques—A comparison, *J. Membr. Sci.* 415–416, 459–468.
- Peng H., H. Xiong, J. Li, M. Xie, Y. Liu, C. Bai, L. Chen (2010) Vanillin cross-linked chitosan microspheres for controlled release of resveratrol, *Food Chem.* 121, 23–28.

- Peng S.J., R.A. Williams (1998) Controlled production of emulsions using a crossflow membrane. Part I: Droplet formation from a single pore, *Chem. Eng. Res. Des.* 76, 894–901.
- Pickering S.U. (1907) Emulsions, *J. Chem. Soc. Trans.* 91, 2001–2021.
- Pilcer G., K. Amighi (2010) Formulation strategy and use of excipients in pulmonary drug delivery, *Int. J. Pharm.* 392, 1–19.
- Priest C., S. Herminghaus, R. Seemann (2006) Generation of monodisperse gel emulsions in a microfluidic device, *Appl. Phys. Lett.* 88, 024106.
- Princen H.M. (1979) Highly concentrated emulsions: I. Cylindrical systems, *J. Colloid Interface Sci.* 71, 55–66.
- Princen H.M., M.P. Aronson, J.C. Moser (1980) Highly concentrated emulsions: II. Real systems. The effect of thin film thickness and contact angle on the volume fraction in creamed emulsions, *J. Colloid Interface Sci.* 75, 246–270.
- Princen H.M., A.D. Kiss (1986) Rheology of foams and highly concentrated emulsions. III. Static shear modulus, *J. Colloid Interface Sci.* 112, 427–437.
- Qv X.-Y., Z.-P. Zeng, J.-G. Jiang (2011) Preparation of lutein microencapsulation by complex coacervation method and its physicochemical properties and stability, *Food Hydrocolloids* 25, 1596–1603.
- Ramakrishnan S., M. Ferrando, L. Aceña-Muñoz, S. De Lamio-Castellví, C. Güell (2013a) Fish oil microcapsules from O/W emulsions produced by premix membrane emulsification, *Food Bioprocess Technol.* 6, 3088–3101.
- Ramakrishnan S., M. Ferrando, L. Aceña-Muñoz, S. De Lamio-Castellví, C. Güell (2013b) Influence of emulsification technique and wall composition on physicochemical properties and oxidative stability of fish oil microcapsules produced by spray drying, *Food Bioprocess Technol.* DOI 10.1007/s11947-013-1187-4
- Ramsden W. (1903) Separation of solids in the surface-layers of solutions and suspensions (Observations on surface-membranes, bubbles, emulsions, and mechanical coagulation)—Preliminary account, *Proc. R. Soc. London* 72, 156–164.
- Rayner M., G. Trägårdh (2002) Membrane emulsification modelling: how can we get from characterisation to design?, *Desalination* 145, 165–172.
- Rayner M., G. Trägårdh, C. Trägårdh, P. Dejmek (2004) Using the Surface Evolver to model droplet formation processes in membrane emulsification, *J. Colloid Interface Sci.* 279, 175–185.
- Rayner M., G. Trägårdh, C. Trägårdh (2005) The impact of mass transfer and interfacial tension expansion rate on droplet size in membrane emulsification processes, *Colloid Surf. A-Physicochem. Eng. Asp.* 266, 1–17.

- Rayner M., M. Sjöö, A. Timgren, P. Dejmek (2012) Quinoa starch granules as stabilizing particles for production of Pickering emulsions, *Faraday Discuss.* 158, 139–155.
- Reynolds P.A., E.P. Gilbert, M.J. Henderson, J.W. White (2009) Structure of high aqueous-in-oil emulsions and related inverse micelle solutions. 4. Surfactant mixtures, *J. Phys. Chem. B* 113, 12243–12256.
- Rondón-González M., V. Sadtler, L. Choplin, J.L. Salager (2006) Emulsion catastrophic inversion from abnormal to normal morphology. 5. Effect of the water-to-oil ratio and surfactant concentration on the inversion produced by continuous stirring, *Ind. Eng. Chem. Res.* 45, 3074–3080.
- Rondón-González M., V. Sadtler, P. Marchal, L. Choplin, J.L. Salager (2008) Emulsion catastrophic inversion from abnormal to normal morphology. 7. Emulsion evolution produced by continuous stirring to generate a very high internal phase ratio emulsion, *Ind. Eng. Chem. Res.* 47, 2314–2319.
- Rosen M.J. (2004) *Surfactants and Interfacial Phenomena*, 3<sup>rd</sup> Ed. Wiley Interscience, Hoboken, USA.
- Rossier-Miranda F.J., K. Schroën, R. Boom (2010) Mechanical characterisation and release properties of fibril-reinforced microcapsules prepared by layer-by-layer adsorption, *Langmuir* 26, 19106–19113.
- Saiko P., A. Szakmary, W. Jaeger, T. Szekeres (2008) Resveratrol and its analogs: defense against cancer, coronary disease and neurodegenerative maladies or just a fad?, *Mutat. Res.-Rev. Mutat. Res.* 658, 68–94.
- Saint Ruth H., D. Attwood, G. Ktistis, C.J. Taylor (1995) Phase studies and particle size analysis of oil-in-water phospholipid microemulsions, *Int. J. Pharm.* 116, 253–261.
- Sapei L., M.A. Naqvi, D. Rousseau (2012) Stability and release properties of double emulsions for food applications, *Food Hydrocolloids* 27, 316–323.
- Sawalha H., N. Purwanti, A. Rinzema, K. Schroën, R. Boom (2008) Polylactide microspheres prepared by premix membrane emulsification-Effects of solvent removal rate, *J. Membr. Sci.* 310, 484–493.
- Schmidts T., D. Dobler, A.-C. Guldan, N. Paulus, F. Runkel (2010) Multiple W/O/W emulsions—Using the required HLB for emulsifier evaluation, *Colloid Surf. A-Physicochem. Eng. Asp.* 372, 48–54.
- Schröder V., H. Schubert (1999) Production of emulsions using microporous ceramic membranes, *Colloid Surf. A-Physicochem. Eng. Asp.* 152, 103–109.
- Seifriz W. (1924) Studies in emulsions. III-V, *J. Phys. Chem.* 29, 738–749
- Shao J., X. Li, X. Lu, C. Jiang, Y. Hu, Q. Li, Y. You, Z. Fu (2009) Enhanced growth inhibition effect of Resveratrol incorporated into biodegradable nanoparticles against

glioma cells is mediated by the induction of intracellular reactive oxygen species levels, *Colloid Surf. B-Biointerfaces* 72, 40–47.

Shinoda K., M. Araki, A. Sadaghiani, A. Khan, B. Lindman (1991) Lecithin-based microemulsions; phase behavior and microstructure, *J. Phys. Chem.* 95, 989–993.

Solans C., J. Esquena, N. Azemar (2003) Highly concentrated (gel) emulsions, versatile reaction media, *Curr. Opin. Colloid Interface Sci.* 8, 156–163.

Steegmans M.L.J., C.G.P.H. Schroën, R.M. Boom (2009) Generalised insights in droplet formation at T-junctions through statistical analysis, *Chem. Eng. Sci.* 64, 3042–3050.

Stubenrauch C., B. Paeplow, G.H. Findenegg (1997) Microemulsions supported by octyl monoglucoside and geraniol. 1. The role of alcohol in the interfacial layer, *Langmuir* 13, 3652–3658.

Su J., J. Flanagan, Y. Hemar, H. Singh (2006) Synergistic effects of polyglycerol ester of polyricinoleic acid and sodium caseinate on the stabilisation of water-oil-water emulsions, *Food Hydrocolloids* 20, 261–268.

Suárez M.Á., J. Coca, C. Pazos (2012) Membrane emulsification: factors influencing the size and distribution of the drops, *Ing. Quím.* 505, 58–73.

Sugiura S., M. Nakajima, N. Kumazawa, S. Iwamoto, M. Seki (2002) Characterization of spontaneous transformation-based droplet formation during microchannel emulsification, *J. Phys. Chem. B.* 106, 9405–9409.

Surh J., Y.G. Jeong, G.T. Vladisavljevic (2008) On the preparation of lecithin-stabilized oil-in-water emulsions by multi-stage premix membrane emulsification, *J. Food Eng.* 89, 164–170.

Suzuki K., I. Shuto, Y. Hagura (1996) Characteristics of the membrane emulsification method combined with preliminary emulsification for preparing corn oil-in-water emulsions, *Food Sci. Technol. Int.* 2, 43–47.

Tcholakova S., N.D. Denkov, A. Lips (2008) Comparison of solid particles, globular proteins and surfactants as emulsifiers, *Phys. Chem. Chem. Phys.* 10, 1608–1627.

Tcholakova S., I. Lesov, K. Golemanov, N.D. Denkov, S. Judat, R. Engel, T. Danner (2011) Efficient emulsification of viscous oils at high drop volume fraction, *Langmuir* 27, 14783–14796.

Teskac K., J. Kristl (2010) The evidence for solid lipid nanoparticles mediated cell uptake of resveratrol, *Int. J. Pharm.* 390, 61–69.

Thevenin M.A., J.L. Grossiord, M.C. Poelman (1996) Sucrose esters cosurfactant microemulsion systems for transdermal delivery—Assesment of bicontinuous structures, *Int. J. Pharm.* 137, 177–186.

- Timgren A., G. Trägårdh, C. Trägårdh (2009) Effects of cross-flow velocity, capillary pressure and oil viscosity on oil-in-water drop formation from a capillary, *Chem. Eng. Sci.* 64, 1111–1118.
- Timgren A., G. Trägårdh, C. Trägårdh (2010) A model for drop size prediction during cross-flow emulsification, *Chem. Eng. Res. Des.* 88, 229–238.
- Timgren A., M. Rayner, M. Sjöö, P. Dejmek (2011) Starch particles for food based Pickering emulsions, *Procedia Food Sci.* 1, 95–103.
- Trentin A., M. Ferrando, F. López, C. Güell (2009) Premix membrane O/W emulsification: effect of fouling when using BSA as emulsifier, *Desalination* 245, 388–395.
- Trentin A., C. Güell, F. López, M. Ferrando (2010) Microfiltration membranes to produce BSA-stabilized emulsions by premix membrane emulsification, *J. Membr. Sci.* 356, 22–32.
- Trentin A., S. De Lamio, C. Güell, F. López, M. Ferrando (2011) Protein-stabilized emulsions containing beta-carotene produced by premix membrane emulsification, *J. Food Eng.* 106, 267–274
- Van der Graaf S., C.G.P.H. Schroën, R.M. Boom (2005a) Preparation of double emulsions by membrane emulsification—a review, *J. Membr. Sci.* 251, 7–15.
- Van der Graaf S., M.L.J. Steegmans, R.G.M. van der Sman, C.G.P.H. Schroën, R.M. Boom (2005b) Droplet formation in a T-shaped microchannel junction: a model system for membrane emulsification, *Colloid Surf. A-Physicochem. Eng. Asp.* 266, 106–116.
- Van der Zwan E., K. Schroën, K. van Dijke, R. Boom (2006) Visualization of droplet break-up in pre-mix membrane emulsification using microfluidic devices, *Colloid Surf. A: Physicochem. Eng. Asp.* 277, 223–229
- Tyrode E., J. Allouche, L. Choplin, J.L. Salager (2005) Emulsion catastrophic inversion from abnormal to normal morphology 4. Following the emulsion viscosity during three inversion protocols and extending the critical dispersed-phase concept, *Ind. Eng. Chem. Res.* 44, 67–74.
- Tzoumaki M.V., T. Moschakis, V. Kiosseoglou, C.G. Biliaderis (2011) Oil-in-water emulsions stabilized by chitin nanocrystal particles, *Food Hydrocolloids* 25, 1521–1529.
- Vladisavljevic G.T., S. Tesch, H. Schubert (2002) Preparation of water-in-oil emulsions using microporous polypropylene hollow fibers: influence of some operating parameters on droplet size distribution, *Chem. Eng. Process.* 41, 231–238.
- Vladisavljevic G.T., M. Shimizu, T. Nakashima (2004) Preparation of monodisperse multiple emulsions at high production rates by multi-stage premix membrane emulsification, *J. Membr. Sci.* 244, 97–106.

- Vladisavljevic G.T., R.A. Williams (2005) Recent developments in manufacturing emulsions and particulate products using membranes. *Adv. Colloid Interface Sci.* 113, 1–20.
- Vladisavljevic G.T., M. Shimizu, T. Nakashima (2005) Permeability of hydrophilic and hydrophobic Shirasu-porous-glass (SPG) membranes to pure liquids and its microstructure, *J. Membr. Sci.* 250, 69–77.
- Vladisavljevic G.T., R.A. Williams (2006) Manufacture of large uniform droplets using rotating membrane emulsification, *J. Colloid Interface Sci.* 299, 396–402.
- Vladisavljevic G.T., M. Shimizu, T. Nakashima (2006a) Production of multiple emulsions for drug delivery systems by repeated SPG membrane homogenization: influence of mean pore size, interfacial tension and continuous phase viscosity, *J. Membr. Sci.* 284, 373–383.
- Vladisavljevic G.T., J. Surh, J.D. McClements (2006b) Effect of emulsifier type on droplet disruption in repeated Shirasu porous glass membrane homogenization, *Langmuir* 22, 4526–4533.
- Wang X.-X., Y.-B. Li, H.-J. Yao, R.-J. Ju, Y. Zhang, R.-J. Li, Y. Yu, L. Zhang, W.-L. Lu (2011) The use of mitochondrial targeting resveratrol liposomes modified with a dequalinium polyethylene glycol-distearoylphosphatidyl ethanolamine conjugate to induce apoptosis in resistant lung cancer cells, *Biomaterials* 32, 5673–5687.
- Williams R.A., S.J. Peng, D.A. Wheeler, N.C. Morley, D. Taylor, M. Whalley, D.W. Houldsworth (1998) Controlled production of emulsions using a crossflow membrane. Part II: Industrial scale manufacture, *Chem. Eng. Res. Des.* 76, 902–910.
- Wilson R., B.J. van Schie, D. Howes (1998) Overview of the preparation, use and biological studies on polyglycerol polyricinoleate (PGPR), *Food Chem. Toxicol.* 36, 711–718.
- Xu J.H., G.S. Luo, G.G. Chen, J.D. Wang (2005) Experimental and theoretical approaches on droplet formation from a micrometer screen hole, *J. Membr. Sci.* 266, 121–131.
- Yang J., D.X. Hao, C.X. Bi, Z.G. Su, L.Y. Wang, G.H. Ma (2010) Rapid synthesis of uniform magnetic microspheres by combing premix membrane emulsification and in situ formation techniques, *Ind. Eng. Chem. Res.* 49, 6047–6053.
- Yasuno M., M. Nakajima, S. Iwamoto, T. Maruyama, S. Sugiura, I. Kobayashi, A. Shono, K. Satoh (2002) Visualization and characterization of SPG membrane emulsification, *J. Membr. Sci.* 210, 29–37.
- Yuan Q., N. Aryanti, G. Gutiérrez, R. A. Williams (2009) Enhancing the throughput of membrane emulsification techniques to manufacture functional particles, *Ind. Eng. Chem. Res.* 48, 8872–8880.

Yuan Q., R.A. Williams, N. Aryanti (2010) Innovations in high throughput manufacturing of uniform emulsions and capsules, *Adv. Powder Technol.* 21, 599–608.

Yusoff A., B.S. Murray (2011) Modified starch granules as particle-stabilizers of oil-in-water emulsions, *Food Hydrocolloids* 25, 42–55.